MATHEMATICAL MODELLING AND NUMERICAL SIMULATION OF THE CARDIOVASCULAR SYSTEM

ALFIO QUARTERONI AND LUCA FORMAGGIA

Date: 11 January, 2002.

The authors wish to thank Prof. Alessandro Veneziani and Dr. Fabio Nobile for their valuable contributions during the preparation of these notes and for having provided most of the numerical results here presented.

Our research activity on the mathematical modelling of the cardiovascular system has been partially supported by grants from various research agencies, which we gratefully acknowledge. In particular, grants 21-54139.98, 21-59230.99 and 20-61862.00 from the Swiss National Science Foundation, the project of Politecnico di Milano "LSC-Multiscacle Computing in Biofluiddynamics", the project Agenzia-2000 by the Italian CNR, titled "Modeling the fluid structure interaction in the arterial system", and a research contract Cofin-2000 by the Italian Ministry of Education (MURST), titled "Scientific computing: innovative models and numerical methods" .

To appear as a Chapter in: N. Ayache Ed., *Modelling of Living Systems*, Handbook of Numerical Analysis Series (P.G.Ciarlet and J.L.Lions Eds.), Elsevier, Amsterdam, 2002.

Alfio Quarteroni, MOX, Department of Mathematics, Politecnico di Milano, Italy and Institute of Mathematics, EPFL, Lausanne, Switzerland.

Luca Formaggia, Institute of Mathematics, EPFL, Lausanne, Switzerland.

Contents

INTRODUCTION

In these notes we will address the problem of developing models for the numerical simulation of the human circulatory system. In particular, we will focus our attention on the problem of haemodynamics in large human arteries.

Indeed, the mathematical investigation of blood flow in the human circulatory system is certainly one of the major challenges of the next years. The social and economical relevance of these studies is highlighted by the unfortunate fact that cardiovascular diseases represent the major cause of death in developed countries.

Altered flow conditions, such as separation, flow reversal, low and oscillatory shear stress areas, are now recognised by the medical research community as important factors in the development of arterial diseases. An understanding of the local haemodynamics can then have useful applications for the medical research and, in a longer term perspective, to surgical planning and therapy. The development of effective and accurate numerical simulation tools could play a crucial role in this process.

Besides their possible role in medical research, another possible use of numerical models of vascular flow is to form the basis for simulators to be used as training systems. For instance, a technique now currently used to cure a stenosis (a pathological restriction of an artery, usually due to fat deposition) is angioplasty. It consists of inflating a balloon positioned in the stenotic region by the help of a catheter. The balloon should squash the stenosis and approximately restore the original lumen area. The success of the procedure depends, among other things, on the sensitivity of the surgeon and his ability of placing the catheter in the right position. A training system which couples virtual reality techniques with the simulation of the flow field around the catheter, the balloon and the vessel walls, employing geometries extracted from real patients, could well serve as training bed for new vascular surgeons. A similar perspective could provide specific design indications concerning the realisations of surgical operations. For instance, numerical simulations could help the surgeon in understanding how the different surgical solutions may affect blood circulation and guide the selection of the most appropriate procedure for a specific patient.

In such "virtual surgery" environment, the outcome of alternative treatment plans for the individual patient can be foreseen by simulations. This numerical approach is one of the aspects of a new paradigm of the clinical practise, which is referred to as "predictive medicine" (see [54]).

Since blood flow interacts mechanically with the vessel walls it gives rise to a rather complex fluid-structure interaction problem which requires algorithms able to correctly describe the energy transfer between the fluid (typically modelled by the Navier-Stokes equations) and the structure. This is indeed one of the main subjects of these notes, which will adopt the following steps.

(1) *Analysis of the physical problem.* We illustrate problems related to haemodynamics, focusing on those aspects which are more relevant to human physiology. This will allow us to identify the major mathematical variables useful for our investigation. This part will be covered in Sect. 1.

(2) *Mathematical modelling.* Starting from some basic physical principles, we will derive the partial differential equations which link the variables relevant to the problem. We will address some difficulties associated to the specific characteristics of these equations. Problems such as existence, uniqueness and data dependence of the solution will be briefly analysed. In particular in Sect. 2 we will deal with models for the fluid flow and recall the derivation of the incompressible Navier-Stokes equations starting

from the basic principles of conservation of mass and momentum. In Sec. 4 the attention will be instead focused on the dynamics of the vessel wall structure. Some simple, yet effective, mathematical models for the vessel wall displacement will be derived and discussed.

(3) *Numerical modelling.* We present different schemes which can be employed to solve the equations that have been derived and discuss their properties. In particular, Sect. 3 deals with some relevant mathematical aspects related to the numerical solution of the equations governing the flow field, while Sect. 5 is dedicated to the coupled fluid-structure problem.

Reduced models which make use of a one dimensional description of blood flow in arteries are often used to study the propagation of average pressure and mass flow on segments of the arterial tree. In Sect. 6 we present the derivation of a model of this type, together with a brief analysis of its main mathematical characteristics.

(4) *Numerical simulation.* A final section is dedicated to numerical results obtained on relavant test cases.

1. THE PHYSICAL PROBLEM

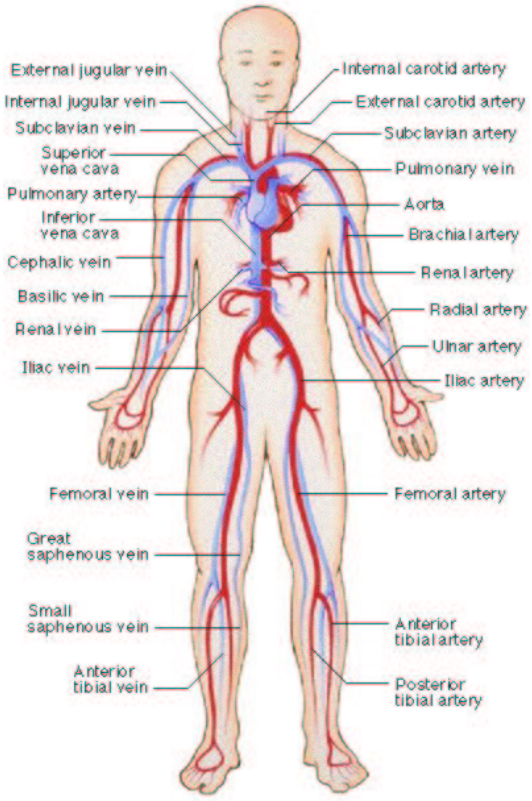

FIGURE 1. The human circulatory system
The human cardiovascular system has the task of supplying the human organs with blood. Its correct working is obviously crucial, and depends on many parameters: external temperature, muscular activity, state of health, just to mention a few. The blood pressure and flow rate then change according to the body needs.

1.1. **A brief description of the human vascular system.** The major components of the cardiovascular system are the heart, the arteries and the veins. It is usually subdivided into two main parts: the *large circulation* system and the *small circulation* system, as shown in Fig. 1. The former brings oxygenated blood from the heart left ventricle to the various organs (arterial system) and then brings it back to right atrium (venous system). The latter pumps the venous blood into the pulmonary artery, where it enters the pulmonary system, get oxygenated and is finally received by the heart left atrium, ready to be sent to the large circulation system.

Figure 2 shows a picture of the human heart. Its functioning is very complex and various research teams are currently trying to develop satisfactory mathematical models of its mechanics, which involves, among other things, the study of the electro-chemical activation of the muscle cells. We will not cover this aspect in these notes, where we rather concentrate on vascular flow, an in particular flow in arteries.

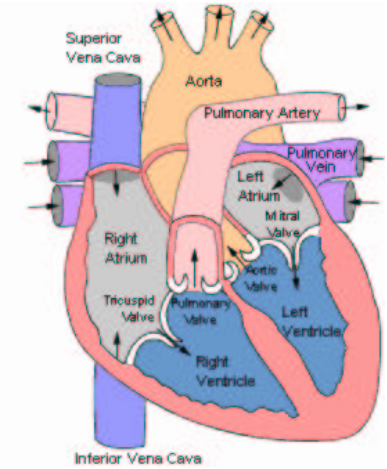

FIGURE 2. The human heart. Courtesy of the Texas Heart®Institute.

Arteries can be regarded as hollow tubes with strongly variable diameters and can be subdivided into *large arteries*, *medium arteries* and *arterioles and capillaries*. The main role of large arteries (1-3 cm of diameter) is to carry a substantial blood flow rate from the heart to the periphery and to act as a "compliant system". They deform under blood pressure and by doing so they are capable of storing elastic energy during the systolic phase and return it during the diastolic phase. As a result the blood flow is more regular than it would be if the large arteries were rigid. We have then a *fluid-structure* interaction problem. The blood may be considered a homogeneous fluid, with "standard" behaviour (Newtonian fluid), the wall may be considered elastic (or mildly visco-elastic).

The smaller arteries (0.2 mm-1 cm of diameter) are characterised by a strong branching. The vessel may in general be considered rigid (apart in the heart, where the vessel movement is mainly determined by the heart motion). Yet, the blood begins to show "non-standard" behaviour typical of a shear-thinning (non-Newtonian) fluid.

The arterioles have an important muscular activity, which is aimed at regulating blood flow to the periphery. Consequently, the vessel wall mechanical characteristics may change depending on parameters such as blood pressure and others. At the smallest levels (capillaries), blood cannot be modelled anymore as a homogeneous fluid, as the dimension of the particles are now of the same order of that of the vessel. Furthermore, the effect of wall permeability on the blood flow becomes important.

The previous subdivision is not a mere taxonomy: the morphology of the vessel walls and the physical characteristics of blood change in dependence of the type of vessel.

Indeed, the blood is not a fluid but a suspension of particles in a fluid called *plasma*. Blood particles must be taken into account in the rheological model in smaller arterioles and capillaries since their size becomes comparable to that of the vessel. The most important blood particles are

- red cells (erythrocytes), responsible for the exchange of oxygen and carbon-dioxide with the cells;
- white cells (leukocytes), which play a major role in the human immune system;

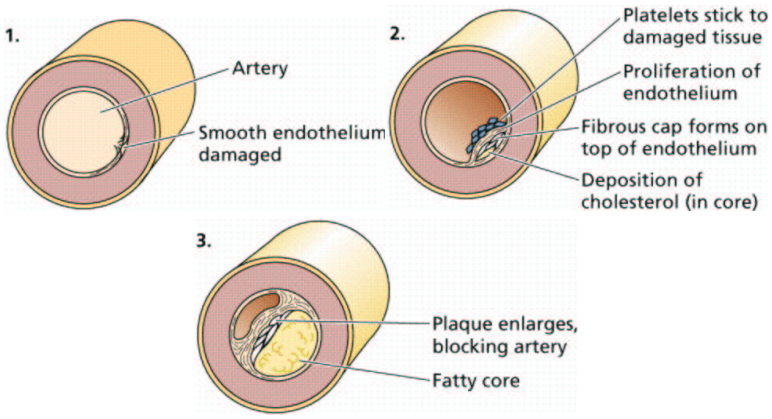

FIGURE 3. The deposition of lipids and cholesterol in the inner wall of an artery (frequently a coronary) can cause a stenosis and eventually a dramatic reduction (or even the interruption) of blood flow. Images taken from "Life: the Science of Biology" by W.K. Purves et al., fourth edition, published by Sinauer Associates Inc. and W.H. Freeman and Company.

- platelets (thrombocytes), main responsible of blood coagulation.

Here, we will limit to flow in *large/medium sized vessels*. We have mentioned that the vascular system is highly complex and able to regulate itself: an excessive decrease in blood pressure will cause the smaller arteries (arterioles) to contract and the heart rate increase. On the contrary, an excessive blood pressure is counter-reacted by a relaxation of the arterioles wall (which causes a reduction of the periphery resistance to the flow) and decreasing the heart beat. Yet, it may happen that some pathological conditions develop, for example the arterial wall may become more rigid, due to illness or excessive smoking habits, fat may accumulate in some areas causing a stenosis, that is a reduction of the vessel section as illustrated in Fig. 3, aneurysms may develop. The consequence of these pathologies on the blood field as well as the possible outcome of a surgical intervention may be studied by numerical tools.

1.2. **The main variables for the mathematical description of blood flow.** The principal quantities which describe blood flow are the *velocity* $\mathbf{u}$ and *pressure* P. Knowing these fields allows the computation of the *stresses* to which an arterial wall is subjected due to the blood movement. Since we will treat fluid-structure interaction problems, the *displacement* of the vessel wall due to the action of the flow field is another quantity of relevance. Pressure, velocity and vessel wall displacement will be functions of time and the spatial position.

The knowledge of the *temperature* field may also be relevant in some particular context, such as the hyperthermia treatment, where some drugs are activated through an artificial localised increase in temperature. Temperature may also have a notable influence on blood properties, in particular on blood viscosity. Yet, this aspect is relevant only in the flow through very small arterioles/veins and in the capillaries, a subject which is not covered in these notes.

Another aspect of blood flow which we will not cover in these notes, is the *chemical interaction* with the vessel wall, which is relevant both for the physiology of the blood vessels and for the development of certain vascular diseases.

Not mentioning the potential relevance of such investigation for the study of the propagation/absorption of pharmaceutical chemicals. Some numerical models and numerical studies for the chemical transport/diffusion process in blood and through arterial wall may be found in [47, 45].

1.3. **Some relevant issues.** Among the difficulties in the modelling of blood flow in large vessels, we mention the following ones.

- *The flow is transient.* Blood flow is obviously pulsatile. This means that one cannot neglect the time by considering a "steady state" solution, function only of the spatial position, as it is often done in many other situations (for example the study of the flow field around an aeroplane or a car). With some approximation one may think the blood flow to be periodic in time. Yet, this is usually true only for relatively short periods, since the various human activities require to change the amount of blood sent to the various organs.

  The cardiac cycle can be subdivided into two phases. The *systole* corresponds to the instant in which the heart is pumping the blood into the arterial system. The systolic period is then characterised by the highest flow rate. The *diastole*, instead, corresponds to the instant in which the heart is filling up with the blood coming from the venous system and the aortic valve is closed. The blood flow is then at its minimum. Fig. 4 illustrates a typical flow rate curve on a large artery during the cardiac cycle.

  Unsteady flow is usually much more complex than its transient counterpart. For instance, if we consider a steady flow of a fluid like water inside an "infinitely long" cylindrical tube, it is possible to derive the analytical steady state solution (also called the *Poiseuille flow* solution), characterised by a parabolic velocity profile. Transient flow in the same geometrical configuration becomes much more complex. The solution may still be obtained analytically if we assume time periodicity, giving rise to the so called *Womersley flow*[57], whose expression may be found for instance in [42]. Just as an example, in figure 5 we show the velocity profile in a tube for a Poiseuille and for a Womersley flow (the latter, obviously, at a given instant).

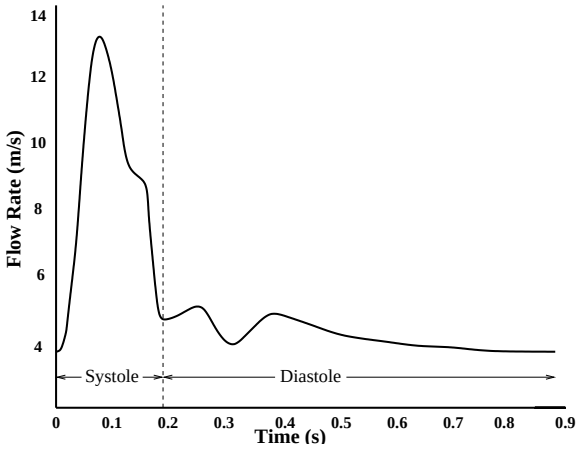

FIGURE 4. A typical flow rate in an artery during the cardiac cycle.

- *The wall interacts mechanically with the flow field.* This aspect is relevant for relatively large vessels. In the aorta, for example, the radius may vary in a range of 5% to 10% between diastole and systole. This is quite

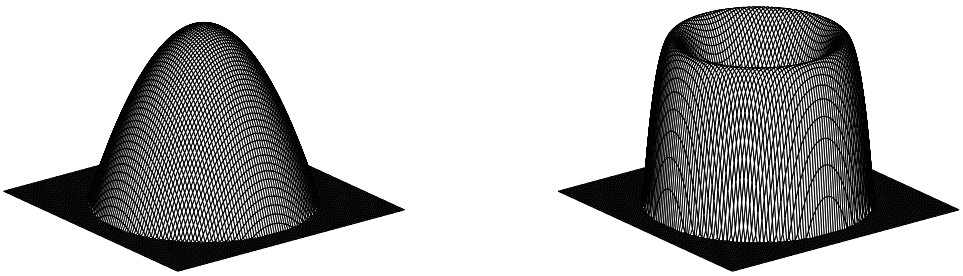

FIGURE 5. Three-dimensional velocity profiles for a Poiseuille flow (left) and Womersley unsteady flow at a given instant (right).

a large displacement, which affects the flow field. The fluid structure interaction problem is the responsible of the propagation of pulse pressure waves. Indeed, no propagative phenomena would otherwise occur in an incompressible fluid like blood. The interaction problem is a rather complex one, since the time scales associated to the interaction phenomena are two orders of magnitude greater than those associated to the bulk flow field.

In arterioles and capillaries the movement of the wall may be considered negligible.

- *Lack of boundary data.* We are normally interested in modelling only a section of the cardiovascular system by means of partial differential equations. A proper setting of a differential problem requires to provide appropriate conditions at the domain boundary, i.e, on the sections at the ends of the region of interest. For instance, let us consider figure 6. "Standard" conditions for the inlet section Γ^{in} and the outlet sections Γ^{out}, may be derived from the analysis of the differential equations governing the fluid flow. A possible choice is to prescribe all components of the velocity on Γ^{in} and the velocity derivative along the normal direction (or the normal stress components) on Γ^{out}. Unfortunately, in practise one never has enough data for prescribing all these conditions. Normally, only "averaged" data are available (mean velocity and mean pressure), which are not sufficient for a "standard" treatment of the mathematical problem. One has thus to devise alternative formulations for the boundary conditions which, on one hand reflect the physics and exploit the available data, on the other hand, permit to formulate a mathematically well posed problem. In these notes we will not investigate this particular aspect. A possible formulation for the flow boundary conditions which is particularly suited for vascular flow problems is illustrated and analysed in [18].

We have not used the terms "inflow" and "outflow" to indicate boundary conditions at Γ^{in} and Γ^{out} since they would be incorrect. Indeed, outflow would indicate the normal component of the velocity is everywhere positive (while it is negative at an inflow section). However, in vascular problems, this assumption is seldom true because the pulsating nature of blood flow might (and typically does) induce a flow reversal on portions of an artery during the cardiac beat. Indeed, the Womersley solution [57] of a pulsatile flow in circular cylinders, which provides a reasonable approximation of the general flow pattern encountered in arteries, shows a periodic flow reversal.

In the medical literature, one encounters the terms "proximal" to indicate the section which is reached first by the flow exiting from the heart, while "distal" is the term associated to the sections which are farther from the heart. Here we have

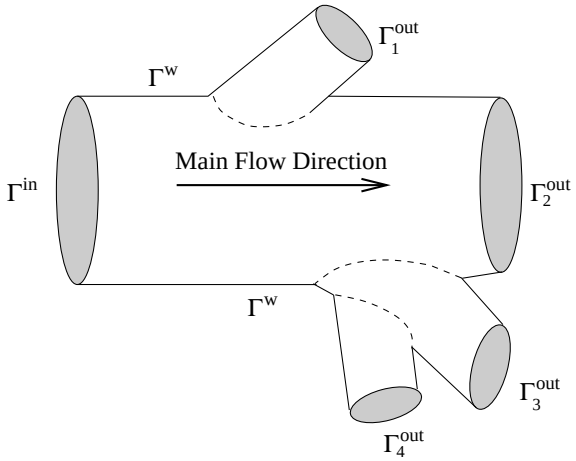

FIGURE 6. An example of a computational domain made of a section of vascular system. We need to provide proper boundary conditions at Γ^{in}, Γ^{out} and Γ^{w}.

preferred instead the terms "inlet" and "outlet" which refer to the behaviour of the mean flow rate across the section. At an inlet (outlet) section the mean flow is entering (exiting) the vascular element under consideration.

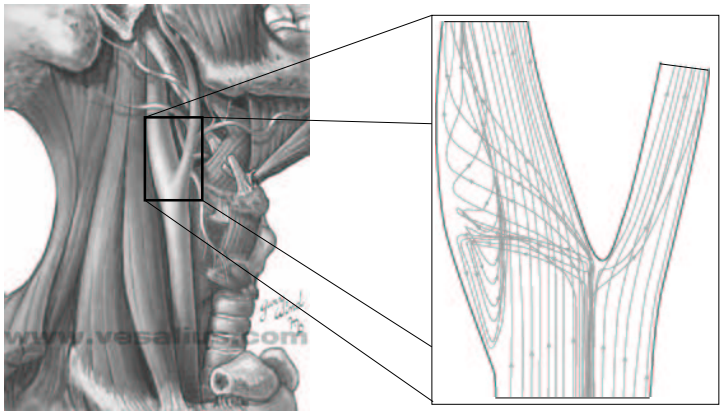

FIGURE 7. Recirculation in the carotid bifurcation. On the left we illustrate the location of the carotid bifurcation. The image on the right shows the particle path during the diastolic period in a model of the carotid bifurcation. A strong recirculation occurs inside the carotid sinus. The image on the left is courtesy of vesalius.com.

Some of the problems which the simulation of blood flow in large arteries may help in answering are summarised below.

- *Study of the physiological behaviour of vessel walls.* For example, are there any characteristics of the flow field which may be related to the formation of stenoses? In particular, in some sites like the carotid bifurcation (see Fig. 7) it is quite usual to have a reversal of the flow during the cardiac cycle which generates a *recirculation zone.* These recirculation zones have been found to be possible sites for fat accumulation and, consequently, the appearance of stenosis. There is some evidence that one of the factors

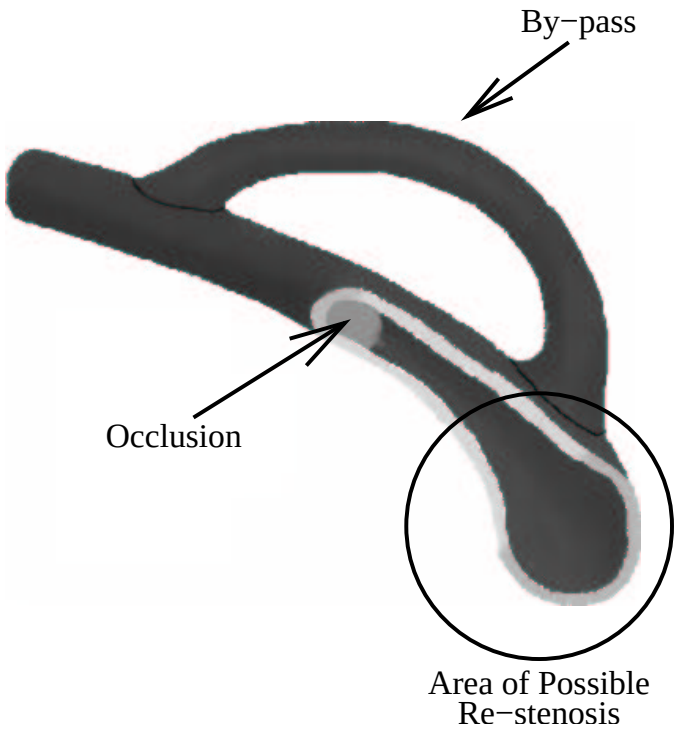

FIGURE 8. A schematic example of a coronary by-pass. The alteration of the flow field due to the by-pass may cause the formation of a new stenosis, typically immediately downstream the by-pass.

which prompt fat accumulation is linked to the oscillatory nature of the vessel wall stresses induced by the fluid in the flow reversal zone. Wall stresses are quantities very difficult to measure "in vivo" while are easily computed once the flow field is known. Numerical simulations may then help in assessing the effectiveness of such theory.

- *Study of post-surgical situations.* Is it possible to predict the flow behaviour after the geometry has been modified by a surgical operation like a by-pass? (see figure 8). It has been found that the flow pattern in the by-pass region may affect the insurgence of post-surgery pathologies. Again, a zone with recirculating or stagnant fluid has negative consequences. Numerical simulations may allow to predict the post-surgery flow pattern and determine, say, the best by-pass configuration.

2. THE DERIVATION OF THE EQUATIONS FOR THE FLOW FIELD

The flow field is governed by a set of partial differential equations in a region whose boundary changes in time. Their derivation, moving from the basic physical principles of conservation of mass and momentum, is the scope of this section.

2.1. **Nomenclature.** The space $\mathbb{R}^3$ is equipped with a Cartesian coordinate system defined by the orthonormal basis $(\mathbf{e}_1, \mathbf{e}_2, \mathbf{e}_3)$, where

$$\mathbf{e}_1 = \begin{bmatrix} 1 \\ 0 \\ 0 \end{bmatrix} \quad \mathbf{e}_2 = \begin{bmatrix} 0 \\ 1 \\ 0 \end{bmatrix} \quad \mathbf{e}_3 = \begin{bmatrix} 0 \\ 0 \\ 1 \end{bmatrix}.$$

Vectors are understood as column vectors. A vector $\mathbf{f} \in \mathbb{R}^3$ may then be written as

$$\mathbf{f} = \sum_{i=1}^{3} f_i \mathbf{e}_i$$

where f_i is the $i-$th component of $\mathbf{f}$ with respect to the chosen basis. Vectors will be always indicated using bold letters while their components will be generally denoted by the same letter in normal typeface. Sometimes, when necessary for clarity, we will indicate the $i-$th component of a vector $\mathbf{f}$ by $(\mathbf{f})_i$ or simply f_i. These definitions apply as well to vectors in $\mathbb{R}^2$.

With the term *domain* we will indicate an open, bounded, connected subset of $\mathbb{R}^N$, $N = 2, 3$, with orientable boundary. We will indicate with $\mathbf{n}$ the outwardly oriented unit vector normal to the boundary. We will also assume that the domain boundary be Lipschitz continuous (for instance, a piecewise polynomial, or a C^1 curve). In figure 9 some admissible domains are shown. If a quantity f (like

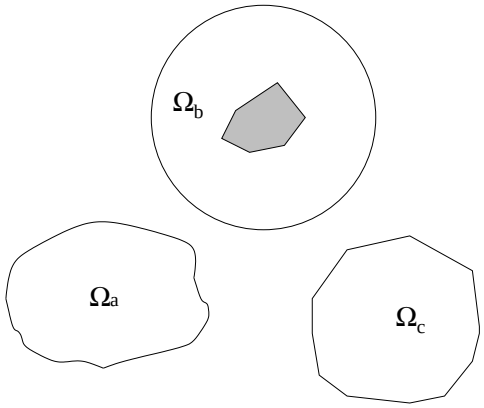

FIGURE 9. Example of admissible domains. Ω_a has a boundary formed by piecewise C^1 curves. Ω_b is a multi-connected domain, with a polygonal internal and a C^∞ external boundary. Finally Ω_c has a polygonal boundary.

temperature or pressure) takes a scalar value on a domain Ω, we say that the quantity defines a *scalar field* on Ω, which we will indicate with $f : \Omega \to \mathbb{R}$. If instead a quantity $\mathbf{f}$ associates to each point in Ω a vector (as in the case of the velocity), we say that it defines a *vector field* on Ω, and we will indicate it with $\mathbf{f} : \Omega \to \mathbb{R}^3$. Finally, if a quantity $\mathbf{T}$ associates to each point in Ω a $\mathbb{R}^{N \times N}$ matrix, we will say that it defines a (second order) *tensor* field on Ω if it obeys the ordinary

transformation rules for tensors[1]. Its components will be indicated by either $(\mathbf{T})_{ij}$, or simply T_{ij}, with $i, j = 1, \ldots, 3$.

Given a function $f : \Omega \to \mathbb{R}, \quad \mathbf{x} \to f(\mathbf{x})$, and a domain $V \subset \Omega$ we will use the shorthand notation

$$\int_V f$$

to indicate the integral

$$\int_V f(\mathbf{x}) d\mathbf{x},$$

and

$$\int_{\partial V} f$$

to indicate the surface (or line) integral

$$\int_{\partial V} f d\sigma,$$

unless the context requires otherwise.

When referring to a physical quantity f, we will indicate with $[f]$ its measure units (in the international system). For instance if $\mathbf{v}$ indicates a velocity, $[\mathbf{v}] = m/s$, where m stands for meters and s for seconds.

2.2. **The motion of continuous media.** In order to derive the differential equations which govern the fluid motion, we need to introduce some kinematic concepts and quantities. The kinematics of a continuous medium studies the property of the motion of a medium which may be thought as continuously occupying, at each time, a portion of space. This allows the use of standard methods of analysis. We will set the derivation in $\mathbb{R}^3$, since this is the natural spatial dimension. However, the definitions and final differential equations are valid also in $\mathbb{R}^2$. Furthermore, we will assume that the motion will take place during a time interval $I = (t_0, t_1)$.

The motion itself is described by a family of mappings $\mathcal{L}_t$ which associate the position $\mathbf{x}$ of a fluid particle at time $t \in I$ to a point $\boldsymbol{\xi} \in \Omega_0$, Ω_0 being the domain occupied by the fluid at the reference initial time t_0. More precisely, we denote with Ω_t the portion of space occupied by the fluid at time t and we indicate with $\mathcal{L}_t$ the mapping

$$\mathcal{L}_t : \Omega_0 \to \Omega_t, \qquad \boldsymbol{\xi} \to \mathbf{x} = \mathbf{x}(t, \boldsymbol{\xi}) = \mathcal{L}_t(\boldsymbol{\xi}),$$

which will be denoted *Lagrangian* mapping at time t. We assume that $\mathcal{L}_t$ is continuous and invertible in $\overline{\Omega_0}$, with continuous inverse.

We call Ω_0 the *reference* configuration, while Ω_t is called *current* (or spatial) configuration. The position of the material particle located at the point $\mathbf{x}$ in the current configuration Ω_t is a function of time and of the position of the same material particle at the reference time.

We may thus relate the variables $(t, \mathbf{x})$ to $(t, \boldsymbol{\xi})$. The former couple is referred to as the *Eulerian* variables while the latter are called the *Lagrangian* variables.

It is worthwhile to point out that when using the Eulerian variables as independent variables, we are concentrating our attention on a position in space $\mathbf{x} \in \Omega_t$ and on the fluid particle which, at that particular time, is located at $\mathbf{x}$. When using the Lagrangian variables as independent variables (Lagrangian frame) we are instead targeting the fluid particle "labelled" $\boldsymbol{\xi}$ (that is the fluid particle which was located at position $\boldsymbol{\xi}$ at the reference time). That is, we are following the *trajectory* $T_{\boldsymbol{\xi}}$ of fluid particle $\boldsymbol{\xi} \in \Omega_0$, defined as

$$T_{\boldsymbol{\xi}} = \{(t, \mathbf{x}(t, \boldsymbol{\xi})), \quad t \in I\}. \tag{2.1}$$

The basic principles of mechanics are more easily formulated with reference to the moving particles, thus in the Lagrangian frame. Yet, in practice is more convenient to work with the Eulerian variables. Therefore, we need to rewrite the equations stemming from those basic principles into the Eulerian frame. We will see later on that for the numerical approximation of the problem at hand it will be necessary to introduce yet another, intermediate, frame of reference, called *Arbitrary Lagrangian Eulerian.*

Being the mapping surjective, a quantity associated with the fluid may be described as function of either the Lagrangian or the Eulerian variables, depending on convenience. We will in general use the same symbol for the functions which describe the evolution of the same quantity in the Lagrangian and in the Eulerian frame, unless the context needs otherwise. In the latter case, we will mark with the hat symbol " $\widehat{\ }$ " a quantity expressed as function of the Lagrangian variables, that is, if $f : I \times \Omega_t \to \mathbb{R}$ we have the equality

$$\widehat{f}(t, \boldsymbol{\xi}) = f(t, \mathbf{x}), \quad \text{with } \mathbf{x} = \mathcal{L}_t(\boldsymbol{\xi}).$$

We will often use the following alternative notation

$$\widehat{f} = f \circ \mathcal{L}_t, \quad \text{or } f = \widehat{f} \circ \mathcal{L}_t^{-1}$$

with the understanding that the composition operator applies only to the spatial variables.

The symbol $\boldsymbol{\nabla}$ is used exclusively to indicate the gradient *with respect to the Eulerian variable* $\mathbf{x}$. When we need to indicate the gradient with respect to the Lagrangian variable $\boldsymbol{\xi}$ we will use the symbol $\boldsymbol{\nabla}_{\boldsymbol{\xi}}$, that is

$$\boldsymbol{\nabla}_{\boldsymbol{\xi}} \widehat{f} = \sum_{i=1}^{3} \frac{\partial \widehat{f}}{\partial \xi_i} \mathbf{e}_i$$

The same convention applies to other spatial differential operators (divergence, Laplacian etc.) as well.

In the following we will put $I \times \Omega_t = \{(t, \mathbf{x}),\ t \in I,\ x \in \Omega_t\}$.

2.2.1. *The velocity.* The *fluid velocity* is the major kinematic quantity of our problem. In the Lagrangian frame it is expressed by means of a vector field $\widehat{\mathbf{u}} = \widehat{\mathbf{u}}(t, \boldsymbol{\xi})$ defined as

$$\widehat{\mathbf{u}} = \frac{\partial \mathbf{x}}{\partial t}, \quad \text{i.e} \quad \widehat{\mathbf{u}}(t, \boldsymbol{\xi}) = \frac{\partial}{\partial t} \mathbf{x}(t, \boldsymbol{\xi}). \tag{2.2}$$

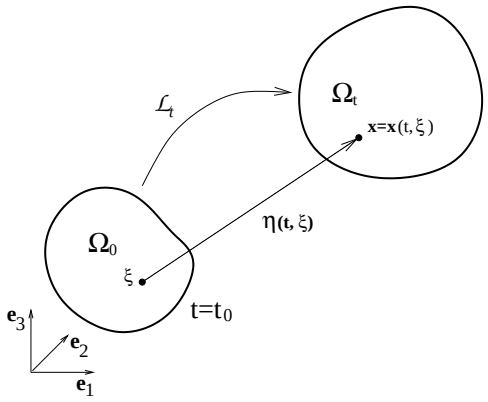

FIGURE 10. The Lagrangian mapping

$\widehat{\mathbf{u}}$ is called the *Lagrangian* velocity field (or velocity field in the Lagrangian frame), and it denotes the time derivative along the trajectory $T_{\boldsymbol{\xi}}$ of the fluid particle $\boldsymbol{\xi}$. The velocity $\mathbf{u}$ on the Eulerian frame is defined for $(t, \mathbf{x}) \in I \times \Omega_t$ as

$$\mathbf{u} = \widehat{\mathbf{u}} \circ \mathcal{L}_t^{-1}, \quad \text{i.e} \quad \mathbf{u}(t, \mathbf{x}) = \widehat{\mathbf{u}}(t, \mathcal{L}_t^{-1}(\mathbf{x})).$$

Example 2.1. Let us consider a 2D case and the following movement law, for $t \geq 0$

$$\begin{aligned} x_1 &= \xi_1 e^t \qquad \xi_1 \in (-1, 1) \\ x_2 &= \xi_2 \qquad \xi_2 \in (-1, 1) \end{aligned}$$

The domain at time $t > 0$ occupies the rectangle $(-e^t, e^t) \times (-1, 1)$. The mapping is clearly invertible for all $t \geq 0$.

We have

$$\widehat{u}_1 = \partial x_1 / \partial t = \xi_1 e^t, \qquad \widehat{u}_2 = \partial x_2 / \partial t = 0.$$

We can immediately compute the velocity field as function of the Eulerian variable as

$$u_1 = x_1 \qquad u_2 = 0.$$

Once the velocity field and the reference configuration is known, the motion may be derived by solving the following Cauchy problem:

For any $\boldsymbol{\xi} \in \Omega_0$, find the function $\mathbf{x} = \mathbf{x}(t, \boldsymbol{\xi})$ which satisfies

$$\begin{cases} \dfrac{\partial \mathbf{x}}{\partial t}(t, \boldsymbol{\xi}) = \widehat{\mathbf{u}}(t, \boldsymbol{\xi}), \forall t \in I \\ \mathbf{x}(t_0, \boldsymbol{\xi}) = \boldsymbol{\xi}. \end{cases}$$

2.2.2. *The material derivative.* We can relate time derivatives computed with respect to the different frames. The *material* (or *Lagrangian*) time derivative of a function f, which we will denote $\frac{Df}{Dt}$, is defined as the time derivative in the Lagrangian frame, yet expressed as function of the Eulerian variables.

That is, if $f : I \times \Omega_t \to \mathbb{R}$ and $\widehat{f} = f \circ \mathcal{L}_t$,

$$\frac{Df}{Dt} : I \times \Omega_t \to \mathbb{R}, \qquad \frac{Df}{Dt}(t, \mathbf{x}) = \frac{\partial \widehat{f}}{\partial t}(t, \boldsymbol{\xi}), \quad \boldsymbol{\xi} = \mathcal{L}_t^{-1}(\mathbf{x}). \tag{2.3}$$

Therefore, for any fixed $\boldsymbol{\xi} \in \Omega_0$ we may also write

$$\frac{Df}{Dt}(t, \mathbf{x}) = \frac{d}{dt} f(t, \mathbf{x}(t, \boldsymbol{\xi})),$$

by which we can observe that the material derivative represents the rate of variation of f along the trajectory $T_{\boldsymbol{\xi}}$.

By applying the chain-rule of derivation of composed functions, we have

$$\frac{Df}{Dt} = \frac{\partial f}{\partial t} + \mathbf{u} \cdot \boldsymbol{\nabla} f. \tag{2.4}$$

Indeed,

$$\frac{Df}{Dt} = \left[\frac{\partial}{\partial t} (f \circ \mathcal{L}_t) \right] \circ \mathcal{L}_t^{-1} = \frac{\partial f}{\partial t} + \boldsymbol{\nabla} f \cdot \left(\frac{\partial \mathbf{x}}{\partial t} \circ \mathcal{L}_t^{-1} \right) = \frac{\partial f}{\partial t} + \mathbf{u} \cdot \boldsymbol{\nabla} f.$$

A quantity which satisfies

$$\frac{\partial f}{\partial t} = 0$$

is called *stationary*, and a motion for which

$$\frac{\partial \mathbf{u}}{\partial t} = 0$$

is said a *stationary motion.* Clearly, blood flow ought not to be stationary!

Example 2.2. Let us consider again the motion of Example 2.1 and consider the function $f(x_1, x_2) = 3x_1 + x_2$ (which is is independent of t). The application of relation (2.4) gives

$$\frac{Df}{Dt} = 0 + \begin{bmatrix} x_1 \\ 0 \end{bmatrix} \cdot \begin{bmatrix} 3 \\ 1 \end{bmatrix} = 3x_1.$$

On the other hand,

$$\widehat{f} = 3\xi_1 e^t + \xi_2,$$

and

$$\frac{\partial \widehat{f}}{\partial t} = 3\xi_1 e^t,$$

by which we deduce that,

$$\frac{\partial \widehat{f}}{\partial t} \circ \mathcal{L}_t^{-1} = 3x_1.$$

This example, besides verifying relation (2.4), shows that a function $f = f(t, \mathbf{x})$ with $\partial f/\partial t = 0$ in general has $Df/Dt \neq 0$.

2.2.3. *The acceleration.* In the Lagrangian frame the acceleration is a vector field $\widehat{\mathbf{a}} : I \times \Omega_0 \to \mathbb{R}^3$ defined as

$$\widehat{\mathbf{a}} = \frac{\partial \widehat{\mathbf{u}}}{\partial t} = \frac{\partial^2 \mathbf{x}}{\partial t^2}.$$

By recalling the definition of material derivative, we may write the acceleration in Eulerian frame as

$$\mathbf{a} = \frac{D\mathbf{u}}{Dt} = \frac{\partial \mathbf{u}}{\partial t} + (\mathbf{u} \cdot \boldsymbol{\nabla})\mathbf{u}. \tag{2.5}$$

Componentwise,

$$a_i = \frac{\partial u_i}{\partial t} + \sum_{j=1}^{3} u_j \frac{\partial u_i}{\partial x_j}. \tag{2.6}$$

2.2.4. *The deformation gradient.* Another kinematic quantity necessary for the derivation of the mathematical model is the *deformation gradient* $\widehat{\mathbf{F}}_t$, which is defined, for each $t \in I$, as

$$\widehat{\mathbf{F}}_t : \Omega_0 \to \mathbb{R}^{N \times N}, \qquad \widehat{\mathbf{F}}_t = \boldsymbol{\nabla}_{\boldsymbol{\xi}} \mathcal{L}_t = \frac{\partial \mathbf{x}}{\partial \boldsymbol{\xi}}. \tag{2.7}$$

Componentwise,

$$(\widehat{\mathbf{F}}_t)_{ij} = \frac{\partial x_i}{\partial \xi_j}.$$

In particular, its determinant,

$$\widehat{J}_t = \det \widehat{\mathbf{F}}_t, \tag{2.8}$$

is called the Jacobian of the mapping $\mathcal{L}_t$. As usual, its counterpart in the Eulerian frame is indicated J_t.

It is possible to show that the time continuity and the invertibility of the Lagrangian mapping is sufficient to have, for all $t \in I$

$$\widehat{J}_t(\boldsymbol{\xi}) > 0 \qquad \forall \boldsymbol{\xi} \in \Omega_0. \tag{2.9}$$

The importance of J_t is clearly linked to the rule which transforms integrals from the current to the reference configuration. We recall the following theorem of elementary calculus (without providing its proof).

Theorem 2.1. *Let $V_t \subset \Omega_t$ be a subdomain of Ω_t and let us consider the function $f : I \times V_t \to \mathbb{R}$. Then, f is integrable on V_t iff $(f \circ \mathcal{L}_t)J_t$ is integrable on $V_0 = \mathcal{L}_t^{-1}(V_t)$, and*

$$\int_{V_t} f(t,\mathbf{x})d\mathbf{x} = \int_{V_0} \widehat{f}(t,\boldsymbol{\xi})\,\widehat{J}_t(\boldsymbol{\xi})d\boldsymbol{\xi},$$

where $\widehat{f}(t,\boldsymbol{\xi}) = f(t,\mathcal{L}_t(\boldsymbol{\xi}))$. In short,

$$\int_{V_t} f = \int_{V_0} \widehat{f}\widehat{J}_t.$$

2.2.5. *The Reynolds transport theorem.* An interesting property of the Jacobian is that its time derivative is linked to the divergence of the velocity field.

Lemma 2.1. *Let J_t denote the Jacobian (2.8) in the Eulerian frame. Then*

$$\frac{D}{Dt}J_t = J_t \operatorname{div}\mathbf{u} \tag{2.10}$$

This relation is sometimes called Euler expansion formula.

Proof. We have, by direct application of the chain-rule,

$$\boldsymbol{\nabla}_{\boldsymbol{\xi}}\widehat{\mathbf{u}} = \boldsymbol{\nabla}_{\boldsymbol{\xi}}(\mathbf{u}\circ\mathcal{L}_t) = \widehat{\boldsymbol{\nabla}\mathbf{u}}\,\boldsymbol{\nabla}_{\boldsymbol{\xi}}\mathcal{L}_t = \widehat{\boldsymbol{\nabla}\mathbf{u}}\,\widehat{\mathbf{F}}_t.$$

On the other hand, by recalling the definition of the velocity (2.2),

$$\boldsymbol{\nabla}_{\boldsymbol{\xi}}\widehat{\mathbf{u}} = \boldsymbol{\nabla}_{\boldsymbol{\xi}}\left(\frac{\partial\mathbf{x}}{\partial t}\right) = \frac{\partial}{\partial t}\boldsymbol{\nabla}_{\boldsymbol{\xi}}\mathbf{x} = \frac{\partial\widehat{\mathbf{F}}_t}{\partial t}.$$

Thus, we may write

$$\widehat{\mathbf{F}}_{t+\epsilon} = \widehat{\mathbf{F}}_t + \epsilon\frac{\partial\widehat{\mathbf{F}}_t}{\partial t} + \mathbf{o}(\epsilon) = \widehat{\mathbf{F}}_t + \epsilon\widehat{\boldsymbol{\nabla}\mathbf{u}}\,\widehat{\mathbf{F}}_t + \mathbf{o}(\epsilon) = (\mathbf{I} + \epsilon\widehat{\boldsymbol{\nabla}\mathbf{u}})\,\widehat{\mathbf{F}}_t + \mathbf{o}(\epsilon).$$

We now exploit the well known result that for any non-singular matrix $\mathbf{A}$

$$\det(\mathbf{I} + \epsilon\mathbf{A}) = 1 + \epsilon\,\mathrm{tr}\,\mathbf{A} + o(\epsilon),$$

where $\mathrm{tr}\,\mathbf{A} = \sum_i A_{ii}$ denotes the trace of the matrix A, to write

$$\widehat{J}_{t+\epsilon} = \det(\widehat{\mathbf{F}}_{t+\epsilon}) = (1 + \epsilon\,\mathrm{tr}\,\widehat{\boldsymbol{\nabla}\mathbf{u}})\widehat{J}_t + o(\epsilon) = (1 + \epsilon\operatorname{div}\widehat{\mathbf{u}})\widehat{J}_t + o(\epsilon).$$

We have used the identity $\mathrm{tr}\,\widehat{\boldsymbol{\nabla}\mathbf{u}} = \operatorname{div}\widehat{\mathbf{u}}$. Then, by applying the definition of material derivative and exploiting the continuity of the Lagrangian mapping, we may write

$$\frac{DJ_t}{Dt} = \left(\lim_{\epsilon\to 0}\frac{\widehat{J}_{t+\epsilon} - \widehat{J}_t}{\epsilon}\right)\circ\mathcal{L}_t^{-1} = (\operatorname{div}\widehat{\mathbf{u}}\,\widehat{J}_t)\circ\mathcal{L}_t^{-1} = \operatorname{div}\mathbf{u}\,J_t.$$

□

Example 2.3. For the movement law given by Example 2.1 we have

$$\widehat{J}_t = \det\begin{bmatrix} e^t & 0 \\ 0 & 1 \end{bmatrix} = e^t$$

and $J_t = e^t$ as well. We may verify directly relation (2.10) since

$$J_t \operatorname{div}\mathbf{u} = e^t(1+0) = e^t = \frac{d}{dt}\widehat{J}_t = (\text{by relation (2.3)}) = \frac{D}{Dt}J_t.$$

We have now the following fundamental result.

Theorem 2.2 (Reynolds transport theorem). *Let $V_0 \subset \Omega_0$, and $V_t \subset \Omega_t$ be its image under the mapping $\mathcal{L}_t$. Let $f : I \times \Omega_t \to \mathbb{R}$ be a continuously differentiable function with respect to both variables $\mathbf{x}$ and t.*

Then,

$$\frac{d}{dt}\int_{V_t} f = \int_{V_t} (\frac{Df}{Dt} + f \operatorname{div} \mathbf{u}) = \int_{V_t} (\frac{\partial f}{\partial t} + \operatorname{div}(f\mathbf{u})) \tag{2.11}$$

Proof. Thanks to Theorem 2.1 and relations (2.10) and (2.3), we have

$$\frac{d}{dt}\int_{V_t} f(t,\mathbf{x})d\mathbf{x} = \frac{d}{dt}\int_{V_0} \widehat{f}(t,\boldsymbol{\xi})\widehat{J}_t(\boldsymbol{\xi})d\boldsymbol{\xi} =$$

$$\int_{V_0} \frac{\partial}{\partial t}\left[\widehat{f}(t,\boldsymbol{\xi})\widehat{J}_t(\boldsymbol{\xi})\right] d\boldsymbol{\xi} = \int_{V_0} \left[\frac{\partial \widehat{f}}{\partial t}(t,\boldsymbol{\xi})\widehat{J}_t(\boldsymbol{\xi}) + \widehat{f}(t,\boldsymbol{\xi})\frac{\partial}{\partial t}\widehat{J}_t(\boldsymbol{\xi})\right] d\boldsymbol{\xi}$$

We now use Theorem 2.1 and the definition of material derivative (2.3) to write

$$\int_{V_0} \frac{\partial \widehat{f}}{\partial t}(t,\boldsymbol{\xi})\widehat{J}_t(\boldsymbol{\xi})d\boldsymbol{\xi} = \int_{V_t} \frac{Df}{Dt}(t,\mathbf{x})d\mathbf{x}.$$

Furthermore, we exploit again the definition of material derivative (2.3) in order to rewrite relation (2.10) in the following equivalent form

$$\frac{\partial}{\partial t}\widehat{J}_t(\boldsymbol{\xi}) = \widehat{J}_t(\boldsymbol{\xi}) \operatorname{div} \mathbf{u}(t,\mathbf{x}(t,\boldsymbol{\xi})).$$

Consequently,

$$\frac{d}{dt}\int_{V_t} f(t,\mathbf{x})d\mathbf{x} = \int_{V_t} \frac{Df}{Dt}(t,\mathbf{x})d\mathbf{x} + \int_{V_0} \widehat{f}(t,\boldsymbol{\xi})J_t(\mathbf{x}(t,\boldsymbol{\xi})) \operatorname{div} \mathbf{u}(t,\mathbf{x}(t,\boldsymbol{\xi}))d\boldsymbol{\xi} =$$

$$\int_{V_t} \frac{Df}{Dt}(t,\mathbf{x})d\mathbf{x} + \int_{V_t} f(t,\mathbf{x}) \operatorname{div} \mathbf{u}(t,\mathbf{x})d\mathbf{x} = \int_{V_t} \frac{Df}{Dt}(t,\mathbf{x}) + f(t,\mathbf{x}) \operatorname{div} \mathbf{u}(t,\mathbf{x})d\mathbf{x}.$$

The second equality in (2.11) is a consequence of (2.4). □

Relation (2.11) is given the name of *Reynolds transport formula*, or simply *transport formula* (sometimes the name *convection formula* is used as well).

By the application of the divergence theorem the previous expression becomes

$$\frac{d}{dt}\int_{V_t} f = \int_{V_t} \frac{\partial f}{\partial t} + \int_{\partial V_t} f\mathbf{u}\cdot\mathbf{n}.$$

2.3. **The derivation of the basic equations of fluid mechanics.** In the sequel, the symbol V_t will always be used to indicate a *material volume* at time t, i.e. V_t is the image under the Lagrangian mapping of a subdomain $V_0 \subset \Omega_0$, i.e. $V_t = \mathcal{L}_t(V_0)$ (as already done in Theorem 2.2).

2.3.1. *Continuity equation or mass conservation.* We assume that there exists a strictly positive, measurable function $\rho : I \times \Omega_t \to \mathbb{R}$, called *density* such that on each $V_t \subset \Omega_t$

$$\int_{V_t} \rho = m(V_t)$$

where $m(V_t)$ is the mass of the material contained in V_t. The density ρ has dimensions $[\rho] = kg/m^3$.

A fundamental principle of classical mechanics, called principle of *mass conservation*, states that mass is neither created nor destroyed during the motion. This principle translates into the following mathematical statement:

Given any material volume $V_t \subset \Omega_t$ the following equality holds

$$\frac{d}{dt}\int_{V_t} \rho = 0.$$

We can apply the transport theorem, obtaining

$$\int_{V_t} \left(\frac{D\rho}{Dt} + \rho \operatorname{div} \mathbf{u} \right) = 0. \tag{2.12}$$

By assuming that the terms under the integral are continuous, the arbitrariness of V_t allows us to write the *continuity equation* in differential form

$$\frac{\partial \rho}{\partial t} + \operatorname{div} \rho\mathbf{u} = 0.$$

In these cases for which we can make the assumption that ρ is constant (like for blood flow), we obtain

$$\operatorname{div} \mathbf{u} = 0. \tag{2.13}$$

Relation (2.13), which has been derived from the continuity equation in the case of a *constant density* fluid (sometimes also called incompressible fluid), is indeed a kinematic constraint. Thanks to (2.10), relation (2.13) is equivalent to

$$\frac{D}{Dt} J_t = 0, \tag{2.14}$$

which is the *incompressibility constraint*. A flow which satisfies the incompressibility constraint is called *incompressible*. By the continuity equation we derive the following implication:

$$\text{constant density fluid} \Rightarrow \text{incompressible flow}$$

whereas the converse is not true in general.

By employing the transport formula (2.11) with $f = 1$ we may note that the incompressibility constraint is equivalent to

$$\frac{d}{dt}\int_{V_t} d\mathbf{x} = 0 \qquad \forall V_t \subset \Omega_t,$$

which means that the only possible motions of an incompressible flow are those which preserve the fluid volume.

2.3.2. *The momentum equation.* Another important principle allows the derivation of an additional set of differential equations, that is the principle of *conservation of momentum*. It is an extension of the famous Newton Law, "force=mass×acceleration", to a continuous medium.

Remark 2.1. In the dimension unit specifications we will use the symbol *Ne* to indicate the *Newtons* (the dimension units of a force), $Ne = kgm/s^2$, instead of the more standard symbol N, since we have used the latter to indicate the number of space dimensions.

$\diamondsuit$

Three different types of forces may be acting on the material inside Ω_t

- *Body forces.* These forces are proportional to the mass. They are normally represented by introducing a vector field $\mathbf{f}^b : I \times \Omega_t \to \mathbb{R}^3$, called *specific body force*, whose dimension unit, $[\mathbf{f}^b]=Ne/kg=m/s^2$, is that of an acceleration. The body force acting on a volume V_t is given by

$$\int_{V_t} \rho \mathbf{f}^b,$$

whose dimension unit is clearly Ne. An example is the gravity force, given by $\mathbf{f}^b = -g\mathbf{e}_3$, where $\mathbf{e}_3$ represents the vertical direction and g the gravitational acceleration.

- *Applied surface forces.* They represent that part of the forces which are imposed on the media through its surface. We will assume that they may be represented through a vector field $\mathbf{t}^e : I \times \Gamma_t^n \to \mathbb{R}^3$, called *applied stresses*, defined on a measurable subset of the domain boundary $\Gamma_t^n \subset \partial\Omega_t$ and with dimension unit $[\mathbf{t}^e] = Ne/m^2$. The resultant force acting through the surface is then given by

$$\int_{\Gamma_t^n} \mathbf{t}^e.$$

  An example of a surface stress is that caused by the friction of the air flowing over the surface of a lake.
- *Internal "continuity" forces.* These are the forces that the continuum media particles exert on each other and are responsible for maintaining material continuity during the movement. To model these forces let us recall the following principle.

The Cauchy principle. *There exists a vector field* $\mathbf{t}$*, called* Cauchy stress*,*

$$\mathbf{t} : I \times \Omega_t \times \mathbf{S}_1 \to \mathbb{R}^3$$

with

$$\mathbf{S}_1 = \{\mathbf{n} \in \mathbb{R}^3 : \quad |\mathbf{n}| = 1\}$$

such that its integral on the surface of any material domain $V_t \subset \Omega_t$*, given by*

$$\int_{\partial V_t} \mathbf{t}(t, \mathbf{x}, \mathbf{n}) d\sigma \tag{2.15}$$

is equivalent *to the resultant of the material continuity forces acting on* V_t*. In (2.15),* $\mathbf{n}$ *indicates the outward normal of* ∂V_t*.*

Furthermore, we have that

$$\mathbf{t} = \mathbf{t}^e \qquad \text{on } \partial V_t \cap \Gamma_t^n.$$

This principle is of fundamental importance because it states that the only dependence of the internal forces on the geometry of ∂V_t is through $\mathbf{n}$.

We may now state the following *principle of conservation of linear momentum.*

For any $t \in I$, on any sub-domain $V_t \subset \Omega_t$ *completely contained in* Ω_t, the following relation holds,

$$\frac{d}{dt}\int_{V_t} \rho(t, \mathbf{x})\mathbf{u}(t, \mathbf{x}) d\mathbf{x} = \int_{V_t} \rho(t, \mathbf{x})\mathbf{f}^b(t, \mathbf{x}) d\mathbf{x} + \int_{\partial V_t} \mathbf{t}(t, \mathbf{x}, \mathbf{n}) d\sigma, \tag{2.16}$$

where all terms dimension unit is Ne. Relation (2.16) expresses the property that the variation of the *linear momentum* of V_t (represented by the integral at the left hand side) is balanced by the resultant of the internal and body forces.

With some further assumptions on the regularity of the Cauchy stresses, we are now able to relate the internal continuity forces to a *tensor field*, as follows.

Theorem 2.3 (Cauchy stress tensor theorem.)**.** *Let us assume that* $\forall t \in I$*, the body forces* $\mathbf{f}^b$*, the density* ρ *and* $\dfrac{D}{Dt}\mathbf{u}$ *are all bounded functions on* Ω_t *and that the Cauchy stress vector field* $\mathbf{t}$ *is continuously differentiable with respect to the variable* $\mathbf{x}$ *for each* $\mathbf{n} \in \mathbf{S}_1$*, and continuous with respect to* $\mathbf{n}$*. Then, there exists a*

continuously differentiable symmetric[1]*. tensor field, called* Cauchy stress tensor,

$$\mathbf{T} : I \times \overline{\Omega_t} \to \mathbb{R}^{3\times 3}, \quad [\mathbf{T}] = Ne/m^2,$$

such that

$$\mathbf{t}(t, \mathbf{x}, \mathbf{n}) = \mathbf{T}(t, \mathbf{x}) \cdot \mathbf{n} \quad \forall t \in I,\ \forall \mathbf{x} \in \Omega_t,\ \forall \mathbf{n} \in \mathbf{S}_1.$$

The proof is omitted. The interested reader may refer to [1, 50].

Therefore, under the hypotheses of the Cauchy theorem, we have

$$\mathbf{T} \cdot \mathbf{n} = \mathbf{t}^e, \quad \text{on } \partial V_t \cap \Gamma_t^n, \tag{2.17}$$

and that the resultant of the internal forces on V_t is expressed by

$$\int_{\partial V_t} \mathbf{T} \cdot \mathbf{n}, \tag{2.18}$$

and we may rewrite the principle of linear momentum (2.16) as follows.

For all $t \in I$, on any sub-domain $V_t \subset \Omega_t$ *completely contained in* Ω_t, the following relation holds,

$$\frac{d}{dt}\int_{V_t} \rho\mathbf{u} = \int_{V_t} \rho\mathbf{f}^b + \int_{\partial V_t} \mathbf{T} \cdot \mathbf{n}. \tag{2.19}$$

Since ρ is constant and $\operatorname{div}\mathbf{u} = 0$, by invoking the transport formula (2.11) we obtain

$$\frac{d}{dt}\int_{V_t} \rho\mathbf{u} = \int_{V_t} \left(\frac{D}{Dt}(\rho\mathbf{u}) + \rho\mathbf{u}\operatorname{div}\mathbf{u}\right) = \int_{V_t} \rho\frac{D\mathbf{u}}{Dt}.$$

By using the divergence theorem, and assuming that $\operatorname{div}\mathbf{T}$ is integrable, relation (2.19) becomes

$$\int_{V_t} \left[\rho\frac{D\mathbf{u}}{Dt} - \mathbf{div}\,\mathbf{T} - \rho\mathbf{f}^b\right] = 0.$$

Thanks to the arbitrariness of V_t and under the hypothesis that the terms under the integrals are continuous in space, we derive the following differential equation

$$\rho\frac{D\mathbf{u}}{Dt} - \mathbf{div}\,\mathbf{T} = \rho\mathbf{f}^b \qquad \text{in } \Omega_t. \tag{2.20}$$

Remark 2.2. In deriving (2.20) we have assumed that V_t is completely contained into Ω_t. We may however extend the derivation to the case where V_t has a part of boundary in common with Γ_t^n. In that case, we should use in place of (2.19) the following,

$$\frac{d}{dt}\int_{V_t} \rho\mathbf{u} = \int_{\partial V_t \setminus \Gamma_t^n} \mathbf{T} \cdot \mathbf{n} + \int_{\partial V_t \cap \Gamma_t^n} \mathbf{t}^e + \int_{V_t} \rho\mathbf{f}^b. \tag{2.21}$$

Even now we would re-obtain (2.20) in view of property (2.17) of the Cauchy stress tensor, which should now be regarded as *boundary condition.*

$\diamondsuit$

We may note that $\dfrac{D\mathbf{u}}{Dt}$ is indeed the fluid acceleration. Referring to relation (2.5), it may be written as

$$\frac{D\mathbf{u}}{Dt} = \frac{\partial\mathbf{u}}{\partial t} + (\mathbf{u} \cdot \boldsymbol{\nabla})\mathbf{u},$$

[1]The symmetry of the Cauchy tensor may indeed be derived from the conservation of angular momentum.

where $(\mathbf{u}\cdot\boldsymbol{\nabla})\mathbf{u}$ is a vector whose components are

$$((\mathbf{u}\cdot\boldsymbol{\nabla})\mathbf{u})_i = \sum_{j=1}^{3} u_j \frac{\partial u_i}{\partial x_j}\ , i = 1,\dots,3.$$

For ease of notation, from now on we will omit the subscript b to indicate the body force density applied to the fluid, which will be indicated just as $\mathbf{f}$.

Relation (2.20) may finally be written as

$$\rho\frac{\partial \mathbf{u}}{\partial t} + \rho(\mathbf{u}\cdot\boldsymbol{\nabla})\mathbf{u} - \mathbf{div}\,\mathbf{T} = \rho\mathbf{f} \tag{2.22}$$

Componentwise,

$$\rho\frac{\partial u_i}{\partial t} + \rho\sum_{j=1}^{3} u_j\frac{\partial u_i}{\partial x_j} - \sum_{j=1}^{3}\frac{\partial T_{ij}}{\partial x_j} = \rho f_i^b, \quad i = 1,\dots,3.$$

The non linear term $\rho(\mathbf{u}\cdot\boldsymbol{\nabla})\mathbf{u}$ is called the *convective term*.

Remark 2.3. We note the convective term may be written in the so called *divergence form* $\mathbf{div}(\mathbf{u}\otimes\mathbf{u})$, where

$$(\mathbf{div}\,\mathbf{u}\otimes\mathbf{u})_{ij} = \sum_{j=1}^{3}\frac{\partial}{\partial x_j}(u_i\,u_j), \quad i = 1,\dots,3,\ j = 1,\dots,3.$$

Indeed, thanks to the incompressibility of the fluid

$$(\mathbf{u}\cdot\boldsymbol{\nabla})\mathbf{u} = (\mathbf{u}\cdot\boldsymbol{\nabla})\mathbf{u} + \mathbf{u}\,\mathrm{div}\,\mathbf{u} = \mathbf{div}(\mathbf{u}\otimes\mathbf{u}).$$

The momentum equation in divergence form is then

$$\rho\frac{\partial \mathbf{u}}{\partial t} + \mathbf{div}\,(\rho\mathbf{u}\otimes\mathbf{u} - \mathbf{T}) = \rho\mathbf{f}. \tag{2.23}$$

♢

2.3.3. *The constitutive law.* In order to close the system of equations (2.22) and (2.13) just derived, we need to link the Cauchy stress tensor to the kinematic quantities, and in particular, the velocity field. Such relation, called *constitutive law*, provides a characterization of the mechanical behavior of the particular fluid under consideration.

The branch of science which studies the behavior of a moving fluid and in particular the relation between stresses and kinematic quantities is called *rheology*. We have already anticipated in the introduction that blood rheology could be complex, particularly in vessels with small size.

Here, we will assume for the fluid a *Newtonian behavior* (an approximation valid for many fluids and also for blood flow in large vessels, which is the case in our presentation). *In a Newtonian incompressible fluid*, the Cauchy stress tensor may be written as a linear function of the velocity derivatives [50], according to

$$\mathbf{T} = -P\mathbf{I} + \mu(\boldsymbol{\nabla}\mathbf{u} + \boldsymbol{\nabla}\mathbf{u}^T), \tag{2.24}$$

where P is a scalar function called *pressure*, $\mathbf{I}$ is the identity matrix, μ is the *dynamic viscosity* of the fluid and is a positive quantity. The tensor

$$\mathbf{D}(\mathbf{u}) = \frac{(\boldsymbol{\nabla}\mathbf{u} + \boldsymbol{\nabla}\mathbf{u}^T)}{2}, \quad D_{ij} = \frac{1}{2}(\frac{\partial u_i}{\partial x_j} + \frac{\partial u_j}{\partial x_i}), \quad i = 1,\dots,3,\ j = 1,\dots,3$$

is called the *strain rate* tensor. Then,

$$\mathbf{T} = -P\mathbf{I} + 2\mu\mathbf{D}(\mathbf{u}).$$

The term $2\mu\mathbf{D}(\mathbf{u})$ in the definition of the Cauchy stress tensor is often referred to as *viscous stress* component of the stress tensor. We have that $[P]$=Ne/m^2 and

$[\mu]=kg/ms$. The viscosity may vary with respect to time and space. For example, it may depend on the fluid temperature. The assumption of Newtonian fluid, however, implies that μ is *independent from kinematic quantities*. Simple models for non-Newtonian fluids, often used for blood flow simulations, express the viscosity as function of the shear stress rate, that is $\mu = \mu(\mathbf{D}(\mathbf{u}))$. The treatment of such cases is rather complex and will not be considered here, the interested reader may consult, for instance, [46, 12].

We now recall that, if P is a scalar and $\mathbf{\Sigma}$ a vector field, then

$$\mathbf{div}(P\mathbf{\Sigma}) = \boldsymbol{\nabla} P\mathbf{\Sigma} + P\,\mathbf{div}\,\mathbf{\Sigma},$$

and, therefore,

$$\mathbf{div}(P\mathbf{I}) = \boldsymbol{\nabla} P\mathbf{I} + P\,\mathbf{div}\,\mathbf{I} = \boldsymbol{\nabla} P.$$

The momentum equation may then be written as

$$\rho\frac{\partial \mathbf{u}}{\partial t} + \rho(\mathbf{u}\cdot\boldsymbol{\nabla})\mathbf{u} + \boldsymbol{\nabla} P - 2\,\mathbf{div}(\mu\mathbf{D}(\mathbf{u})) = \rho\mathbf{f}.$$

Since ρ is constant, it is sometimes convenient to introduce the kinematic viscosity $\nu = \mu/\rho$, with $[\nu]=1/sm^2$, and to write

$$\frac{\partial \mathbf{u}}{\partial t} + (\mathbf{u}\cdot\boldsymbol{\nabla})\mathbf{u} + \boldsymbol{\nabla} p - 2\,\mathbf{div}(\nu\mathbf{D}(\mathbf{u})) = \mathbf{f}, \tag{2.25}$$

where $p = P/\rho$ is a scaled pressure (with $[p]=m^2/s^2$).

Remark 2.4. Under the additional hypothesis that ν is constant, the momentum equation may be further elaborated by considering that

$$\mathbf{div}\,\boldsymbol{\nabla}\mathbf{u} = \Delta\mathbf{u},$$

$$\mathbf{div}\,\boldsymbol{\nabla}\mathbf{u}^T = \boldsymbol{\nabla}(\mathrm{div}\,\mathbf{u}) = (\text{by relation (2.13)}) \;= \mathbf{0}.$$

Consequently, the momentum equation for an incompressible Newtonian fluid with constant viscosity may be written in the alternative form

$$\frac{\partial \mathbf{u}}{\partial t} + (\mathbf{u}\cdot\boldsymbol{\nabla})\mathbf{u} + \boldsymbol{\nabla} p - \nu\Delta\mathbf{u} = \mathbf{f}. \tag{2.26}$$

However, for reasons that will appear clear later on (and that have to see with the way the fluid stresses act on the vessel structure) we prefer to use the Navier-Stokes equations in the form (2.25), even when considering a constant viscosity.

$\diamondsuit$

2.4. **The Navier-Stokes equations.** The set of differential equations formed by the continuity equation and the momentum equations in the form derived in the previous section provides the *Navier-Stokes equations* for incompressible fluids.

They are in particular valid on any fixed spatial domain Ω which is for all times of interest inside the portion of space filled by the fluid, i.e $\Omega \subset \Omega_t$. Indeed, in most cases, as with the flow around a car or an aeroplane, the flow motion is studied in a fixed domain Ω (usually called computational domain) embodying the region of interest. We will see in Sect. 5 that this is not possible anymore when considering the fluid-structure interaction problem arising when blood is flowing in a large artery.

Yet, before addressing this more complex situation, we will analyze the Navier Stokes equations in a fixed domains, that is, we will consider, for any $t \in I$, the system of equations

$$\begin{aligned} &\frac{\partial \mathbf{u}}{\partial t} + (\mathbf{u}\cdot\boldsymbol{\nabla})\mathbf{u} + \boldsymbol{\nabla} p - 2\,\mathbf{div}(\nu\mathbf{D}(\mathbf{u})) = \mathbf{f}, \quad \text{in } \Omega \\ &\mathrm{div}\,\mathbf{u} = 0, \quad \text{in } \Omega. \end{aligned} \tag{2.27}$$

Furthermore, we need to prescribe the initial status of the fluid velocity, for instance

$$\mathbf{u}(t = t_0, \mathbf{x}) = \mathbf{u}_0(\mathbf{x}) \qquad \mathbf{x} \in \Omega. \tag{2.28}$$

The principal unknowns are the velocity $\mathbf{u}$ and the "scaled" pressure $p = P/\rho$.

Let's take a practical case-study, namely the blood flow in an artery, for example the carotid (ref. Fig. 3), which we will here consider rigid. We proceed by identifying the area of interest, which may be the carotid sinus, and a domain Ω which will contain that area and which extends into the vessels up to a certain distance. For obvious practical reasons we will need to "truncate" the domain at certain sections. Inside such domain, the Navier-Stokes equations are valid, yet in order to solve them we need to provide appropriate boundary conditions.

2.4.1. *Boundary conditions for the Navier Stokes equations.* The Navier-Stokes equations must be supplemented by proper boundary conditions that allow the determination of the velocity field up to the boundary of the computational domain Ω. The more classical boundary conditions which are mathematically compatible with the Navier Stokes equations are

(1) *Applied stresses* (or *Neumann* boundary condition). We have already faced this condition when discussing the Cauchy principle. With the current definition for the Cauchy stresses it becomes

$$\mathbf{T} \cdot \mathbf{n} = -P\mathbf{n} + 2\mu\mathbf{D}(\mathbf{u}) \cdot \mathbf{n} = \mathbf{t}^e \quad \text{on } \Gamma^n \subset \partial\Omega, \tag{2.29}$$

where Γ^n is a measurable subset (possibly empty) of the whole boundary $\partial\Omega$.

(2) *Prescribed velocity* (or *Dirichlet* boundary condition). A given velocity field is imposed on Γ^d, a measurable subset of $\partial\Omega$ (which may be empty). This means that a vector field

$$\mathbf{g} : I \times \Gamma^d \to \mathbb{R}^3.$$

is prescribed and we impose that

$$\mathbf{u} = \mathbf{g} \qquad \text{on } \Gamma^d.$$

Since $\operatorname{div} \mathbf{u} = 0$ in Ω, it must be noted that if $\Gamma^d = \partial\Omega$ then at any time $\mathbf{g}$ must satisfy the following compatibility condition

$$\int_{\partial\Omega} \mathbf{g} \cdot \mathbf{n} = 0. \tag{2.30}$$

Clearly for a proper boundary condition specification we must have $\Gamma^n \cup \Gamma^d = \partial\Omega$.

The conditions to apply are normally driven by physical considerations. For instance, for a viscous fluid ($\mu > 0$) like the one we are here considering here, physical consideration lead to impose the homogeneous Dirichlet condition $\mathbf{u} = \mathbf{0}$ at a solid fixed boundary. When dealing with an "artificial boundary", that is a boundary which truncates the space occupied by the fluid (for computational reasons) the choice of appropriate conditions is often more delicate and should in any case guarantee the well-posedness of the resulting differential problem.

For example, for the flow field inside a 2D model for the carotid artery such the one shown in figure 11, we could impose Dirichlet boundary condition on Γ^{in}, by prescribing a velocity field $\mathbf{g}$.

On the "wall" boundary Γ^w, which is in this case assumed to be fixed, we will impose homogeneous Dirichlet conditions, that is $\mathbf{u} = \mathbf{0}$ on Γ^w. When we will consider the coupled problem between fluid and vessel wall, Γ^w will be moving, hence the homogeneous Dirichlet condition will be replaced by $\mathbf{u} = \mathbf{w}$, where $\mathbf{w}$ is the wall velocity.

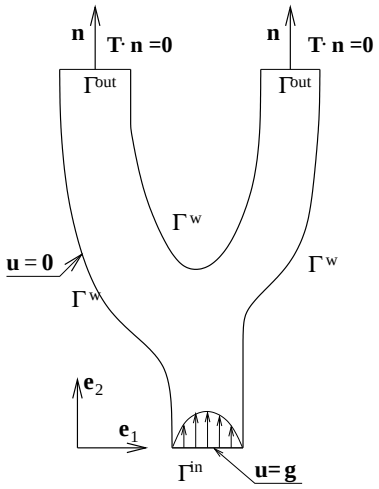

FIGURE 11. A possible boundary subdivision for the flow in a carotid bifurcation

At the exit Γ^{out}, we could, for instance, impose homogeneous Neumann conditions, i.e relation (2.29) with $\mathbf{t}^e = \mathbf{0}$. For the case illustrated in Fig. 11 and with that choice of coordinate basis, it becomes (derivation left as exercise)

$$\mu(\frac{\partial u_1}{\partial x_2} + \frac{\partial u_2}{\partial x_1}) = 0,$$
$$-P + 2\mu\frac{\partial u_2}{\partial x_2} = 0.$$

Remark 2.5. We anticipate the fact (without providing the proof) that this choice of boundary conditions, with the hypothesis that at Γ^{out} the velocity satisfies everywhere the condition $\mathbf{u} \cdot \mathbf{n} > 0$, is sufficient to guarantee that the solution of the Navier-Stokes problem exists and is continuously dependent from the data (initial solution, boundary conditions, forcing terms), provided that the initial data and forcing term are sufficiently small.

♢

Unfortunately, the homogeneous Neumann condition, which indeed would simulate a discharge into the open air, is rather unphysical for the case of a human vessel. As a matter of fact, it neglects completely the presence of the remaining part of the circulatory system. The difficulty in devising proper boundary condition for this specific problem was already mentioned in section 1 of these notes. The matter is still open and is the subject of active research. A possibility is provided by coupling the Navier-Stokes equations on the section of the arterial tree of interest with reduced models, like the one that will be presented in section 6, which are able to represent, though in a simplified way, the presence of the remaining part of the circulatory system. Techniques of this type has been used and analysed in [20, 15].

3. THE INCOMPRESSIBLE NAVIER-STOKES EQUATIONS AND THEIR APPROXIMATION

In this section we introduce the weak formulation of the Navier-Stokes equations for constant density (incompressible) fluids. Then, we address basic issues concerning the approximation of these equations in the context of the finite element method.

3.1. **Some functional spaces.** For the following discussion we need to introduce some Sobolev spaces for vector functions. We assume that the reader is already acquainted with the main definitions and results on Sobolev spaces in one dimension. A simple introduction is provided in [48]. For a deeper insight see, for instance, [4].

We will indicate with $\mathbf{L}^p(\Omega)$ $(1 \leq p \leq \infty)$ the space of vector functions $\mathbf{f} : \Omega \to \mathbb{R}^N$ (with $N = 2$ or 3) whose components belong to $L^p(\Omega)$. Its norm is

$$\|\mathbf{f}\|_{\mathbf{L}^p(\Omega)} = \left(\sum_{i=1}^{N} \|f_i\|^p_{L^p(\Omega)} \right)^{\frac{1}{p}}, 1 \leq p < \infty$$

and

$$\|\mathbf{f}\|_{\mathbf{L}^\infty(\Omega)} = \inf\{C \in \mathbb{R} | \quad |f_i| \leq C,\ i = 1, \cdots, N,\ \text{a.e. in } \Omega\},$$

where *a.e* stands for "almost everywhere". We will use the same notation for tensor fields, i.e. we will also indicate with $\mathbf{L}^p(\Omega)$ the space of tensor fields $\mathbf{T} : \Omega \to \mathbb{R}^{N \times N}$ whose components belongs to $L^p(\Omega)$. In this case

$$\|\mathbf{T}\|_{\mathbf{L}^p(\Omega)} = \left(\sum_{i=1}^{N} \sum_{j=1}^{N} \|T_{ij}\|^p_{L^p(\Omega)} \right)^{\frac{1}{p}}, 1 \leq p < \infty.$$

Analogously a vector (or a tensor) function $\mathbf{f}$ belongs to $\mathbf{H}^m(\Omega)$ if all its components belong to $H^m(\Omega)$, and we have

$$\|\mathbf{f}\|_{\mathbf{H}^m(\Omega)} = \left(\sum_{i=1}^{N} \|f_i\|^2_{H^m(\Omega)} \right)^{\frac{1}{2}},$$

while its semi-norm is

$$|\mathbf{f}|_{\mathbf{H}^m(\Omega)} = \left(\sum_{i=1}^{N} |f_i|^2_{H^m(\Omega)} \right)^{\frac{1}{2}}.$$

It is understood that, when $m = 0$,

$$\mathbf{H}^0(\Omega) \equiv \mathbf{L}^2(\Omega).$$

When equipped with the following scalar product

$$(\mathbf{f}, \mathbf{g})_{\mathbf{H}^m(\Omega)} = \sum_{i=1}^{N} (f_i, g_i)_{H^m(\Omega)}, \qquad \mathbf{f}, \mathbf{g} \in \mathbf{H}^m(\Omega),$$

the space $\mathbf{H}^m(\Omega)$ is a Hilbert space.

To ease notation, we will often use the following short-hand notation for the L^2 scalar products,

$$(\mathbf{v}, \mathbf{w}) \equiv (\mathbf{v}, \mathbf{w})_{\mathbf{L}^2(\Omega)}, \qquad (p, q) \equiv (p, q)_{L^2(\Omega)}.$$

We note that the L^2 scalar product of two tensor fields $\mathbf{T}$ and $\mathbf{G}$ belonging to $\mathbf{L}^2(\Omega)$ is defined as

$$(\mathbf{T}, \mathbf{G}) \equiv (\mathbf{T}, \mathbf{G})_{\mathbf{L}^2(\Omega)} = \int_\Omega \mathbf{T} : \mathbf{G} = \sum_{i=1}^{N} \sum_{j=1}^{N} \int_\Omega T_{ij} G_{ij}.$$

For our purposes we will usually have $m = 1$. In that case we have the equality

$$\|\mathbf{f}\|^2_{\mathbf{H}^1(\Omega)} = \|\mathbf{f}\|^2_{\mathbf{L}^2(\Omega)} + \|\boldsymbol{\nabla}\mathbf{f}\|^2_{\mathbf{L}^2(\Omega)}.$$

We often utilise the space $\mathbf{H}^1_0(\Omega)$ defined as

$$\mathbf{H}^1_0(\Omega) = \{\mathbf{v} \in \mathbf{H}^1(\Omega) | \quad \mathbf{v}|_{\partial\Omega} = 0\}.$$

We will consider *bounded* domains Ω with regular (i.e. *Lipschitz continuous*) boundary $\partial\Omega$, so that both the Sobolev embedding theorems in $\mathbb{R}^N$ and the *Green* integration formula hold. Some important results are here recalled, without providing the demonstration, which may be found in [34] or [4].

Theorem 3.1 (Sobolev embeddings (simplified form)). *Let Ω be a bounded domain of $\mathbb{R}^N$ with Lipschitz continuous boundary. The following properties hold*

$$\begin{cases} \text{If } 0 \le s < \frac{N}{2}, & \mathbf{H}^s(\Omega) \hookrightarrow \mathbf{L}^p(\Omega), \quad p = \frac{2N}{N-2s}, \\ \text{If } s = \frac{N}{2}, & \mathbf{H}^s(\Omega) \hookrightarrow \mathbf{L}^q(\Omega), \quad 2 \le q < \infty, \\ \text{If } s > \frac{N}{2}, & \mathbf{H}^s(\Omega) \hookrightarrow [C^0(\overline{\Omega})]^N, \end{cases}$$

where $A \hookrightarrow B$ means that A is included in B with continuous embedding.

Theorem 3.2 (Green integration formula). *Let Ω be a bounded domain of $\mathbb{R}^N$ with Lipschitz continuous boundary and let $\mathbf{n}$ denote the unit outer normal along $\partial\Omega$. Let $u, v \in H^1(\Omega)$, then the integral*

$$\int_{\partial\Omega} uv\, n_i$$

exists and is finite for each component n_i of $\mathbf{n}$. In addition we have

$$\int_\Omega \frac{\partial u}{\partial x_i} v = -\int_\Omega u \frac{\partial v}{\partial x_i} + \int_{\partial\Omega} uvn_i, \; i = 1, \ldots, N.$$

Lemma 3.1 (Poincaré inequality - multidimensional case). *Let $f : \mathbb{R}^N \to \mathbb{R}$ be a function of $\mathbf{H}^1(\Omega)$, with $f = 0$ on $\Gamma \subset \partial\Omega$ of strictly positive measure. Then, there exists a positive constant C_P, (depending only on the domain Ω and on Γ), such that*

$$\|f\|_{L_2(\Omega)} \le C_P \|\boldsymbol{\nabla} f\|_{\mathbf{L}_2(\Omega)}. \tag{3.1}$$

Lemma 3.2. *Let Ω be a bounded and connected subset of $\mathbb{R}^N$, where $N = 2$ or 3. Furthermore, let us assume that the velocity field $\mathbf{u} \in \mathbf{H}^1(\Omega)$ vanishes on $\Gamma \subset \partial\Omega$ of strictly positive measure. Then, there exists a constant $C_K > 0$ so that the following inequality holds,*

$$\int_\Omega \mathbf{D}(\mathbf{u}) : \mathbf{D}(\mathbf{u}) \ge C_K \|\boldsymbol{\nabla}\mathbf{u}\|^2_{\mathbf{L}^2(\Omega)}. \tag{3.2}$$

This theorem is a consequence of the *Korn inequality*, whose precise statement may be found for instance in [9, 14].

Lemma 3.3 (Gronwall Lemma). *Let f be a non-negative function which is integrable in $I = (t_0, t_1)$ and g and ϕ be two continuous functions in I, with g non-decreasing. If*

$$\phi(t) \le g(t) + \int_{t_0}^t f(\tau)\phi(\tau)d\tau \quad \forall t \in I, \tag{3.3}$$

then

$$\phi(t) \leq g(t) \exp \int_{t_0}^{t} f(\tau) d\tau \quad \forall t \in I. \tag{3.4}$$

3.2. **Weak form of Navier-Stokes equations.** The incompressible Navier-Stokes equations read

$$\frac{\partial \mathbf{u}}{\partial t} + (\mathbf{u} \cdot \boldsymbol{\nabla})\mathbf{u} + \boldsymbol{\nabla} p - 2\,\mathbf{div}(\nu \mathbf{D}(\mathbf{u})) = \mathbf{f}, \qquad \text{in } \Omega,\ t \in I, \tag{3.5a}$$

$$\operatorname{div} \mathbf{u} = 0, \qquad \text{in } \Omega,\ t \in I, \tag{3.5b}$$

$$\mathbf{u} = \mathbf{u}_0, \qquad \text{in } \Omega,\ t = t_0. \tag{3.5c}$$

We assume that ν is a bounded strictly positive function, precisely we assume that there exist two constants $\nu_0 > 0$ and $\nu_1 > 0$ such that $\forall t \in I$,

$$\nu_0 \leq \nu \leq \nu_1 \text{ almost everywhere in } \Omega.$$

We consider the case in which the system of differential equations (3.5) is equipped with the following boundary conditions.

$$\mathbf{u} = \mathbf{g} \qquad \text{on } \Gamma^d,\ t \in I, \tag{3.6a}$$

$$-p\mathbf{n} + 2\nu \mathbf{D}(\mathbf{u}) \cdot \mathbf{n} = \mathbf{h} \qquad \text{on } \Gamma^n,\ t \in I, \tag{3.6b}$$

We have indicated with Γ^d and Γ^n the portions of $\partial\Omega$ where Dirichlet and Neumann boundary conditions are applied, respectively. We must have $\Gamma^d \cup \Gamma^n = \partial\Omega$.

Remark 3.1. If $\Gamma^d = \partial\Omega$ we call the problem formed by (3.5) and (3.6) a *Dirichlet problem*. We will instead use the term *Neumann problem* when $\Gamma^n = \partial\Omega$. The conditions $\mathbf{g} = \mathbf{0}$ and $\mathbf{h} = \mathbf{0}$ are called *homogeneous boundary conditions*.

In the case of a Dirichlet problem, the boundary datum has to satisfy the following compatibility relation for all $t \in I$:

$$\int_{\partial\Omega} \mathbf{g} \cdot \mathbf{n} = 0.$$

$\diamondsuit$

Remark 3.2. For the problem at hand, we normally have $\mathbf{f} = \mathbf{0}$, since the only external force which one may eventually consider in blood flow is the gravity force. Even in this case, we may still adopt the Navier-Stokes equations with $\mathbf{f} = \mathbf{0}$ by replacing p with $p^*(t, \mathbf{x}) = p(t, \mathbf{x}) + gz(\mathbf{x})\mathbf{e}_z$, where g is the gravity acceleration, $\mathbf{e}_z$ the unit vector defining the vertical direction (upwardly oriented) and $z(\mathbf{x})$ the (known) quota of point $\mathbf{x}$ with respect to a reference horizontal plane. Yet, for the sake of completeness, many of the derivations of this as well as the following sections refer to the general case $\mathbf{f} \neq \mathbf{0}$.

$\diamondsuit$

The *weak form* of the Navier-Stokes equations is (formally) obtained by taking the scalar product of the momentum equations with a vector function $\mathbf{v}$ belonging to a functional space $\mathbf{V}$ (called *test function space*), which will be better specified later on, integrating over Ω and applying the Green integration formula. We operate similarly on the continuity equation, by multiplying it by a function $q \in Q$ and integrating. Also the space Q will be specified at a later stage.

We formally obtain

$$(\frac{\partial \mathbf{u}}{\partial t}, \mathbf{v}) + ((\mathbf{u}\cdot\boldsymbol{\nabla})\mathbf{u}, \mathbf{v}) + 2\int_\Omega \nu \mathbf{D}(\mathbf{u}) : \mathbf{D}(\mathbf{v}) - (p, \operatorname{div}\mathbf{v})$$

$$= (\mathbf{f}, \mathbf{v}) + \int_{\partial\Omega} \mathbf{v}\cdot(2\nu\mathbf{D}(\mathbf{u})\cdot\mathbf{n} - p\mathbf{n}),$$

$$(\operatorname{div}\mathbf{u}, q) = 0.$$

We have exploited the identity

$$\int_\Omega \nu\mathbf{D}(\mathbf{u}) : \boldsymbol{\nabla}\mathbf{v} = \int_\Omega \nu\mathbf{D}(\mathbf{u}) : \mathbf{D}(\mathbf{v}),$$

which derives from the symmetry of $\mathbf{D}(\mathbf{u})$.

The boundary term may now be split into two parts

$$\int_{\partial\Omega} \mathbf{v}\cdot(2\nu\mathbf{D}(\mathbf{u})\cdot\mathbf{n} - p\mathbf{n}) = \int_{\Gamma^d} \mathbf{v}\cdot(2\nu\mathbf{D}(\mathbf{u})\cdot\mathbf{n} - p\mathbf{n}) + \int_{\Gamma^n} \mathbf{v}\cdot\mathbf{h}$$

We note that the contribution from the Neumann boundary is now a *given data*, while contribution from the Dirichlet boundary can be eliminated by appropriately choosing the test space $\mathbf{V}$.

By inspection, we may recognise that all terms make sense if we choose as test function spaces

$$\mathbf{V} = \{\mathbf{v}\in\mathbf{H}^1(\Omega), \quad \mathbf{v}|_{\Gamma^d} = \mathbf{0}\},$$
$$Q = \{q\in L^2(\Omega), \quad \text{with } \int_\Omega q = 0 \quad \text{if } \Gamma^d = \partial\Omega\},$$

and if we seek, at each time t, the velocity in

$$\mathbf{V}_\mathbf{g} = \{\mathbf{u}\in\mathbf{H}^1(\Omega), \quad \mathbf{u}|_{\Gamma^d} = \mathbf{g}\}$$

and the pressure in Q.

Remark 3.3. The request that Q is formed by functions with zero mean on Ω when we treat a Dirichlet problem derives from the fact that in such a case the pressure is determined only up to a constant, as it appears in the equations only through its gradient. To compute a unique value for the pressure it is then necessary to fix the constant. This is obtained by the zero-mean constraint.

♢

Finally, the *weak form* of the Navier-Stokes problem (3.5) and (3.6), reads:

Find, $\forall t\in I$, $\mathbf{u}(t)\in\mathbf{V}_\mathbf{g}$ *and* $p(t)\in Q$ *such that*

$$\text{(3.7)}\quad \begin{cases} (\frac{\partial\mathbf{u}}{\partial t}, \mathbf{v}) + a(\mathbf{u},\mathbf{v}) + c(\mathbf{u},\mathbf{u},\mathbf{v}) + b(\mathbf{v},p) = (\mathbf{f},\mathbf{v}) + \int_{\Gamma^n}\mathbf{v}\cdot\mathbf{h}, \quad \forall\mathbf{v}\in\mathbf{V}, \\ b(\mathbf{u},q) = 0, \quad \forall q\in Q, \end{cases}$$

where

$$\text{(3.8)}\qquad a(\mathbf{u},\mathbf{v}) = 2\int_\Omega \nu\mathbf{D}(\mathbf{u}) : \mathbf{D}(\mathbf{v}),$$

$$\text{(3.9)}\qquad c(\mathbf{w},\mathbf{u},\mathbf{v}) = \int_\Omega (\mathbf{w}\cdot\boldsymbol{\nabla})\mathbf{u}\cdot\mathbf{v},$$

$$\text{(3.10)}\qquad b(\mathbf{v},p) = -\int_\Omega p\operatorname{div}\mathbf{v}.$$

3.2.1. *The homogeneous Dirichlet problem.* In this section we will focus on the homogeneous Dirichlet problem, that is the case when $\Gamma^d = \partial\Omega$ and $\mathbf{g} = \mathbf{0}$ in (3.6a). Therefore,

$$\mathbf{V} = \mathbf{H}_0^1(\Omega), \qquad Q = L_0^2(\Omega) = \{q \in L^2(\Omega), \quad \int_\Omega q = 0\} \tag{3.11}$$

and the weak form reads:

Find, $\forall t \in I$, $\mathbf{u}(t) \in \mathbf{V}$ *and* $p(t) \in Q$ *such that*

$$\begin{cases} (\dfrac{\partial \mathbf{u}}{\partial t}, \mathbf{v}) + a(\mathbf{u}, \mathbf{v}) + c(\mathbf{u}, \mathbf{u}, \mathbf{v}) + b(\mathbf{v}, p) = (\mathbf{f}, \mathbf{v}), \quad \forall \mathbf{v} \in \mathbf{V}, \\ \\ b(\mathbf{u}, q) = 0, \quad \forall q \in Q. \end{cases} \tag{3.12}$$

Lemma 3.4. *The forms* $a : \mathbf{V} \times \mathbf{V} \to \mathbb{R}$, $c : \mathbf{V} \times \mathbf{V} \times \mathbf{V} \to \mathbb{R}$ *and* $b : \mathbf{V} \times Q \to \mathbb{R}$ *are continuous with respect to their arguments. In addition,* $a(\cdot, \cdot)$ *is coercive, i.e.* $\exists \alpha > 0$ *such that*

$$a(\mathbf{v}, \mathbf{v}) \geq \alpha \|\mathbf{v}\|^2_{\mathbf{H}^1(\Omega)}, \quad C > 0, \forall \mathbf{v} \in \mathbf{V}.$$

Proof. The continuity the bilinear forms a and b is an immediate consequence of the Cauchy-Schwarz inequality. Indeed, $\forall \mathbf{u}, \mathbf{v} \in V$ and $\forall q \in Q$

$$\begin{aligned} |a(\mathbf{u}, \mathbf{v})| \leq & \nu_1 |\mathbf{u}|_{\mathbf{H}^1(\Omega)} |\mathbf{v}|_{\mathbf{H}^1(\Omega)} \leq \nu_1 \|\mathbf{u}\|_{\mathbf{H}^1(\Omega)} \|\mathbf{v}\|_{\mathbf{H}^1(\Omega)}, \\ |b(\mathbf{u}, p)| \leq & \| \operatorname{div} \mathbf{u}\|_{L^2(\Omega)} \|p\|_{L^2(\Omega)} \leq \|\mathbf{u}\|_{\mathbf{H}^1(\Omega)} \|p\|_{L^2(\Omega)} \end{aligned}$$

For the tri-linear form c we first have to note that thanks to the Sobolev embedding theorem $\mathbf{H}^1(\Omega) \hookrightarrow \mathbf{L}^6(\Omega)$ (as $N = 2, 3$) and consequently $\mathbf{H}^1(\Omega) \hookrightarrow \mathbf{L}^4(\Omega)$. Then, $\mathbf{wu} \in \mathbf{L}^2(\Omega)$, and considering the expression of $c(\cdot, \cdot, \cdot)$ component-wise, we have

$$\int_\Omega w_i \frac{\partial u_k}{\partial x_i} v_k \leq \|w_i v_k\|_{L^2(\Omega)} \| \frac{\partial u_k}{\partial x_i} \|_{L^2(\Omega)} \leq \|w_i\|_{L^4(\Omega)} \|v_k\|_{L^4(\Omega)} \| \frac{\partial u_k}{\partial x_i} \|_{L^2(\Omega)}.$$

Then

$$\begin{aligned} \int_\Omega w_i \frac{\partial u_k}{\partial x_i} v_k \leq & C \|w_i\|_{H^1(\Omega)} \| \frac{\partial u_k}{\partial x_i} \|_{L^2(\Omega)} \|v_k\|_{H^1(\Omega)} \leq \\ & C \|w_i\|_{H^1(\Omega)} |u_k|_{H^1(\Omega)} \|v_k\|_{H^1(\Omega)} \leq C \|w_i\|_{H^1(\Omega)} \|u_k\|_{H^1(\Omega)} \|v_k\|_{H^1(\Omega)}, \end{aligned} \tag{3.13}$$

where C is a positive constant.

It follows that, $\forall \mathbf{u}, \mathbf{v}, \mathbf{v} \in \mathbf{V}$

$$c(\mathbf{w}, \mathbf{u}, \mathbf{v}) \leq C_1 \|\mathbf{w}\|_{\mathbf{H}^1(\Omega)} \|\mathbf{u}\|_{\mathbf{H}^1(\Omega)} \|\mathbf{v}\|_{\mathbf{H}^1(\Omega)},$$

by which the continuity of the tri-linear form is proved (C_1 is a positive constant).

The coercivity of the linear form a derives from inequalities (3.1) and (3.2), since

$$a(\mathbf{v}, \mathbf{v}) \geq 2\nu_0 \int_\Omega \mathbf{D}(\mathbf{v}) : \mathbf{D}(\mathbf{v}) \geq 2\nu_0 C_K |\mathbf{v}|^2_{\mathbf{H}^1(\Omega)} \geq \alpha \|\mathbf{v}\|^2_{\mathbf{H}^1(\Omega)}, \forall \mathbf{v} \in \mathbf{V}, \tag{3.14}$$

with $\alpha = \frac{2\nu_0 C_K}{C_P^2 + 1}$, being C_P and C_K the constants in (3.1) and (3.2), respectively. □

We now introduce the space

$$\mathbf{V}_{\text{div}} = \{\mathbf{f} \in V | \quad \operatorname{div} \mathbf{f} = 0 \text{ a.e. in } \Omega\}.$$

Theorem 3.3. *If* $\mathbf{u}$ *is a solution of the weak formulation (3.12), then it satisfies*

$$(\frac{\partial \mathbf{u}}{\partial t}, \mathbf{v}) + a(\mathbf{u}, \mathbf{v}) + c(\mathbf{u}, \mathbf{u}, \mathbf{v}) = (\mathbf{f}, \mathbf{v}), \quad \forall \mathbf{v} \in \mathbf{V}_{\text{div}},\ t \in I. \tag{3.15}$$

Conversely, if, $\forall t \in I$, $\mathbf{u}(t) \in \mathbf{V}_{\text{div}}$ *is a solution of (3.15) and* $\dfrac{\partial \mathbf{u}}{\partial t} \in \mathbf{L}^2(\Omega)$, *then there exists a unique* $p \in Q$ *such that* $(\mathbf{u}, p)$ *satisfies (3.12).*

Proof. The first part of the proof is trivial. If $\mathbf{u}$ satisfies (3.12) then it belongs to $\mathbf{V}_{\text{div}}$ and it satisfies (3.15), since $\mathbf{V}_{\text{div}} \subset \mathbf{V}$.

The demonstration of the inverse implication requires first to state the following result.

Lemma 3.5. *Let* Ω *be a domain of* $\mathbb{R}^N$ *and let* $L \in \mathbf{V}'$. *Then* $L(\mathbf{v}) = 0\ \forall \mathbf{v} \in \mathbf{V}_{\text{div}}$ *if and only if there exists a function* $p \in L^2(\Omega)$ *such that*

$$L(\mathbf{v}) = (p, \operatorname{div} \mathbf{v}),\ \forall \mathbf{v} \in \mathbf{V}.$$

For the proof see Lemma 2.1 of [24].

The application L defined as

$$L(\mathbf{v}) = (\frac{\partial \mathbf{u}}{\partial t}, \mathbf{v}) + a(\mathbf{u}, \mathbf{v}) + c(\mathbf{u}, \mathbf{u}, \mathbf{v}) - (\mathbf{f}, \mathbf{v}) \quad \forall \mathbf{v} \in \mathbf{V}$$

belongs to $\mathbf{V}'$, being a linear continuous functional on $\mathbf{V}$. We can therefore apply lemma (3.5) and obtain the desired result. □

3.3. **An energy inequality for the Navier-Stokes equations.** We now prove an energy inequality for problem (3.12), by which we may assess a continuous dependence of the solution from the given data.

Theorem 3.4 (Energy inequalities). *Let* $\mathbf{u}(t) \in \mathbf{V}_{\text{div}}$ *be a solution of (3.12),* $\forall t \in I$. *Then the following inequalities hold*

$$\|\mathbf{u}(t)\|^2_{\mathbf{L}^2(\Omega)} + C_1 \int_0^t \|\boldsymbol{\nabla}\mathbf{u}(\tau)\|^2_{\mathbf{L}^2(\Omega)} d\tau \leq \left(\|\mathbf{u}_0\|^2_{\mathbf{L}^2(\Omega)} + \int_0^t \|\mathbf{f}(\tau)\|^2_{\mathbf{L}^2(\Omega)} d\tau \right) e^t,$$

where $C_1 = 4\nu_0 C_K$, *and*

$$\|\mathbf{u}(t)\|^2_{\mathbf{L}^2(\Omega)} + C_2 \int_0^t \|\boldsymbol{\nabla}\mathbf{u}\|^2_{\mathbf{L}^2(\Omega)}(\tau) d\tau \leq \|\mathbf{u}_0\|^2_{\mathbf{L}^2(\Omega)} + \frac{C_P}{C_2} \int_0^t , \|\mathbf{f}(\tau)\|^2_{\mathbf{L}^2(\Omega)} d\tau,$$

where $C_2 = 2\nu_0 C_K$. *Here,* C_K *and* C_P *are the constants in the Poincaré inequality (3.1 and in (3.2), respectively.*

We first prove the following result

Lemma 3.6. *If* $\mathbf{u}$ *is a solution of (3.12) then* $c(\mathbf{u}, \mathbf{u}, \mathbf{u}) = 0$.

Proof. It follows from the Green formula and the fact that $\mathbf{u}|_{\partial\Omega} = \mathbf{0}$. Indeed,

$$c(\mathbf{u}, \mathbf{u}, \mathbf{u}) = \int_\Omega (\mathbf{u} \cdot \boldsymbol{\nabla})\mathbf{u} \cdot \mathbf{u} = \int_\Omega \frac{1}{2} \boldsymbol{\nabla} \left(|\mathbf{u}|^2 \right) \cdot \mathbf{u} = -\frac{1}{2} \int_\Omega |\mathbf{u}|^2 \operatorname{div} \mathbf{u} + \frac{1}{2} \int_{\partial\Omega} |\mathbf{u}|^2 \mathbf{u} \cdot \mathbf{n}.$$

Now, the last integral is zero since $\mathbf{u} = 0$ on $\partial\Omega$. Moreover, for the same reason

$$\int_\Omega \operatorname{div} \mathbf{u} = \int_{\partial\Omega} \mathbf{u} \cdot \mathbf{n} = 0.$$

Then, if we set

$$c = \int_\Omega |\mathbf{u}|^2,$$

we have

$$\int_\Omega |\mathbf{u}|^2 \operatorname{div} \mathbf{u} = \int_\Omega |\mathbf{u}|^2 \operatorname{div} \mathbf{u} - c \int_\Omega \operatorname{div} \mathbf{u} = \int_\Omega (|\mathbf{u}|^2 - c) \operatorname{div} \mathbf{u} = b(\mathbf{u}, (|\mathbf{u}|^2 - c)) = 0,$$

where the last equality is obtained since $(|\mathbf{u}|^2 - c) \in Q$ and $b(\mathbf{u}, q) = 0$, $\forall q \in Q$. □

We now give the demonstration of theorem 3.4.

Proof. For all fixed t, take $\mathbf{v} = \mathbf{u}(t)$ in the momentum equation of (3.15). We have

$$\frac{1}{2}\frac{d}{dt}\|\mathbf{u}\|^2_{\mathbf{L}^2(\Omega)} + c(\mathbf{u},\mathbf{u},\mathbf{u}) + b(\mathbf{u},p) + a(\mathbf{u},\mathbf{u}) = (\mathbf{f},\mathbf{u}). \tag{3.16}$$

Then,

$$\frac{1}{2}\frac{d}{dt}\|\mathbf{u}\|^2_{\mathbf{L}^2(\Omega)} + a(\mathbf{u},\mathbf{u}) = (\mathbf{f},\mathbf{u}).$$

Now, thanks to (3.2)

$$a(\mathbf{u},\mathbf{u}) = 2\int_\Omega \nu \mathbf{D}(\mathbf{u}) : \mathbf{D}\mathbf{u} \geq 2\nu_0 C_K \|\boldsymbol{\nabla}\mathbf{u}\|^2_{\mathbf{L}^2(\Omega)},$$

then

$$\frac{d}{dt}\|\mathbf{u}\|^2_{\mathbf{L}^2(\Omega)} + 4\nu_0 C_K \|\boldsymbol{\nabla}\mathbf{u}\|^2_{\mathbf{L}^2(\Omega)} \leq 2(\mathbf{f},\mathbf{u}) \leq \frac{1}{2\epsilon}\|\mathbf{f}\|^2_{\mathbf{L}^2(\Omega)} + 2\epsilon\|\mathbf{u}\|^2_{\mathbf{L}^2(\Omega)}, \tag{3.17}$$

for any $\epsilon > 0$. The first inequality is obtained by choosing $\epsilon = \frac{1}{2}$. By integrating between t_0 and t we have

$$\|\mathbf{u}(t)\|^2_{\mathbf{L}^2(\Omega)} + 4\nu_0 C_K \int_{t_0}^t \|\boldsymbol{\nabla}\mathbf{u}(\tau)\|^2_{\mathbf{L}^2(\Omega)} d\tau \leq$$
$$\int_{t_0}^t \|\mathbf{f}(\tau)\|^2_{\mathbf{L}^2(\Omega)} d\tau + \int_{t_0}^t \|\mathbf{u}(\tau)\|^2_{\mathbf{L}^2(\Omega)} d\tau + \|\mathbf{u}_0\|^2_{\mathbf{L}^2(\Omega)}.$$

We apply Gronwall lemma (Lemma 3.3) by identifying

$$\|\mathbf{u}(t)\|^2_{\mathbf{L}^2(\Omega)} + 4\nu_0 C_K \int_{t_0}^t \|\boldsymbol{\nabla}\mathbf{u}(\tau)\|^2_{\mathbf{L}^2(\Omega)} d\tau$$

with $\phi(t)$, obtaining the first result. By using instead the Poincaré inequality on the last term of (3.17), and by taking $\epsilon = \frac{\nu_0 C_K}{C_P^2}$, we obtain

$$\frac{d}{dt}\|\mathbf{u}\|^2_{\mathbf{L}^2(\Omega)} + 2\nu_0 C_K \|\boldsymbol{\nabla}\mathbf{u}\|^2_{\mathbf{L}^2(\Omega)} \leq \frac{C_P^2}{2\nu_0 C_K}\|\mathbf{f}\|^2_{\mathbf{L}^2(\Omega)}.$$

By integrating between t_0 and t we obtain the second inequality of the theorem. □

Remark 3.4. In the case where $\mathbf{f} = \mathbf{0}$ we may derive the simpler estimate

$$\|\mathbf{u}(t)\|^2_{\mathbf{L}^2(\Omega)} + 4\nu_0 C_K \int_0^t \|\boldsymbol{\nabla}\mathbf{u}(\tau)\|^2_{\mathbf{L}^2(\Omega)} d\tau \leq \|\mathbf{u}_0\|^2_{\mathbf{L}^2(\Omega)}, \forall t \geq t_0$$

♢

3.4. **The Stokes equations.** The space discretisation of the Navier-Stokes equations give rise to a *non-linear* set of ordinary differential equations because of the presence of the convective term. This makes both the analysis and the numerical solution more difficult. In some cases, when the fluid is highly viscous, the contribution of the non-linear convective term may be neglected. The key parameter which allow us to make that decision is the *Reynolds number* Re, which is an a-dimensional number defined as

$$Re = \frac{|\mathbf{u}|L}{\nu},$$

where L represents a length-scale for the problem at hand and $|\mathbf{u}|$ the Euclidean norm of the velocity. For the flow in a tube L is the tube diameter.

Contrary to other fluid dynamic situations, the high variation in time and space of the velocity in the vascular system does not allow to select a single representative

value of the Reynolds number, [2] nevertheless in the situations where $Re << 1$ (for instance, flow in smaller arteries or capillaries) we may say that the convective term is negligible compared to the viscous contribution and may be discarded. We have then the *Stokes* equations, which read (in the case of homogeneous Dirichlet conditions)

$$\frac{\partial \mathbf{u}}{\partial t} + \nabla p - 2\,\mathbf{div}(\nu \mathbf{D}(\mathbf{u})) = \mathbf{f}, \qquad \text{in } \Omega,\ t \in I, \tag{3.18a}$$

$$\operatorname{div} \mathbf{u} = 0, \qquad \text{in } \Omega,\ t \in I, \tag{3.18b}$$

$$\mathbf{u} = \mathbf{0} \qquad \text{on } \partial\Omega,\ t \in I, \tag{3.18c}$$

$$\mathbf{u} = \mathbf{u}_0, \qquad \text{in } \Omega,\ t = t_0. \tag{3.18d}$$

The corresponding weak form reads

Find, $\forall t \in I$, $\mathbf{u}(t) \in \mathbf{V}$, $p(t) \in Q$, *such that*

$$\begin{aligned} &(\frac{\partial \mathbf{u}}{\partial t}, \mathbf{v}) + a(\mathbf{u}, \mathbf{v}) + b(\mathbf{v}, p) = (\mathbf{f}, \mathbf{v}), \quad \forall \mathbf{v} \in \mathbf{V}, \\ &b(\mathbf{u}, q) = 0, \quad \forall q \in Q. \end{aligned} \tag{3.19}$$

In the case of a *steady problem*, that is when we consider $\dfrac{\partial \mathbf{u}}{\partial t} = \mathbf{0}$, the solution $(\mathbf{u}, p)$ of the Stokes problem (3.19) is a saddle point for the functional

$$\mathcal{S}(\mathbf{v}, q) = \frac{1}{2} a(\mathbf{v}, \mathbf{v}) + b(\mathbf{v}, q) - (\mathbf{f}, \mathbf{v}), \quad \mathbf{v} \in \mathbf{V},\ q \in Q.$$

This means

$$\mathcal{S}(\mathbf{u}, p) = \min_{\mathbf{v} \in \mathbf{V}} \max_{q \in Q} \mathcal{S}(\mathbf{v}, q).$$

In this respect, the pressure p may be considered as a *Lagrange multiplier* associated to the incompressibility constraint.

Remark 3.5. In those cases when instead $Re >> 1$ (*high Reynolds number flows*) the flow becomes *unstable*. High frequency fluctuations in the velocity and pressure field appear, which might give rise to *turbulence*. This phenomenon is particularly complex and its numerical simulation may be extremely difficult. To make the problem amenable to numerical solution it is often necessary to adopt a *turbulence model*, which allows to give a more or less accurate description of the effect of turbulence on the main flow variables.

In normal physiological situations, the typical values of the Reynolds number reached in the cardiovascular system do not allow the formation of full scale turbulence. Some flow instabilities may occur only at the exit of the aortic valve and limited to the systolic phase. Indeed, in this region the Reynolds number may reach the value of few thousands only for the portion of the cardiac cycle corresponding the the peak systolic velocity. Therefore, there is no sufficient time for a full turbulent flow to develop.

The situation is different in some pathological circumstances, e.g in the presence of a stenotic artery. The increase of the velocity at the location of the vessel restriction may induce turbulence to develop. This fact could explain the high increase in the noise produced caused by the blood stream in this situation.

♢

[2] Another a-dimensional number which measures the relative importance of inertia versus viscous in oscillatory flow is the Womersley number [21]

3.5. **Numerical approximation of Navier-Stokes equations.** In this section we give a very short account on possible numerical methods for the solution of the Navier-Stokes equations. This subject is far from being simple, and we will not make any attempt to be exhaustive. The interested reader can consult, for instance, chapters 9,10 and 13 of A. Quarteroni, A. Valli [43] and the classic books on the subject by V. Girault and P.A. Raviart [24] and R. Temam [55].

Here, we will simply mention a few methods to advance the Navier-Stokes equations from a given time-level to a new one and we will point out some of the mathematical problems that have to be faced. For the sake of simplicity we will confine ourselves to the homogeneous Dirichlet problem (3.12).

3.5.1. *Time advancing by finite differences.* The Navier-Stokes problem (2.27) (equivalently, its weak form 3.12)) can be advanced in time by suitable finite difference schemes.

The simulation will cover the $I = (0,T)$ which we subdivide into sub-intervals (time-steps) $I^k = (t^k, t^{k+1})$ with $k = 0, \cdots, N$ and where $t^{k+1} - t^k = \Delta t$ is constant. We have thus partitioned the space-time domain $I \times \Omega$ into several *time-slabs* $I^k \times \Omega$. We assume that on each slab we know the solution at $t = t^k$ and that we wish to find the solution at $t = t^{k+1}$. Clearly, for the first time slab the assumption is true since at $t = 0$ the approximate solution is obtained from the initial data. If we treat the time slabs in their natural order as soon as the solution on the k-th time slab has been found, it is made available as initial condition for the computation on the next time slab. This is a *time-advancing* procedure.

We will indicate by $(\mathbf{u}^k, p^k)$ the approximate solution at time t^k, that is

$$(\mathbf{u}^k, p^k) \approx (\mathbf{u}(t^k), p(t^k)).$$

A family of simple time-advancing schemes is obtained by using the Taylor expansion formula to write

$$\frac{\partial \mathbf{u}}{\partial t}(t^{k+1}) = \frac{\mathbf{u}(t^{k+1}) - \mathbf{u}(t^k)}{\Delta t} + O(\Delta t).$$

Then, by making the first order approximation

$$\frac{\partial \mathbf{u}}{\partial t}(t^{k+1}) \approx \frac{\mathbf{u}^{k+1} - \mathbf{u}^k}{\Delta t},$$

into (2.27) we may write the following time-stepping scheme to calculate $\mathbf{u}^{k+1}$ and p^{k+1}:

$$\frac{\mathbf{u}^{k+1} - \mathbf{u}^k}{\Delta t} - 2\,\mathbf{div}\,\nu\mathbf{D}(\mathbf{u}^{k+1}) + (\mathbf{u}^* \cdot \boldsymbol{\nabla})\mathbf{u}^{**} + \boldsymbol{\nabla} p^{k+1} = \mathbf{f}^{k+1}, \quad \text{in } \Omega, \tag{3.20a}$$

$$\operatorname{div} \mathbf{u}^{k+1} = 0, \quad \text{in } \Omega, \tag{3.20b}$$

$$\mathbf{u}^{k+1} = \mathbf{0} \qquad \text{on } \partial\Omega. \tag{3.20c}$$

Here, $\mathbf{f}^{k+1}$ stands for $\mathbf{f}(t^{k+1})$.

The value of $\mathbf{u}^*$ and $\mathbf{u}^{**}$ in the non-linear convective term may be taken, for instance, as follows

$$(\mathbf{u}^* \cdot \boldsymbol{\nabla})\mathbf{u}^{**} = \begin{cases} (\mathbf{u}^k \cdot \boldsymbol{\nabla})\mathbf{u}^k, & \text{fully explicit treatment,} \\ (\mathbf{u}^k \cdot \boldsymbol{\nabla})\mathbf{u}^{k+1}, & \text{semi-implicit treatment,} \\ (\mathbf{u}^{k+1} \cdot \boldsymbol{\nabla})\mathbf{u}^{k+1}, & \text{fully implicit treatment.} \end{cases}$$

In the case of the fully implicit treatment, equations (3.20) give rise to a non-linear system. The semi-implicit and fully explicit treatments, instead, perform a *linearisation* of the convective term, thus eliminating the non-linearity.

Let us consider the scheme resulting from the *fully explicit treatment* of the convective term. Problem (3.20) is then rewritten as

(3.21a)
$$\frac{1}{\Delta t}\mathbf{u}^{k+1} - 2\,\mathbf{div}(\nu\mathbf{D}(\mathbf{u}^{k+1})) + \boldsymbol{\nabla} p^{k+1} = \mathbf{f}^{k+1} + \frac{1}{\Delta t}\mathbf{u}^{k} - (\mathbf{u}^{k}\cdot\boldsymbol{\nabla})\mathbf{u}^{k} \quad \text{in } \Omega,$$

(3.21b)
$$\operatorname{div}\mathbf{u}^{k+1} = 0 \quad \text{in } \Omega,$$

(3.21c)
$$\mathbf{u}^{k+1} = \mathbf{0} \qquad \text{on } \partial\Omega.$$

We will now denote $\mathbf{u}^{k+1}$ and p^{k+1} by $\mathbf{w}$ and π, respectively, and by $\mathbf{q}$ and a_0 the quantities

(3.22)
$$\mathbf{q} = \mathbf{f}^{k+1} + \frac{1}{\Delta t}\mathbf{u}^{k} - (\mathbf{u}^{k}\cdot\boldsymbol{\nabla})\mathbf{u}^{k}, \quad a_0 = \frac{1}{\Delta t}.$$

Problem (3.21) may be written in the form

(3.23a)
$$a_0\mathbf{w} - 2\,\mathbf{div}(\nu\mathbf{D}(\mathbf{w})) + \boldsymbol{\nabla}\pi = \mathbf{q}, \quad \text{in } \Omega,$$

(3.23b)
$$\operatorname{div}\mathbf{w} = 0, \quad \text{in } \Omega,$$

(3.23c)
$$\mathbf{w} = \mathbf{0} \qquad \text{on } \partial\Omega,$$

which is called the *generalised Stokes problem.*

For its approximation, a Galerkin finite element procedure can be set up by considering two finite element spaces $\mathbf{V}_h$ for the velocity and Q_h for the pressure, and seeking $\mathbf{w}_h \in \mathbf{V}_h$ and $\pi_h \in Q_h$ such that

(3.24)
$$\begin{cases} \tilde{a}(\mathbf{w}_h, \mathbf{v}_h) + b(\mathbf{w}_h, \pi_h) = (\mathbf{q}, \mathbf{v}_h), \quad \forall \mathbf{v}_h \in \mathbf{V}_h, \\ \\ b(\mathbf{w}_h, q_h) = 0, \quad \forall q_h \in Q_h, \end{cases}$$

where $\tilde{a}(\mathbf{w}, \mathbf{v}) = a_0(\mathbf{w}, \mathbf{v}) + a(\mathbf{w}, \mathbf{v})$.

The algebraic form of problem (3.24) is derived by denoting with

$$\{\boldsymbol{\varphi}_i, \quad i = 1, \ldots, N_{\mathbf{V}_h}\}, \quad \{\psi_i, \quad i = 1, \ldots, N_{Q_h}\}$$

the bases of $\mathbf{V}_h$ and Q_h, respectively. Here $N_{\mathbf{V}_h} = \dim(\mathbf{V}_h)$ and $N_{Q_h} = \dim(Q_h)$. Then, by setting

(3.25)
$$\mathbf{w}_h(\mathbf{x}) = \sum_{i=1}^{N_{\mathbf{V}_h}} w_i\boldsymbol{\varphi}_i(\mathbf{x}), \quad p_h(\mathbf{x}) = \sum_{i=1}^{N_{Q_h}} \pi_i\psi_i(\mathbf{x})$$

we obtain the following system from (3.24):

(3.26)
$$\begin{pmatrix} C & D^T \\ D & 0 \end{pmatrix}\begin{pmatrix} \mathbf{W} \\ \boldsymbol{\Pi} \end{pmatrix} = \begin{pmatrix} \mathbf{F_s} \\ \mathbf{0} \end{pmatrix}.$$

where $\mathbf{W}$, $\boldsymbol{\Pi}$ and $\mathbf{F_s}$ denote three vectors defined respectively as

$$(\mathbf{W})_i = w_i, \qquad (\boldsymbol{\Pi})_i = \pi_i, \qquad (\mathbf{F_s})_i = (\mathbf{q}, \boldsymbol{\varphi}_i),$$

while C, K and D are matrices whose components are defined as

$$(C)_{ij} = \tilde{a}(\boldsymbol{\varphi}_j, \boldsymbol{\varphi}_i), \quad (D)_{ij} = b(\boldsymbol{\varphi}_j, \psi_i).$$

The global matrix

(3.27)
$$A = \begin{pmatrix} C & D^T \\ D & 0 \end{pmatrix}$$

is a square matrix with dimension $(N_{\mathbf{V}_h} + N_{Q_h}) \times (N_{\mathbf{V}_h} + N_{Q_h})$.

In the case of a finite element approximation, p_i represents the pressure at the i-th mesh node. The interpretation of w_i is made more complex by the fact that the velocity is a vector function, while w_i is a scalar. Let us assume that we are

considering a three dimensional problem and let the basis for $\mathbf{V}_h$ be chosen by grouping the vector functions $\boldsymbol{\varphi}_i$ into 3 families, as follows:

$$\boldsymbol{\varphi}_i^1 = \begin{bmatrix} \varphi_i \\ 0 \\ 0 \end{bmatrix}, \quad \boldsymbol{\varphi}_i^2 = \begin{bmatrix} 0 \\ \varphi_i \\ 0 \end{bmatrix}, \quad \boldsymbol{\varphi}_i^3 = \begin{bmatrix} 0 \\ 0 \\ \varphi_i \end{bmatrix}.$$

Finally, let $M_{\mathbf{V}_h} = \frac{N_{\mathbf{V}_h}}{3}$. Then, we may rewrite the first expansion in (3.25) as

$$\mathbf{w}_h(\mathbf{x}) = \sum_{i=1}^{M_{\mathbf{V}_h}} \sum_{j=1}^{3} w_i^j \boldsymbol{\varphi}_i^j(\mathbf{x}),$$

where w_i^j here represents the j-th component of $\mathbf{w}$ at the i-th mesh node.

Lemma 3.7. *If* $\ker D^T = \mathbf{0}$*, then matrix* A *is non-singular.*

Proof. We first prove the non-singularity of C. For any $\mathbf{W} \in \mathbb{R}^{N_{\mathbf{V}_h}}$, $\mathbf{W} \neq \mathbf{0}$

$$\mathbf{W}^T C \mathbf{W} = \sum_{i=1}^{N_{\mathbf{V}_h}} \sum_{j=1}^{N_{\mathbf{V}_h}} w_i w_j C_{ij} = \tilde{a}(\mathbf{w}, \mathbf{w}) > 0,$$

where $\mathbf{w} = \sum_{i=1}^{N_{\mathbf{V}_h}} w_i \boldsymbol{\varphi}_i$. Consequently, C is positive-definite, and thus non-singular. From (3.26) we have

$$\mathbf{W} = C^{-1} \left(\mathbf{F_s} - D^T \boldsymbol{\Pi} \right), \quad D\mathbf{W} = \mathbf{0}.$$

Then we may formally compute the discrete pressure terms by

$$- \left(D C^{-1} D^T \right) \boldsymbol{\Pi} = - D C^{-1} \mathbf{F_s}.$$

Proving that A is non-singular thus reduces to show that the matrix

$$S = D C^{-1} D^T$$

is non singular. If we take any $\mathbf{q} \in \mathbb{R}^{N_{Q_h}}$ with $|\mathbf{q}| \neq 0$ we have by hypothesis that $D^T \mathbf{q} \neq 0$. Then

$$\mathbf{q}^T S \mathbf{q} = (D^T \mathbf{q})^T C^{-1} D^T \mathbf{q} \neq 0,$$

since C^{-1} is symmetric positive definite. Thus matrix S (which is clearly symmetric) has all eigenvalues different from zero and, consequently, is non-singular. This concludes the proof. □

The scheme we have presented, with an explicit treatment of just the convective term, is only one of the many possible ways of producing a time discretisation of the Navier-Stokes equations. Another choice is to resort to a fully implicit scheme.

3.5.2. *Fully implicit schemes.* By employing in (3.20) a full implicit treatment of the convective part we would obtain a non-linear system of the following type

$$\begin{pmatrix} E(\mathbf{W}) & D^T \\ D & 0 \end{pmatrix} \begin{pmatrix} \mathbf{W} \\ \boldsymbol{\Pi} \end{pmatrix} = \begin{pmatrix} \mathbf{F_s} \\ \mathbf{0} \end{pmatrix}, \tag{3.28}$$

where now the matrix E is a function of the unknown velocity,

$$(E(\mathbf{W}))_{ij} = \widetilde{a}(\boldsymbol{\varphi}_i, \boldsymbol{\varphi}_j) + c(\mathbf{u}^{k+1}, \boldsymbol{\varphi}_j, \boldsymbol{\varphi}_i) = C_{ij} + \sum_{m=1}^{N_{\mathbf{V}_h}} c(\boldsymbol{\varphi}_m, \boldsymbol{\varphi}_j, \boldsymbol{\varphi}_i) W_m.$$

A possible way to solve it is to resort to *Newton's method*:

Given $\begin{pmatrix}\mathbf{W}^0\\ \mathbf{\Pi}^0\end{pmatrix}$, solve for $\quad l=0,\cdots$

$$\begin{pmatrix}\dfrac{\partial E}{\partial \mathbf{W}}(\mathbf{W}^l)\cdot\mathbf{W}^l+E(\mathbf{W}^l) & D^T\\ D & 0\end{pmatrix}\begin{pmatrix}\mathbf{W}^{l+1}-\mathbf{W}^l\\ \mathbf{\Pi}^{l+1}-\mathbf{\Pi}^l\end{pmatrix} = \begin{pmatrix}\mathbf{F_s}\\ \mathbf{0}\end{pmatrix}-\begin{pmatrix}E(\mathbf{W}^l) & D^T\\ D & 0\end{pmatrix}\begin{pmatrix}\mathbf{W}^l\\ \mathbf{\Pi}^l\end{pmatrix}, \tag{3.29}$$

until a suitable convergence criterion is met.

The solution of a non-linear system is now reduced to a series of solutions of linear systems. Going back to the Navier-Stokes equations, we may note that a full implicit scheme would require to solve *at each time step* a series of linear systems of form (3.29), that resembles the Stokes problem. The resulting numerical scheme is thus in general very *computationally intensive*.

3.6. **Projection methods.** We now follow another route for the solution of the incompressible Navier-Stokes equations which does not lead to a Stokes problem but to a series of simpler systems of partial differential equations. We start from the Navier-Stokes equations already discretised in time and we will consider again a single time step, that is

$$\frac{\mathbf{u}^{k+1}-\mathbf{u}^k}{\Delta t}+(\mathbf{u}^k\cdot\boldsymbol{\nabla})\mathbf{u}^{k+1}-2\,\mathbf{div}(\nu\mathbf{D}(\mathbf{u}^{k+1}))+\boldsymbol{\nabla}p^{k+1}=\mathbf{f}^{k+1},\quad \text{in } \Omega, \tag{3.30}$$

plus (3.20b) and (3.20c). Here, for the sake of simplicity (and without any loss of generality) we have chosen a semi-implicit treatment of convective term. We wish now to split the system in order to consider the effects of the velocity and the pressure terms separately. We define an intermediate velocity $\tilde{\mathbf{u}}$, obtained by solving the momentum equation where the pressure contribution has been dropped, precisely

$$\frac{\tilde{\mathbf{u}}-\mathbf{u}^k}{\Delta t}+(\mathbf{u}^k\cdot\boldsymbol{\nabla})\tilde{\mathbf{u}}-2\,\mathbf{div}(\nu\mathbf{D}(\tilde{\mathbf{u}}))=\mathbf{f}^{k+1},\quad \text{in } \Omega, \tag{3.31a}$$

$$\tilde{\mathbf{u}}=\mathbf{0}\qquad \text{on } \partial\Omega. \tag{3.31b}$$

We may recognise that (3.31a) is now a problem on the velocity only, which could be re-interpreted as the time discretisation of a parabolic differential equation of the following type

$$\frac{\partial\tilde{\mathbf{u}}}{\partial t}+(\mathbf{w}\cdot\boldsymbol{\nabla})\tilde{\mathbf{u}}-2\,\mathbf{div}(\nu\mathbf{D}(\tilde{\mathbf{u}}))=\mathbf{f},$$

with $\mathbf{w}$ a given vector field. We cannot at this stage impose the incompressibility condition because we would obtain an over-constrained system.

We then consider the contribution given by the pressure term and the incompressibility constraint, that is

$$\frac{\mathbf{u}^{k+1}-\tilde{\mathbf{u}}}{\Delta t}+\boldsymbol{\nabla}p^{k+1}=\mathbf{0},\quad \text{in } \Omega, \tag{3.32a}$$

$$\operatorname{div}\mathbf{u}^{k+1}=0,\quad \text{in } \Omega. \tag{3.32b}$$

System (3.32) depends on both the velocity and pressure, yet we may derive an *equation only for the pressure* by taking (formally) the divergence of (3.32a) and exploiting the incompressibility constraint (3.32b). That is,

$$0=\operatorname{div}\left(\frac{\mathbf{u}^{k+1}-\tilde{\mathbf{u}}}{\Delta t}+\boldsymbol{\nabla}p^{k+1}\right)=-\frac{1}{\Delta t}\operatorname{div}\tilde{\mathbf{u}}+\operatorname{div}\boldsymbol{\nabla}p^{k+1}=-\frac{1}{\Delta t}\operatorname{div}\tilde{\mathbf{u}}+\Delta p^{k+1},$$

by which we obtain a *Poisson equation* for the pressure in the form

$$\Delta p^{k+1} = \frac{1}{\Delta t} \operatorname{div} \tilde{\mathbf{u}}, \quad \text{in } \Omega. \tag{3.33}$$

Equation (3.33) must be supplemented by boundary conditions, which are *not directly available from the original problem* (3.30). For that, we need to resort to the following theorem, also known as *Ladhyzhenskaja theorem.*

Theorem 3.5 (Helmholtz Decomposition Principle)**.** *Let Ω be a domain of $\mathbb{R}^N$ with smooth boundary. Any vector function $\mathbf{v} \in \mathbf{L}^2(\Omega)$ (with $N = 2, 3$) can be uniquely represented as $\mathbf{v} = \mathbf{w} + \boldsymbol{\nabla}\psi$ with $\mathbf{w} \in \mathbf{H}_{div}(\Omega)$, where*

$$\mathbf{H}_{div}(\Omega) = \{\mathbf{w} \mid \ \mathbf{w} \in \mathbf{L}^2(\Omega), \operatorname{div} \mathbf{w} = 0, \ a.e \ \ \mathbf{w} \cdot \mathbf{n} = 0 \quad on \ \partial\Omega\},$$

and $\psi \in H^1(\Omega)$.

The proof is rather technical and is here omitted. An outline, valid for the case $\mathbf{v} \in \mathbf{H}^1(\Omega)$, is given in [8]. A more general demonstration is found in Theorem 1.5 of [55].

If we now consider the expression

$$\tilde{\mathbf{u}} = \mathbf{u}^{k+1} + \boldsymbol{\nabla}(\Delta t p^{k+1}), \tag{3.34}$$

derived from (3.32a), we may identify $\tilde{\mathbf{u}}$ with $\mathbf{v}$ and $(\Delta t p^{k+1})$ with ψ in the Helmholtz decomposition principle. Then, the natural space for $\mathbf{u}^{k+1}$ is $\mathbf{H}_{div}(\Omega)$, by which we should impose

$$\mathbf{u}^{k+1} \cdot \mathbf{n} = 0, \quad \text{on } \partial\Omega. \tag{3.35}$$

Unfortunately, (3.35) is still a condition on the velocity, while we are looking for a boundary condition for the pressure. The latter is found by considering the normal component of (3.34) on the boundary,

$$\tilde{\mathbf{u}} \cdot \mathbf{n} = \mathbf{u}^{k+1} \cdot \mathbf{n} + \Delta t \boldsymbol{\nabla} p^{k+1} \cdot \mathbf{n}, \quad \text{on } \partial\Omega,$$

and noting that on $\partial\Omega$ we have $\tilde{\mathbf{u}} \cdot \mathbf{n} = 0$, because of (3.31b), and $\mathbf{u}^{k+1} \cdot \mathbf{n} = 0$. Then,

$$\boldsymbol{\nabla} p^{k+1} \cdot \mathbf{n} = \frac{\partial p^{k+1}}{\partial n} = 0, \quad \text{on } \partial\Omega,$$

which is a *homogeneous Neumann boundary condition* for the Poisson problem (3.33).

The *projection method* here presented for the solution of the Navier-Stokes equations consists then in solving at each time-step a sequence of simpler problems, listed in the following.

(1) *Advection-diffusion problem for the velocity* $\tilde{\mathbf{u}}$. Solve problem (3.31a)-(3.31b).

(2) *Poisson problem for the pressure*

$$\Delta p^{k+1} = \frac{1}{\Delta t} \operatorname{div} \tilde{\mathbf{u}}, \quad \text{in } \Omega, \tag{3.36a}$$

$$\frac{\partial}{\partial n} p^{k+1} = 0, \quad \text{on } \partial\Omega. \tag{3.36b}$$

(3) *Computation of* $\mathbf{u}^{k+1}$ (this is an explicit step)

$$\mathbf{u}^{k+1} = \tilde{\mathbf{u}} - \Delta t \boldsymbol{\nabla} p^{k+1}. \tag{3.37}$$

3.7. **Algebraic Factorisation Methods.** An alternative way of reducing the computational cost of the solution of the full Navier-Stokes problem is to operate at algebraic level. We will consider the generalised Stokes problem in its algebraic form (3.26). This is the typical system that arises at each time step of a time advancing scheme for the solution of the Navier-Stokes by a finite element method, when the convective term is treated explicitly. In this case, the matrix C has the form

$$C = \frac{M}{\Delta t} + K + B,$$

where M is the mass matrix, K the stiffness matrix and B the matrix arising from the explicit treatment of the convective term.

The matrix D derives from the discretisation of the divergence term, while D^T represents a discrete gradient operator. We may formally solve for $\mathbf{W}$

$$\mathbf{W} = C^{-1}(\mathbf{F_s} - D^T\mathbf{\Pi}), \tag{3.38}$$

and by substituting into (3.26) we have

$$DC^{-1}D^T\mathbf{\Pi} = DC^{-1}\mathbf{F_s}. \tag{3.39}$$

The matrix $DC^{-1}D^T$ is called *Stokes pressure matrix* and is somehow akin to a discrete Laplace operator. Having obtained $\mathbf{\Pi}$ from (3.39), we can then compute the velocity by solving (3.38).

However, the inversion of C is in general prohibitive in terms of memory and computational cost (indeed C is sparse, but C^{-1} is usually not).

A way to simplify the computation can be found by recognising that steps (3.39) and (3.38) may be derived from the following LU factorisation of the global matrix A

$$A = \begin{pmatrix} C & D^T \\ D & 0 \end{pmatrix} = \begin{pmatrix} C & 0 \\ D & -DC^{-1}D^T \end{pmatrix} \begin{pmatrix} I_{\mathbf{W}} & C^{-1}D^T \\ D & I_{\mathbf{\Pi}} \end{pmatrix} = LU, \tag{3.40}$$

where $I_{\mathbf{W}}$ and $I_{\mathbf{\Pi}}$ indicate the identity matrices of dimension equal to the number of velocity and pressure degrees of freedom, respectively. We then consider the LU solution

$$\begin{cases} C\widetilde{\mathbf{W}} = \mathbf{F_s} \\ D\widetilde{\mathbf{W}} - DC^{-1}D^T\widetilde{\mathbf{\Pi}} = 0 \end{cases} \qquad \begin{cases} \mathbf{W} + C^{-1}D^T\mathbf{\Pi} = \widetilde{\mathbf{W}} \\ \mathbf{\Pi} = \widetilde{\mathbf{\Pi}} \end{cases}$$

where $\widetilde{\mathbf{W}}$ and $\widetilde{\mathbf{\Pi}}$ are intermediate velocities and pressures.

The scheme may be written in the following alternative form,

$$\textit{Intermediate velocity} \quad C\widetilde{\mathbf{W}} = \mathbf{F_s}, \tag{3.41a}$$

$$\textit{Pressure computation} \quad -DC^{-1}D^T\mathbf{\Pi} = -D\widetilde{\mathbf{W}}, \tag{3.41b}$$

$$\textit{Velocity update} \quad \mathbf{W} = \widetilde{\mathbf{W}} - C^{-1}D^T\mathbf{\Pi}. \tag{3.41c}$$

The key to reduce complexity is to replace C by a matrix simpler to invert, which, however, is "similar" to C, in a sense that we will make precise. This technique is called *inexact factorisation*. In practise we replace A in (3.40) by an approximation A^* obtained by replacing in the LU factorisation the matrix C^{-1} by convenient approximations, which we indicate by H_1 and H_2, that is

$$A^* = L^*U^* = \begin{pmatrix} C & 0 \\ D & -DH_1D^T \end{pmatrix} \begin{pmatrix} I_{\mathbf{W}} & H_2D^T \\ D & I_{\mathbf{\Pi}} \end{pmatrix} = \begin{pmatrix} C & CH_2D^T \\ D & D(H_2 - H_1)D^T \end{pmatrix}. \tag{3.42}$$

If we choose $H_2 = H_1$ the discrete continuity equation is unaltered, that means that the approximated system still guarantees *mass conservation* at discrete level. If $H_2 = C^{-1}$, the discrete momentum equations are unaltered, and the resulting

scheme satisfies the discrete conservation of momentum. In particular, we can consider the two special cases

$$H_1 = H_2 = H \quad \Rightarrow \quad A^* = \begin{pmatrix} C & CHD^T \\ D & 0 \end{pmatrix}$$

$$H_1 = C^{-1} \neq H_2 \quad \Rightarrow \quad A^* = \begin{pmatrix} C & D^T \\ D & Q \end{pmatrix}, \quad Q = D(H_1 - C^{-1})D^T.$$

3.7.1. *The algebraic Chorin-Temam Scheme.* We note that

$$C = \frac{M}{\Delta t} + K + B = \frac{1}{\Delta t}(M + \Delta t(K + B)) = \frac{1}{\Delta t} M(I_{\mathbf{W}} + \Delta t M^{-1}(K + B)).$$

We recall the well known Neumann expansion formula [35]

$$(I + \epsilon A)^{-1} = \sum_{j=0}^{\infty} (-1)^j (\epsilon A)^j,$$

which converges for any matrix A and any positive number ϵ small enough so that the spectral radius of ϵA is strictly less than one. We can apply this formula to C^{-1} to get

$$C^{-1} = \Delta t M (I_{\mathbf{W}} + \Delta t M^{-1}(K + B))^{-1} M^{-1} = \tag{3.43}$$

$$\Delta t \sum_{j=0}^{\infty} (-1)^j \left[\Delta t M^{-1}(K + B)\right]^j M^{-1} = \Delta t (I_{\mathbf{W}} - \Delta t M^{-1} S + \cdots) M^{-1},$$

where we have put $S = K + B$.

A way to find a suitable approximation is to replace C^{-1} with just some terms of the series. The simplest choice considers just a first order approximation, which corresponds to put into (3.42)

$$H_1 = H_2 = H = \Delta t M^{-1}. \tag{3.44}$$

Consequently,

$$A^* = A_{CT} = \begin{pmatrix} C & \Delta t C M^{-1} D^T \\ D & 0 \end{pmatrix} = \begin{pmatrix} C & D^T + \Delta t S M^{-1} D^T \\ D & 0 \end{pmatrix}. \tag{3.45}$$

The scheme obtained by applying the corresponding LU decomposition reads

$$\textit{Intermediate velocity} \quad C\widetilde{\mathbf{W}} = \mathbf{F_s}, \tag{3.46a}$$

$$\textit{Pressure computation} \quad -\Delta t D M^{-1} D^T \mathbf{\Pi} = -D\widetilde{\mathbf{W}}, \tag{3.46b}$$

$$\textit{Velocity update} \quad \mathbf{W} = \widetilde{\mathbf{W}} - \Delta t M^{-1} D^T \mathbf{\Pi}. \tag{3.46c}$$

This algorithm is known as *algebraic Chorin-Temam scheme.* Comparing with the standard projection method, we may note that the algebraic scheme replaces in the pressure computation step (3.46b) the Laplace operator of the Poisson problem (3.36) with a "discrete Laplacian" $DM^{-1}D^T$, which incorporates the boundary condition of the original problem. No additional boundary condition is required for the pressure, contrary to the standard (differential type) scheme.

Remark 3.6. The finite element mass matrix M is a sparse matrix with the same structure of C. Therefore it may seem that there is little gain in the computational efficiency with respect to the original factorisation (3.41). However, the matrix M may be approximated by a diagonal matrix called *lumped mass matrix* [43], whose inversion is now trivial.

$\Diamond$

Remark 3.7. It is possible to write the algebraic Chorin-Temam scheme in incremental form, as it has been done for its differential counterpart.

$\diamondsuit$

3.7.2. *The Yosida scheme.* If we make the special choice

$$H_1 = \Delta t M^{-1}, \qquad H_2 = C^{-1} \tag{3.47}$$

we have

$$A^* = A_Y = \begin{pmatrix} C & D^T \\ D & Q \end{pmatrix} \quad \text{with } Q = -D(\Delta t M^{-1} - C^{-1})D^T. \tag{3.48}$$

The corresponding scheme reads

$$\text{Intermediate velocity} \quad C\widetilde{\mathbf{W}} = \mathbf{F_s}, \tag{3.49a}$$

$$\text{Pressure computation} \quad -\Delta t D M^{-1} D^T \mathbf{\Pi} = -D\widetilde{\mathbf{W}}, \tag{3.49b}$$

$$\text{Velocity update} \quad \mathbf{W} = \widetilde{\mathbf{W}} - \Delta t C^{-1} D^T \mathbf{\Pi}. \tag{3.49c}$$

The last step (3.49c) is more expensive than its counterpart (3.46c) in the Chorin-Temam scheme, since now we need to invert the full matrix C. An analysis of this method is found in [40].

Remark 3.8. If we consider the Stokes problem we have $C = (\Delta t)^{-1} M + K$ and consequently the matrix $Q = -D(\Delta t M^{-1} - C^{-1})D^T$ in (3.48) may be written as

$$Q = -\Delta t D \left[I_{\mathbf{W}} - (I_{\mathbf{W}} + \Delta t K)^{-1} \right] D^T = -(\Delta t)^2 D Y D^T,$$

where

$$Y = \frac{1}{\Delta t} \left[I_{\mathbf{W}} - (I_{\mathbf{W}} + \Delta t K)^{-1} \right],$$

may be regarded as the *Yosida* regularisation of K, which is the discretisation of the Laplace operator. That is Q may be interpreted as the discretisation of the differential operator

$$(\Delta t)^2 \operatorname{div}(\mathcal{Y}_{\Delta t} \boldsymbol{\nabla}),$$

where $\mathcal{Y}_{\Delta t}$ is the Yosida operator [4].

$\diamondsuit$

Remark 3.9. An incremental form may be found as follows. If $\mathbf{\Pi}^n$ represents the known value of the pressure degrees of freedom from the previous time step, we have

$$\text{Intermediate velocity} \quad C\widetilde{\mathbf{W}} = \mathbf{F_s} - D^T \mathbf{\Pi}^n,$$

$$\text{Pressure increment} \quad -\Delta t D M^{-1} D^T (\mathbf{\Pi} - \mathbf{\Pi}^n) = -D\widetilde{\mathbf{W}},$$

$$\text{Velocity update} \quad \mathbf{W} = \widetilde{\mathbf{W}} - \Delta t C^{-1} D^T (\mathbf{\Pi} - \mathbf{\Pi}^n).$$

$\diamondsuit$

More details on algebraic fractional step methods may be found in [37] and [41].

4. MATHEMATICAL MODELLING OF VESSEL WALLS

The vascular wall has a very complex nature and devising an accurate model for its mechanical behaviour is rather difficult. Its structure is indeed formed by many layers with different mechanical characteristics[22, 30](see Fig. 12). Moreover, experimental results obtained by specimens are only partially significant. Indeed, the vascular wall is a living tissue with the presence of muscular cells which contribute to its mechanical behaviour. It may then be expected that the dead tissue used in the laboratory will have different mechanical characteristics than the living one. Moreover, the arterial mechanics depend also on the type of the surrounding tissues, an aspect almost impossible to reproduce in a laboratory. We are then facing

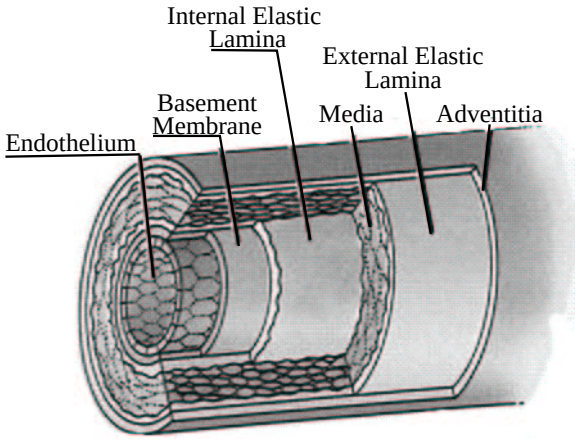

FIGURE 12. The vessel wall is formed by many layers made of tissues with different mechanical characteristics. Image taken from "Life: the Science of Biology" by W.K. Purves et al., fourth edition, published by Sinauer Associates Inc. and W.H. Freeman and Company.

a problem whose complexity is enormous. It is the role of mathematical modelling to find reasonable simplifying assumptions by which major physical characteristics remain present, yet the problem becomes amenable to numerical analysis and computational solution.

The set up of a general mathematical model of the mechanics of a solid continuum may follow the same general route that we have indicated for fluid mechanics. In particular, it is possible to identify again a Cauchy stress tensor $\mathbf{T}$. The major difference between solids and fluids is in the constitutive relation which links $\mathbf{T}$ to kinematics quantities. We have seen in section 2 that for a fluid such a kinematic quantity is the velocity gradient or, more precisely, the strain rate $\mathbf{D}$. For a solid, the Cauchy stress tensor is instead a function of the *deformation gradient*, which we have already defined in (2.7). That is, the *constitutive law* for a solid may be written as

$$\mathbf{T} = \mathbf{T}(\mathbf{F}_t).$$

If we assume that both the deformation gradient and the displacements are small, under the hypothesis of *linear elasticity* and homogeneous material it is possible to derive relatively simple relations for $\mathbf{T}$. For sake of space, we will not pursue that matter here. The interested reader may consult, for instance, Chapter 4 of the book by L.A. Segel [49], or, for a more extensive treatment, the book by P.G. Ciarlet [9].

Another possible situation is the one that involves a constitutive law of the form

$$\mathbf{T} = \mathbf{T}(\mathbf{D}, \mathbf{F}_t), \tag{4.1}$$

which describes the mechanical behaviour of a material with characteristics intermediate to those of a liquid and a solid. In such case, the continuum is said to be *viscoelastic*. An example of such behaviour is given by certain plastics or by liquid suspensions. In particular, also blood exhibits a viscoelastic nature, particularly when flowing in small vessels, e.g. in arterioles and capillaries. Indeed, in that case the presence of suspended particles and their interaction during the motion strongly affect the blood mechanical behaviour. Again, we will not cover this topic here. The book by Y.C. Fung [22] may be used by the reader interested on the peculiar aspects of the mechanics of living tissues.

The geometry of a section of an artery where no branching is present may be described by using a curvilinear cylindrical coordinate system (r, θ, z) with the corresponding base unit vectors $\mathbf{e}_r$, $\mathbf{e}_\theta$, and $\mathbf{e}_z$, where $\mathbf{e}_z$ is aligned with the axis of the artery, as shown in Fig. 13.

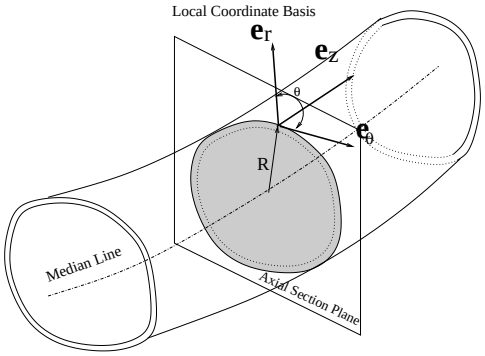

FIGURE 13. A model of a "realistic" section of an artery with the principal geometrical parameters.

Clearly, the vessel structure may be studied using full three dimensional models, which may also account for its multilayer nature. However, it is common practise to resort to simplified 2D or even 1D mechanical models in order to reduce the overall computational complexity when the final aim is to study the coupled fluid-structure problem. In Fig. 14 we sketch some of the approximations normally made. A 2D model may be obtained by either resorting to a shell-type description or considering longitudinal sections (θ =const.) of the vessels. In the first case we exploit the fact that the effective wall thickness is relatively small to reduce the whole structure to a surface. A rigorous mathematical derivation (for the linear case) may be found in [10]. In the second case we neglect the variations of the stresses in the circumferential direction. In this way we are able to eliminate all terms containing derivatives with respect to θ in the equations and we may consider each plane θ = const. independently. The resulting displacement field will depend only parametrically on θ. If, in addition, we assume that the problem has an axial symmetry (which implies the further assumption of a straight axis) the dependence on θ is completely neglected. In this case, also the fluid would be described by a 2D axi-symmetric model.

The simplest models, called 1D models, are derived by making the same assumption on the wall thickness made for the shell model, yet starting from a 2D model. The structure will then be represented by a line on a generic longitudinal section, as shown in the last picture of Fig. 14.

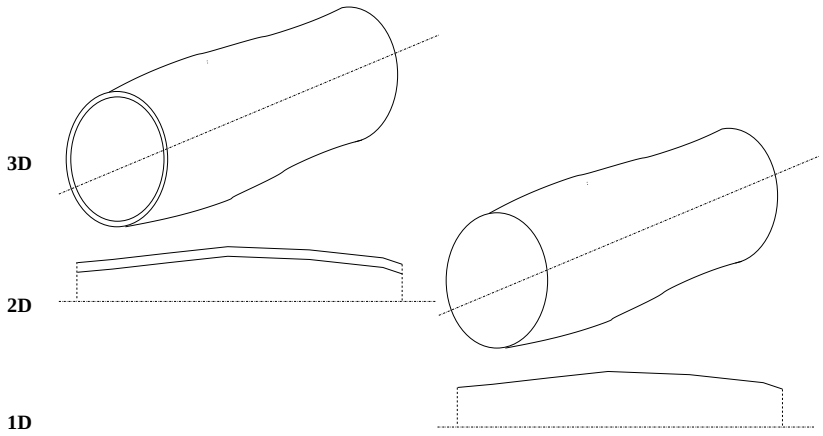

FIGURE 14. Different models for arterial wall mechanics

Even with all these simplifying assumptions an accurate model of the vessel wall mechanics is rather complex. Therefore, in these notes we will only present the simplest models, whose derivation is now detailed.

4.1. **Derivation of 1D models of vessel wall mechanics.** We are going to introduce a hierarchy of 1D models for the vessel structure, of variable complexity. We first present the assumptions common to all models.

The relatively small thickness of the vessel wall allow us to use as basis model a shell model, where the vessel wall geometry is fully described by its median surface, see Fig. 15

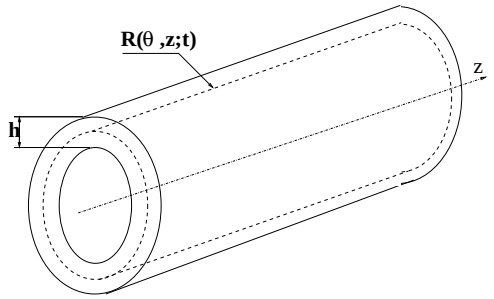

FIGURE 15. A cylindrical model of the vessel geometry. The latter is approximated, at any time t, by a surface $r = R(\theta, z; t)$, which is outlined with dashed lines in figure.

We take as *reference configuration* Γ_0^w the one assumed by the vessel at rest when filled with fluid with zero velocity and whose pressure is equal to the pressure P_{ext} exerted by the tissues external to the vessel. Although in principle P_{ext} can change along the vessel (for instance because of the effect of gravity), for the sake of simplicity (and without any loss of generality) we will consider only the case where P_{ext} is constant.

The cylindrical-like aspect of sections of the arterial system allows us to derive simplified mathematical models for the movement of the arterial wall assuming a straight cylindrical geometry. We thus assume that the reference configuration Γ_0^w be a cylindrical surface with radius R_0 (a regular strictly positive function of z),

i.e.

$$\Gamma_0^w = \{(r,\theta,z) : r = R_0(z),\ \theta \in [0,2\pi),\ z \in [0,L]\},$$

where L indicates the length of the arterial element under consideration. In our cylindrical coordinate system (r,θ,z), the z coordinate is aligned along the vessel axes and a plane $z = \overline{z}\,(=\text{constant})$ defines an *axial section.*

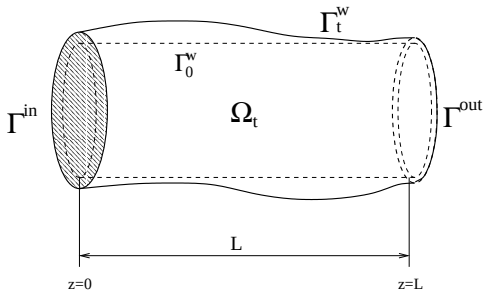

FIGURE 16. The reference configuration Γ_0^w used for the derivation of our models is that of a circular cylinder. Γ_t^w indicates the current configuration at a given time t, while Ω_t is the domain occupied by the fluid.

We assume that the displacement vector $\boldsymbol{\eta}$ has only a radial component, that is

$$\boldsymbol{\eta} = \eta \mathbf{e}_r = (R - R_0)\mathbf{e}_r, \tag{4.2}$$

where $R = R(\theta,z;t)$ is the function that provides, at each t, the radial coordinate $r = R(\theta,z;t)$ of the wall surface. The *current configuration* Γ_t^w at time t of the vessel surface is then given by

$$\Gamma_t^w = \{(r,\theta,z) : r = R(\theta,z;t),\ \theta \in [0,2\pi),\ z \in [0,L]\}.$$

As a consequence, the length of the vessel does not change with time. We will indicate with $\mathbf{n}$ the outwardly oriented unit normal to the surface Γ_t^w at a given point. In Fig. 16 we sketch the reference and current configuration for the model of the section of an artery.

Another important assumption is that of *plain stresses.* We neglect the stress components along the normal direction $\mathbf{n}$, i.e. we assume that the stresses lie on the vessel surface.

We itemise here the main assumptions:

- A1 *Small thickness and plain stresses.* The vessel wall thickness h is sufficiently small to allow a shell-type representation of the vessel geometry. In addition, we will also suppose that it is constant in the reference configuration. The vessel structure is subjected to plain stresses.
- A2 *Cylindrical reference geometry and radial displacements.* The reference vessel configuration is described by a circular cylindrical surface with straight axes.[3] The displacements are only in the radial direction.
- A3 *Small deformation gradients.* We assume that the deformation gradients are small, so that the structure basically behaves like a linear elastic solid and $\frac{\partial R}{\partial \theta}$ and $\frac{\partial R}{\partial z}$ remain uniformly bounded during motion.
- A4 *Incompressibility.* The vessel wall tissue is incompressible, i.e. it maintains its volume during the motion. This is a reasonable assumption since biological tissues are ideed nearly incompressible.

[3]This assumption may be partially dispensed with, by assuming that the reference configuration is "close" to that of a circular cylinder. The model here derived may be supposed valid also in that situation.

The models that we are going to illustrate could be derived from the general laws of solid mechanics. Yet, this is not the route we will follow, preferring to describe them in a more direct way, while trying to give some insight on the physical meaning of the various terms that we are about to introduce.

4.1.1. *Forces acting on the vessel wall.* Let us consider the vessel configuration at a given time t and a generic point on the vessel surface of coordinates $\theta = \overline{\theta}$, $z = \overline{z}$ and $r = R(\overline{\theta}, \overline{z}; t)$, with $\overline{z} \in (0, L)$ and $\theta \in (0, 2\pi)$. In the following derivation, if not otherwise indicated, all quantities are computed at location $(R(\overline{\theta}, \overline{z}; t), \overline{\theta}, \overline{z})$ and at time t.

We will indicate with $d\sigma$ the measure of the following elemental surface

$$d\mathcal{S} = \{(r, \theta, z) : r = R(\theta, z; t),\ \theta \in [\overline{\theta} - \frac{d\theta}{2}, \overline{\theta} + \frac{d\theta}{2}],\ z \in [\overline{z} - \frac{dz}{2}, \overline{z} + \frac{dz}{2}]\}.$$

In figure 17 we have also indicated the two main stresses, the circumferential stress and the longitudinal stress $\boldsymbol{\sigma}_\theta$ and $\boldsymbol{\sigma}_z$, which represent the internal forces acting on the portion under consideration.

We may derive the following expression for $\mathbf{n}$ and $d\sigma$:

$$\mathbf{n} = (R_0 g)^{-1} \left(R\mathbf{e}_r - \frac{\partial R}{\partial \theta}\mathbf{e}_\theta - R\frac{\partial R}{\partial z}\mathbf{e}_z \right), \tag{4.3}$$

$$d\sigma = gR_0 d\theta dz = g d\sigma_0, \tag{4.4}$$

where

$$g = \frac{R}{R_0}\sqrt{1 + \left(\frac{1}{R}\frac{\partial R}{\partial \theta}\right)^2 + \left(\frac{\partial R}{\partial z}\right)^2},$$

and $\sigma_0 = R_0 d\theta dz$ is the measure of the image of $d\mathcal{S}$ in the reference configuration Γ_0^w. In particular we have

$$\mathbf{n} \cdot \mathbf{e}_r = \frac{R}{R_0} g^{-1} \tag{4.5}$$

and

$$\mathbf{n} \cdot \mathbf{e}_r d\sigma = R d\theta dz. \tag{4.6}$$

The linear dimension of the elemental surface $d\mathcal{S}$ along the longitudinal direction has been indicated with dl. I can be easily verified that

$$dl = \sqrt{1 + \left(\frac{\partial R}{\partial z}\right)^2} dz. \tag{4.7}$$

Let us now consider the external forces acting through the elemental surface $d\mathcal{S}$.

- **Forces from the surrounding tissues.** As the tissue surrounding the vessel interacts with the vessel wall structure by exerting a constant pressure P_{ext}, the resulting force acting on $d\mathcal{S}$ is simply given by

$$\mathbf{f}_{\text{tissue}} = -P_{ext}\mathbf{n} d\sigma + o(d\sigma). \tag{4.8}$$

- **Forces from the fluid**. The forces the fluid exerts on the vessel wall are represented by the Cauchy stresses on the wall. Then, if we indicate with $\mathbf{T}_f$ the Cauchy stress tensor for the fluid, we have

$$\mathbf{f}_{\text{fluid}} = -\mathbf{T}_f \cdot \mathbf{n} d\sigma + o(d\sigma) = P\mathbf{n} d\sigma - 2\mu \mathbf{D}(\mathbf{u}) \cdot \mathbf{n} d\sigma + o(d\sigma). \tag{4.9}$$

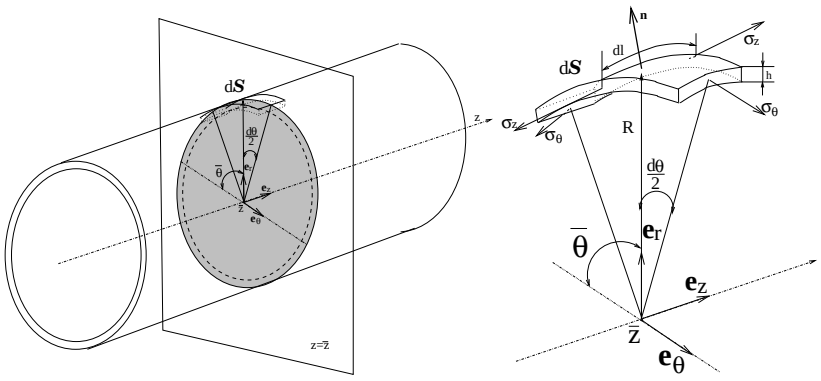

FIGURE 17. A cylindrical model of the vessel geometry (left) and the infinitesimal portion of vessel wall used for the derivation of the equations (right).

4.1.2. *The independent ring model.* The independent ring model is expressed by a differential equation for the time evolution of η, for each z and θ. For the derivation of this model, we will make some additional assumptions:

IR-1 *Dominance of circumferential stresses* $\boldsymbol{\sigma}_\theta$. The stresses $\boldsymbol{\sigma}_z$ acting along longitudinal direction are negligible with respect to $\boldsymbol{\sigma}_\theta$ and are thus neglected when writing the momentum equation.

IR-2 *Cylindrical configuration* The vessel remains a circular cylinder during motion, i.e. $\frac{\partial R}{\partial \theta} = 0$. This hypothesis may be partially dispensed with, by allowing small circumferential variations of the radius, yet we will neglect $\frac{\partial R}{\partial \theta}$ in our model.

IR-3 *Linear elastic behaviour.* Together with hypotheses IR-1 and IR-2 it allows us to write that the circumferential stress is proportional to the relative circumferential elongation, i.e.

$$\sigma_\theta = \frac{E}{1-\xi^2}\frac{\eta}{R_0}, \tag{4.10}$$

where ξ is the *Poisson* ratio (which may be taken equal to 0.5 thanks to the hypothesis A4) and E is the Young modulus.[4]

We will write the balance of momentum along the radial direction by analysing the system of forces acting on $d\mathcal{S}$. We have already examined the external forces, we need now to look in more details at the effect of the internal forces, which, by assumption, are only due to the circumferential stress $\boldsymbol{\sigma}_\theta$.

We may note in Fig. 18 that the two vectors $\mathbf{e}_\theta(\overline{\theta}+\frac{d\theta}{2})$ and $\mathbf{e}_\theta(\overline{\theta}-\frac{d\theta}{2})$ form with $\mathbf{e}_r$ an angle of $\pi/2 + d\theta/2$ and $-(\pi/2 + d\theta/2)$, respectively. The component of the resultant of the internal forces on the radial direction is then

$$f_{int} = \left(\sigma_\theta \mathbf{e}_\theta(\overline{\theta}+\frac{d\theta}{2}) + \sigma_\theta \mathbf{e}_\theta(\overline{\theta}-\frac{d\theta}{2})\right)\cdot \mathbf{e}_r h dl = \tag{4.11}$$

$$= -2\sigma_\theta \sin\frac{d\theta}{2} h dl = -\sigma_\theta h d\theta dl + o(d\theta dl).$$

[4]The presence of the term $1-\xi^2$ is due to the assumption of planar stresses. Some authors (like [21]) consider that the hypothesis of mono-axial stresses is more realistic for the problem at hand. In that case one has to omit the term $1-\xi^2$ from the stress-strain relation and write simply $\sigma_\theta = E\eta R_0^{-1}$.

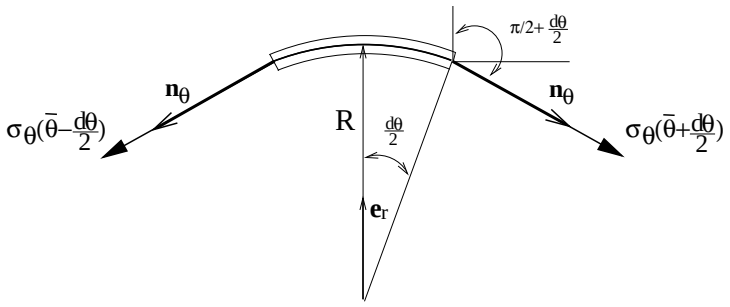

FIGURE 18. Computation of the angle between $\boldsymbol{\sigma}_\theta$ and the radial direction $\mathbf{e}_r$.

Owing to the incompressibility assumption A4 the volume in the current configuration is unchanged with respect to that in the reference configuration, i.e.

$$hRd\theta dl = h_0 R_0 d\theta dz.$$

Then, being $o(dl) = o(dz)$ we may write (4.11) as

$$f_{int} = -\frac{\sigma_\theta}{R} h_0 R_0 + o(d\theta dz) = \frac{Eh_0}{1-\xi^2}\frac{\eta}{R} d\theta dz + o(d\theta dz).$$

Finally, the mass of the portion of vessel wall under consideration is

$$mass = \rho_w h R d\theta dl = \rho_w h_0 R_0 d\theta dz,$$

where ρ_w is the density of the vessel tissue, whereas the acceleration along the radial direction is given by $\dfrac{\partial^2 R}{\partial t^2} = \dfrac{\partial^2 \eta}{\partial t^2}$. By balancing the resultant of the internal and external forces, provided in (4.8) and (4.9), with the inertia term, we have

$$\rho_w h_0 R_0 \frac{\partial^2 \eta}{\partial t^2} d\theta dz + \frac{Eh_0}{1-\xi^2}\frac{\eta}{R} d\theta dz = - (2\mu \mathbf{D}(\mathbf{u})\cdot\mathbf{n})\cdot\mathbf{e}_r d\sigma + (P - P_{ext})\mathbf{n}\cdot\mathbf{e}_r d\sigma + o(d\theta dz). \tag{4.12}$$

By dividing either side by $d\theta dz$ and passing to the limit for $d\theta \to 0$ and $dz \to 0$, and recalling that $d\sigma = g\,\Gamma_0^w d\theta dz = R(\mathbf{n}\cdot\mathbf{e}_r)^{-1} d\theta dz$, thanks to (4.3) and (4.5), we obtain

$$\rho_w h_0 R_0 \frac{\partial^2 \eta}{\partial t^2} + \frac{Eh_0}{1-\xi^2}\frac{\eta}{R} = -(2\mu \mathbf{D}(\mathbf{u})\cdot\mathbf{n})\cdot\mathbf{e}_r g\Gamma_0^w + (P - P_{ext})R.$$

Since the derivation has been made by considering an arbitrary plane $\theta = \overline{\theta}$ and time t, we may finally obtain the *independent ring model*

$$\frac{\partial^2 \eta}{\partial t^2} + b\eta = H, \quad \text{in } \Gamma_0^w,\ t \in I, \tag{4.13}$$

where

$$b = \frac{E}{\rho_w (1-\xi^2) R_0^2}, \tag{4.14}$$

is a positive coefficient linked to the wall mechanical properties, while

$$H = \frac{1}{\rho_w h_0}\left[\frac{R}{R_0}(P - P_{ext}) - 2g\mu(\mathbf{D}(\mathbf{u})\cdot\mathbf{n})\cdot\mathbf{e}_r\right] = \frac{\rho}{\rho_w h_0}\left[\frac{R}{R_0}(p - p_{ext}) - 2g\nu(\mathbf{D}(\mathbf{u})\cdot\mathbf{n})\cdot\mathbf{e}_r\right], \tag{4.15}$$

is the *forcing term* which accounts for the action of external forces.

Remark 4.1. Often, the term R/R_0 in the right hand side of (4.15) is neglected as well as the contribution to the forcing term due to the fluid viscous stresses. In this case, we have just

$$H = \frac{P - P_{ext}}{\rho_w h_0}. \tag{4.16}$$

and the forcing term does not depend anymore on the current geometrical configuration.

$\diamondsuit$

By neglecting the acceleration term in (4.13) we obtain the following *algebraic model*, which is often found in the medical and bioengineering literature,

$$b\eta = H, \quad \text{in } \Gamma_0^w,\ t \in I \tag{4.17}$$

according to which the wall displacement is proportional to the normal component of the applied external stresses.

Remark 4.2. One may account for the *viscoelastic* nature of the vessel wall structure even in this simple model by adding to the constitutive relation (4.10) a term proportional to the displacement velocity, as in a simple Voigt/Kelvin model [22], that is by writing

$$\sigma_\theta = \frac{E}{1-\xi^2}\frac{\eta}{R_0} + \frac{\gamma}{R_0}\frac{\partial \eta}{\partial t},$$

where γ (whose unit is $[\gamma] = kg/ms$) is a positive constant damping parameter.

Then, the resulting differential equation would read

$$\frac{\partial^2 \eta}{\partial t^2} + \frac{\gamma}{R_0^2 \rho_w h_0}\frac{\partial \eta}{\partial t} + b\eta = H, \quad \text{in } \Gamma_0^w, t \in I. \tag{4.18}$$

We may note that the term $\dfrac{1}{R_0}\dfrac{\partial \eta}{\partial t}$ plays the role of the strain rate $\mathbf{D}$ into the general relation for viscoelastic materials (4.1).

$\diamondsuit$

Models (4.13), (4.17) and (4.18) are all apt to provide a solution η for every possible value of θ. In principle, since no differentiation with respect to θ is present in the model, nothing would prevent us to get significant variations of η with θ (or even a discontinuity), which would contradict assumption IR-2. This potential drawback could be eliminated by enriching the models with further terms involving derivatives along θ, as in the case of models derived from shell theory [11]. On the other hand, a more heuristic and less rigorous argument can be put forward moving from (4.17). Since b is relatively large, smooth variations of the forcing term H with respect to θ are damped to tiny one on η. This observation may be extended also to models (4.13) and (4.18) in view of the fact that for the problems at hand the term $b\eta$ dominates the other terms on the left hand side. Similar considerations apply to the model that we will introduce in the next subsection.

4.1.3. *The generalised string model.* A more complete model considers also the effects of the longitudinal stresses $\boldsymbol{\sigma}_z$. Experimental and physiological analysis [22] show that vessel walls are in a "pre-stressed" state. In particular, when an artery is extracted from a body tends to "shrink", i.e. to reduce its length. This fact implies that arteries in the human body are normally subjected to a longitudinal tension.

At the base of the generalised string model is the assumption that this longitudinal tension is indeed the dominant component of the longitudinal stresses.

More precisely, let us refer to Fig. 19; we replace assumption IR-1 by the following

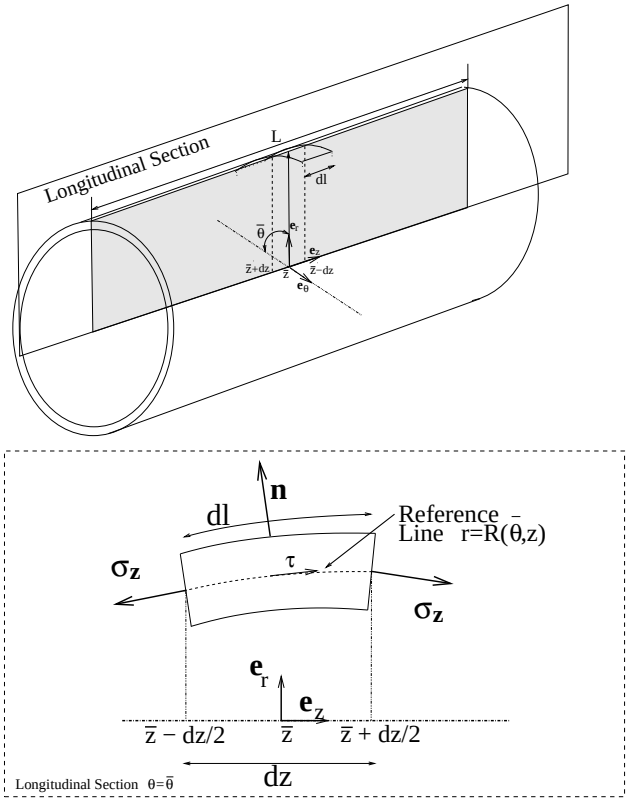

FIGURE 19. A cylindrical model of the vessel geometry (top) and quantities on a longitudinal section (bottom)

GS-1 The longitudinal stress $\boldsymbol{\sigma}_z$ is not negligible and, in particular,

$$\boldsymbol{\sigma}_z = \pm\sigma_z\boldsymbol{\tau}, \tag{4.19}$$

where $\boldsymbol{\tau}$ is the unitary vector tangent to the curve

$$r = R(\overline{\theta}, z; t), \tag{4.20}$$

and its modulus σ_z is constant. Moreover, we assume that it is a *traction stress* (that is with a versus equal to that of the normal to the surface on which it applies).

We also maintain assumption IR-2 of the independent ring model. When considering the forces acting on $d\mathcal{S}$ we have now a further term, namely (referring again to Fig. 19)

$$\begin{aligned}\mathbf{f}_z &= [\boldsymbol{\sigma}_z(\overline{z} + dz/2) + \boldsymbol{\sigma}_z(\overline{z} - dz/2)]\, hRd\theta = \\ &= \sigma_z \frac{\boldsymbol{\tau}(\overline{z} + dz/2) - \boldsymbol{\tau}(\overline{z} - dz/2)}{dl} dl\, hRd\theta = \sigma_z \frac{d\boldsymbol{\tau}}{dl} R_0 h_0 dl d\theta + \mathbf{o}(dz d\theta)\end{aligned}$$

We now exploit the Frenet-Serret formulae to write

$$\frac{d\boldsymbol{\tau}}{dl} = \kappa\mathbf{n},$$

where κ is the curvature of the line $r = R(\overline{\theta}, z; t)$, whose expression is

$$\kappa = \frac{\partial^2 R}{\partial z^2}\left[1 + \left(\frac{\partial R}{\partial z}\right)^2\right]^{-3/2}. \tag{4.21}$$

By recalling (4.7) and (4.5) we obtain

$$\mathbf{f}_z \cdot \mathbf{e}_r = \sigma_z \frac{\partial^2 R}{\partial z^2} \left[1 + \left(\frac{\partial R}{\partial z} \right)^2 \right]^{-3/2} R_0 h_0 dz d\theta + o(dz d\theta).$$

We eliminate the geometric non-linearity in the model by neglecting the term $\left(\frac{\partial R}{\partial z}\right)^2$. Furthermore, we replace $\frac{\partial^2 R}{\partial z^2}$ by $\frac{\partial^2 \eta}{\partial z^2}$.[5]

By proceeding like in the previous section, we may modify the independent ring model into the following differential equation

$$\frac{\partial^2 \eta}{\partial t^2} - a \frac{\partial^2 \eta}{\partial z^2} + b\eta = H, \quad \text{in } \Gamma_0^w,\ t \in I, \tag{4.22}$$

where

$$a = \frac{\sigma_z}{\rho_w h_0}.$$

The final *generalised string* model is obtained by adding to the expression for $\boldsymbol{\sigma}_z$ in (4.19) a term

$$c \frac{\partial}{\partial t} \frac{\partial \eta}{\partial z}, \quad c > 0$$

which is a viscoelastic term linking the longitudinal stress to the rate of rotation of the structure. For small displacements, $\partial\eta/\partial z$ is indeed proportional to the angle of rotation around the circumferential direction of the structure, with respect to the reference configuration.

The result is

$$\frac{\partial^2 \eta}{\partial t^2} - a \frac{\partial^2 \eta}{\partial z^2} + b\eta - c \frac{\partial^3 \eta}{\partial t \partial z^2} = H, \quad \text{in } \Gamma_0^w,\ t \in I. \tag{4.23}$$

4.2. **Analysis of vessel wall models.** In the following we will provide some a-priori estimates for the differential models just proposed.

We recall Poincaré inequality for the one dimensional case.

Lemma 4.1 (Poincaré inequality - one dimensional case). *Let $f \in H^1(a,b)$ with $f(a) = 0$. Then there exists a positive constant C_p such that*

$$\|f\|_{L^2(0,L)} \leq C_p \left\| \frac{df}{dx} \right\|_{L^2(0,L)}. \tag{4.24}$$

Proof. For all $x \in [a,b]$ we have,

$$f(x) = f(a) + \int_a^x \frac{df}{dx}(\tau) d\tau = \int_a^x \frac{df}{dx}(\tau) d\tau$$

Then,

$$\begin{aligned} \int_a^b f^2(s) ds &= \int_a^b \left(\int_a^s \frac{df}{dx}(\tau) d\tau \right)^2 ds \leq \text{(by Cauchy-Schwarz inequality)} \\ &\leq \int_a^b \left(\left(\int_a^s 1^2 d\tau \right)^{1/2} \left\{ \int_a^s [\frac{df}{dx}(\tau)]^2 d\tau \right\}^{1/2} \right)^2 ds \leq \\ &\leq \int_a^b (b-a) \left\| \frac{df}{dx} \right\|^2_{L^2(a,b)} ds = (b-a)^2 \left\| \frac{df}{dx} \right\|^2_{L^2(a,b)}, \end{aligned}$$

by which inequality (4.24) is proved by taking $C_p = (b-a)$. The same inequality holds if $f(b) = 0$. □

[5] This last equality is clearly true whenever R_0 is varying linearly with z.

Thanks to the fact that no derivatives with respect to the variable θ are present in the equations, we may carry out some further analysis of the structure models illustrated so far by considering the equations for a fixed value of θ and z.

We will consider equation (4.13) and address then the following problem:

$$\frac{\partial^2 \eta}{\partial t^2} + b\eta = H, \quad \text{in } \Gamma_0^w,\ t \in I, \tag{4.25}$$

with the following initial values for the displacement and its time rate

$$\eta = \eta_0, \quad \frac{\partial \eta}{\partial t} = \eta_1, \quad \text{in } \Gamma_0^w,\ t = t_0. \tag{4.26}$$

We also introduce the space $L^2(I; L^2(\Gamma_0^w))$ of functions $f : \Gamma_0^w \times I \to \mathbb{R}$ that are square integrable in Γ_0^w for almost every (a.e.) $t \in I$ and such that

$$\int_{t_0}^{t_1} \|f(\tau)\|^2_{L^2(\Gamma_0^w)}\, d\tau < \infty.$$

Lemma 4.2. *If $H \in L^2(I; L^2(\Gamma_0^w))$, the following inequality holds for a.e. $t \in I$*

$$\|\frac{\partial \eta}{\partial t}(t)\|^2_{L^2(\Gamma_0^w)} + b\|\frac{\partial \eta}{\partial t}(t)\|^2_{L^2(\Gamma_0^w)} \leq \left(\|\eta_1\|^2_{L^2(\Gamma_0^w)} + b\|\eta_0\|^2_{L^2(\Gamma_0^w)} + \int_{t_0}^{t} \|H(\tau)\|^2_{L^2(\Gamma_0^w)}\, d\tau\right) e^{(t-t_0)}. \tag{4.27}$$

Proof. It can be obtained by multiplying (4.25) by $\frac{\partial \eta}{\partial t}$ and applying Gronwall lemma (Lemma 3.3). □

Relation (4.27) asserts that the sum of the total kinetic and elastic potential energy associated to equation (4.25) is bounded, at each time t, by a quantity which depends only on the initial condition and the forcing term.

Let us consider the generalised string model (4.23) with the following initial and boundary conditions

$$\eta = \eta_0, \quad \frac{\partial \eta}{\partial t} = \eta_1 \quad \text{in } \Gamma_0^w,\ t = t_0, \tag{4.28a}$$

$$\eta|_{z=0} = \alpha, \quad \eta|_{z=L} = \beta, \quad t \in I. \tag{4.28b}$$

Let us define the following energy function

$$e_s(t) = \frac{1}{2}\left(\|\frac{\partial \eta}{\partial t}(t)\|^2_{L^2(\Gamma_0^w)} + a\|\frac{\partial \eta}{\partial z}(t)\|^2_{L^2(\Gamma_0^w)} + b\|\eta(t)\|^2_{L^2(\Gamma_0^w)}\right) \tag{4.29}$$

Lemma 4.3. *If $H \in L^2(I; L^2(\Gamma_0^w))$ and $\alpha = \beta = 0$, the following inequality holds for a.e. $t \in I$*

$$e_s(t) + \frac{c}{2}\int_{t_0}^{t} \|\frac{\partial^2 \eta}{\partial t \partial z}(\tau)\|^2_{L^2(\Gamma_0^w)}\, d\tau \leq e_s(0) + k\int_{t_0}^{t_1} \|H(\tau)\|^2_{L^2(\Gamma_0^w)}\, d\tau, \tag{4.30}$$

where $k = \dfrac{C_p^2}{2c}$ and C_p is the Poincaré constant.

Proof. We use the short-hand notations $\dot{\eta}$ and $\ddot{\eta}$ for the time derivatives of η. We first multiply the generalised string equation (4.23) by $\dot{\eta}$ and integrate w.r. to z:

$$\int_0^L \dot{\eta}\ddot{\eta} - a\int_0^L \dot{\eta}\frac{\partial^2\eta}{\partial z^2} - c\int_0^L \dot{\eta}\frac{\partial^3\eta}{\partial t\partial z^2} + b\int_0^L \dot{\eta}\eta = \tag{4.31}$$
$$\frac{1}{2}\frac{d}{dt}\int_0^L \dot{\eta}^2 + a\int_0^L \frac{\partial^2\eta}{\partial t\partial z}\frac{\partial\eta}{\partial z} - a\left[\dot{\eta}\frac{\partial\eta}{\partial z}\right]_0^L + c\int_0^L (\frac{\partial^2\eta}{\partial t\partial z})^2 -$$
$$c\left[\frac{\partial^2\eta}{\partial t\partial z}\dot{\eta}\right]_0^L + \frac{b}{2}\frac{d}{dt}\int_0^L \eta^2 = \int_0^L \dot{\eta}H$$

By exploiting the homogeneous boundary conditions and the fact that

$$\frac{\partial^2\eta}{\partial t\partial z}\frac{\partial\eta}{\partial z} = \frac{1}{2}\frac{\partial}{\partial t}\left(\frac{\partial\eta}{\partial z}\right)^2,$$

we have

$$\frac{1}{2}\frac{d}{dt}\int_0^L \dot{\eta}^2 + \frac{a}{2}\frac{d}{dt}\int_0^L \frac{\partial\eta}{\partial z}^2 + c\int_0^L (\frac{\partial^2\eta}{\partial t\partial z})^2 + \frac{b}{2}\frac{d}{dt}\int_0^L \eta^2 = \int_0^L \dot{\eta}H.$$

We now integrate w.r. to the circumferential direction, obtaining

$$\frac{de_s}{dt} + c\|\frac{\partial^2\eta}{\partial t\partial z}\|^2_{L^2(\Gamma_0^w)} = \int_{\Gamma_0^w} \dot{\eta}H. \tag{4.32}$$

The application the Cauchy-Schwarz,Young and Poincaré inequalities to the right-hand side gives

$$\frac{de_s}{dt} + c\|\frac{\partial^2\eta}{\partial t\partial z}\|^2_{L^2(\Gamma_0^w)} \le \frac{1}{4\epsilon}\|H\|^2_{L^2(\Gamma_0^w)} + \epsilon\|\dot{\eta}\|^2_{L^2(\Gamma_0^w)} \le$$
$$\frac{1}{4\epsilon}\|H\|^2_{L^2(\Gamma_0^w)} + C_p^2\epsilon\|\frac{\partial^2\eta}{\partial t\partial z}\|^2_{L^2(\Gamma_0^w)}.$$

for any positive ϵ. If we choose ϵ such that $C_p^2\epsilon = c/2$ and integrate in time between t_0 and t we finally obtain the desired result. □

5. THE COUPLED FLUID-STRUCTURE PROBLEM

In this section we will treat the situation arising when the flow in a vessel interacts mechanically with the wall structure. This aspect is particularly relevant for blood flow in large arteries, where the vessel wall radius may vary up to 10% because of the forces exerted by the flowing blood stream.

We will first illustrate a framework for the Navier-Stokes equations in a moving domain which is particularly convenient for the analysis and for the set up of numerical solution methods.

5.1. **The Arbitrary Lagrangian Eulerian (ALE) formulation of the Navier-Stokes equation.** In section (2.4) we have introduced the Navier Stokes equations in a fixed domain Ω, according to the *Eulerian* approach where the independent spatial variables are the coordinates of a fixed Eulerian system. We now consider the case where the domain is moving. In practical situations, such as the flow inside a portion of a compliant artery, we have to compute the flow solution in a *computational domain* Ω_t varying with time.

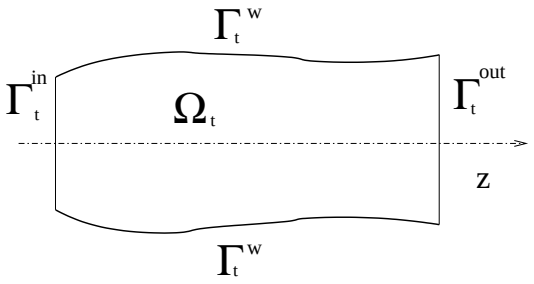

FIGURE 20. The longitudinal section of a model of an artery. The vessel wall Γ_t^w is moving. The location along the z axis of Γ_t^{in} and Γ_t^{out} are fixed.

The boundary of Ω_t may in general be subdivided into two parts. The first part coincides with the physical fluid boundary, i.e. the vessel wall. In the example of Fig. 20, this part is represented by Γ_t^w, which is moving under the effect of the flow field. The other part of $\partial\Omega_t$ corresponds to "fictitious boundaries" (also called artificial boundaries) which delimit the region of interest. They are necessary because solving the fluid equation on the whole portion of space occupied by the fluid under study is in general impractical, if not impossible. In our case, that would mean solving the whole circulatory system!

In the example of Fig. 20, the "fictitious" boundaries are the inlet and outlet boundaries, there indicated by Γ_t^{in} and Γ_t^{out}, respectively. The location of these boundaries is fixed a priori. More precisely, Γ_t^{in} and Γ_t^{out} may change with time because of the displacement of Γ_t^w, however they remain planar and their position along the vessel axis is fixed.

Clearly in this case the Eulerian approach becomes impractical.

A possible alternative would be to use the *Lagrangian approach.* Here, we identify the computational domain on a reference configuration Ω_0 and the corresponding domain in the current configuration, which we indicate with $\Omega_{\mathcal{L}_t}$, will be provided by the Lagrangian mapping (which has been introduced in section 2.2), i.e.

$$\Omega_{\mathcal{L}_t} = \mathcal{L}_t(\Omega_0), \ t \in I. \tag{5.1}$$

Fig. 21 illustrates the situation for the flow inside an artery whose wall is moving. Since the fluid velocity at the wall is equal to the wall velocity, the Lagrangian

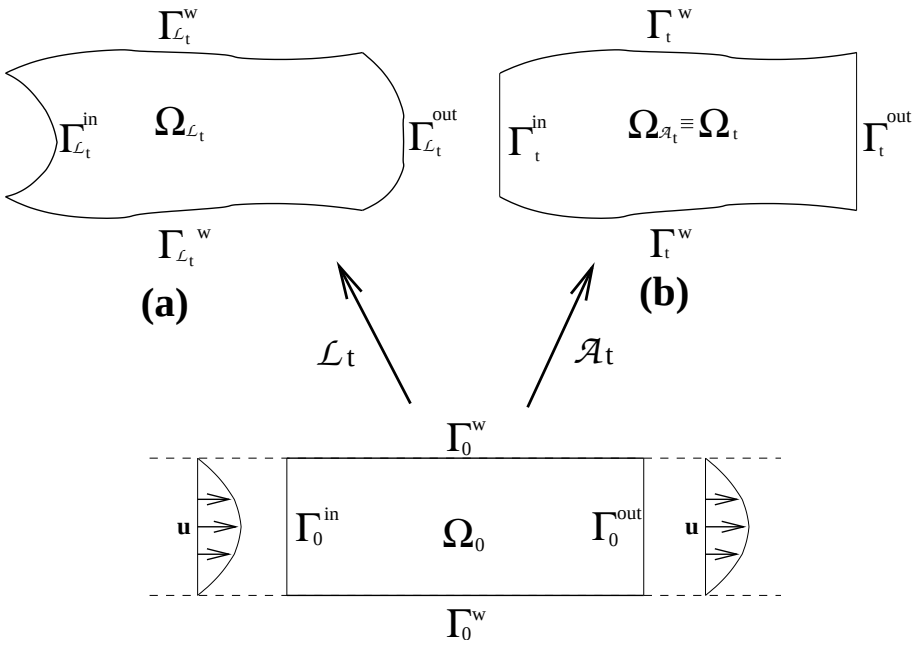

FIGURE 21. Comparison between the Lagrangian and the ALE approach. The reference computational domain Ω_0 is mapped by (a) the Lagrangian mapping $\mathcal{L}_t$ and by (b) the Arbitrary Lagrangian Eulerian mapping.

mapping effectively maps Γ_0^w to the correct wall position Γ_t^w at each time t. However, the "fictitious' boundaries Γ_0^{in} and Γ_0^{out} in the reference configuration will now be transported along the fluid trajectories, into $\Gamma_{\mathcal{L}_t}^{in}$ and $\Gamma_{\mathcal{L}_t}^{out}$. This is clearly not acceptable, particularly if one wants to study the problem for a relatively large time interval. Indeed, the domain rapidly becomes highly distorted.

The ideal situation would then be that indicated in Fig. 21 (b). Even if the wall is moving, one would like to keep the inlet and outlet boundaries at the same spatial location along the vessel axis.

With that purpose, we introduce the *Arbitrary Lagrangian Eulerian* (ALE) mapping

$$\mathcal{A}_t : \Omega_0 \to \Omega_{\mathcal{A}_t}, \qquad \mathbf{Y} \to \mathbf{y}(t, \mathbf{Y}) = \mathcal{A}_t(\mathbf{Y}), \tag{5.2}$$

which provides the spatial coordinates $(t, \mathbf{y})$ in terms of the so-called *ALE coordinates* $(t, \mathbf{Y})$, with the basic requirement that $\mathcal{A}_t$ retrieves, at each time $t \in I$, the desired computational domain, i.e.

$$\Omega_{\mathcal{A}_t} \equiv \mathcal{A}_t(\Omega_0) = \Omega_t, \quad \forall t \in I.$$

The ALE mapping should be continuous and bijective in $\overline{\Omega_0}$. Once given, we may define the *domain* velocity field as

$$\widetilde{\mathbf{w}}(t, \mathbf{Y}) = \frac{\partial}{\partial t}\mathbf{y}(t, \mathbf{Y}), \tag{5.3}$$

which, in the spatial coordinates is expressed as

$$\mathbf{w} = \widetilde{\mathbf{w}} \circ \mathcal{A}_t^{-1}, \quad \text{i.e} \quad \mathbf{w}(t, \mathbf{y}) = \widetilde{\mathbf{w}}(t, \mathcal{A}_t^{-1}(\mathbf{y})). \tag{5.4}$$

Similarly to what has been done for the Lagrangian mapping in Sect. 2.2 we use the convention of indicating by $\widetilde{f}$ the composition of a function f with the ALE mapping, i.e. $\widetilde{f} = f \circ \mathcal{A}_t$.

We define the ALE trajectory $T_{\mathbf{Y}}$ for every $\mathbf{Y} \in \Omega_0$ as

$$T_{\mathbf{Y}} = \{(t, \mathbf{y}(t, \mathbf{Y})), \quad t \in I\} \tag{5.5}$$

and the ALE derivative of a function f, as the time derivative along a trajectory $T_{\mathbf{Y}}$, that is if

$$f : I \times \Omega_t \to \mathbb{R},$$

then

$$\frac{D^{\mathcal{A}}}{Dt} f : I \times \Omega_t \to \mathbb{R}, \qquad \frac{D^{\mathcal{A}}}{Dt} f(t, \mathbf{y}) = \frac{\partial \widetilde{f}}{\partial t}(t, \mathbf{Y}), \quad \mathbf{Y} = \mathcal{A}_t^{-1}(\mathbf{y}). \tag{5.6}$$

Similarly to what already obtained for the Lagrangian mapping (relation (2.4)), we have

$$\frac{D^{\mathcal{A}}}{Dt} f = \frac{\partial f}{\partial t} + \mathbf{w} \cdot \boldsymbol{\nabla} f, \tag{5.7}$$

where now the gradient is made with respect to the $\mathbf{y}$-coordinates.

The Jacobian of the ALE mapping $J^{\mathcal{A}_t}$, defined as

$$J^{\mathcal{A}_t} = \det \left(\frac{\partial \mathbf{y}}{\partial \mathbf{Y}} \right), \tag{5.8}$$

is, for all $t \in I$, a positive quantity because the ALE mapping is surjective at time t_0 is equal to the identity mapping. It satisfies the following relation

$$\frac{D^{\mathcal{A}}}{Dt} J^{\mathcal{A}_t} = J^{\mathcal{A}_t} \operatorname{div} \mathbf{w}. \tag{5.9}$$

Again in a way all analogous to what seen for the Lagrangian mapping we may derive the following result.

Theorem 5.1 (ALE transport theorem). *Let $V_0 \subset \Omega_0$, and let $V^{\mathcal{A}_t} \subset \Omega_t$ be its image under the mapping $\mathcal{A}_t$. Furthermore, let $f : I \times \Omega_t \to \mathbb{R}$ be continuously differentiable with respect to both variables. Then*

$$\begin{aligned} \frac{d}{dt} \int_{V^{\mathcal{A}_t}} f = \int_{V^{\mathcal{A}_t}} \left(\frac{D^{\mathcal{A}}}{Dt} f + f \operatorname{div} \mathbf{w} \right) = \int_{V^{\mathcal{A}_t}} \left(\frac{\partial f}{\partial t} + \operatorname{div}(f \mathbf{w}) \right) \\ = \int_{V^{\mathcal{A}_t}} \frac{\partial f}{\partial t} + \int_{\partial V^{\mathcal{A}_t}} f \mathbf{w} \cdot \mathbf{n}. \end{aligned} \tag{5.10}$$

The proof is similar to that of theorem 2.2, and is omitted.■

The Navier-Stokes equations (2.27) are clearly valid on Ω_t, yet it may be convenient to recast them in order to put into evidence the ALE time derivative. We obtain, by a straightforward application of (5.7) to (2.27),

$$\begin{aligned} &\tfrac{D^{\mathcal{A}}}{Dt} \mathbf{u} + [(\mathbf{u} - \mathbf{w}) \cdot \boldsymbol{\nabla}] \, \mathbf{u} + \boldsymbol{\nabla} p - 2 \, \mathbf{div}(\nu \mathbf{D}(\mathbf{u})) = \mathbf{f}, \\ &\operatorname{div} \mathbf{u} = 0, \end{aligned} \tag{5.11}$$

in Ω_t and for all $t \in I$.

5.2. **Coupling with the structure model.** We now study the properties of the coupled fluid-structure problem, using for the structure the generalised string model (4.23). Referring to Fig. 16, we recall that Γ_t^w is the current configuration of the vessel structure, while Γ_0^w is the reference configuration in which the structure equation is written. We also recall that we take $\mathbf{n}$ always to be the outwardly vector normal to the fluid domain boundary.

We will then address the following problem:

For all $t \in I$, find $\mathbf{u}$, p , η such that

$$\begin{aligned} &\tfrac{D^{\mathcal{A}}}{Dt}\mathbf{u} + [(\mathbf{u}-\mathbf{w})\cdot\boldsymbol{\nabla}]\,\mathbf{u} + \boldsymbol{\nabla} p - 2\,\mathbf{div}(\nu\mathbf{D}(\mathbf{u})) = \mathbf{f}, \\ &\qquad\qquad\qquad\qquad\qquad\qquad\qquad\qquad\qquad\qquad \text{in } \Omega_t, \\ &\operatorname{div}\mathbf{u} = 0, \end{aligned} \tag{5.12}$$

and

$$\frac{\partial^2\eta}{\partial t^2} - a\frac{\partial^2\eta}{\partial z^2} + b\eta - c\frac{\partial^3\eta}{\partial t\partial^2 z} = H \quad \text{in } \Gamma_0^w \tag{5.13}$$

with the following initial conditions for $t = t_0$

$$\mathbf{u} = \mathbf{u}_0, \qquad \mathbf{x} \in \Omega_0, \tag{5.14a}$$

$$\eta = \eta_0, \quad \dot\eta = \eta_1 \quad \text{in } \Gamma_0^w, \tag{5.14b}$$

boundary conditions for $t \in I$

$$[2\nu\mathbf{D}(\mathbf{u}) - (p-p_0)\mathbf{I}]\cdot\mathbf{n} = \mathbf{0} \qquad \text{on } \Gamma_t^{out}, \tag{5.15a}$$

$$\mathbf{u} = \mathbf{g}, \qquad \text{on } \Gamma_t^{in}, \tag{5.15b}$$

$$\eta|_{z=0} = \alpha, \quad \eta|_{z=L} = \beta, \tag{5.15c}$$

and the interface condition

$$\widetilde{\mathbf{u}} = \mathbf{u}\circ\mathcal{A}_t = \frac{\partial\eta}{\partial t}\mathbf{e}_r, \qquad \text{on } \Gamma_0^w,\ t \in I. \tag{5.16}$$

Another interface condition is implicitly provided by the fact that the forcing term H is function of the fluid variables (see (4.15)).

Here, $\mathbf{u}_0$, $\mathbf{g}$, α and β are given functions, H is the forcing term (4.15) and $\mathcal{A}_t$ is an ALE mapping such that $\mathcal{A}_t^{-1}(\partial\Omega_t) = \Gamma^{in} \cup \Gamma^{out} \cup \Gamma_0^w$. We have used the ALE form for the Navier-Stokes equations since it is best suited in view of the numerical solution, as it will be detailed in the next section.

We may then recognise the sources of the coupling between the fluid and the structure models, which are twofold (in view of a possible iterative solution strategy):

- fluid $\rightarrow$ structure. The fluid solution provides the value of H, which is function of the fluid stresses at the wall.
- structure $\rightarrow$ fluid. The movement of the vessel wall changes the geometry on which the fluid equations must be solved. In addition, the proper boundary conditions for the fluid velocity in correspondence to vessel wall are not anymore homogeneous Dirichlet conditions, but they impose the equality between the fluid and the structure velocity. They express the fact that the fluid particle in correspondence of the vessel wall should move at the same velocity as the wall.

Note that we have made some changes with respect to the nomenclature used in (2.27) to indicate that the domain is now moving. We rewrite the expression of the forcing term H, given in (4.15), by noting that while the fluid velocity and pressure are written in the current configuration, H lives in the reference configuration for

the vessel wall Γ_0^w. Therefore, following the nomenclature introduced in the previous subsection, we write

$$H = \frac{\rho}{\rho_w h_0}\left[(\widetilde{p} - p_0)\frac{R}{R_0} - 2g\widetilde{\nu}(\widetilde{\mathbf{D}(\mathbf{u})\cdot\mathbf{n}})\cdot\mathbf{e}_r\right]. \tag{5.17}$$

5.2.1. *Energy inequality for the coupled problem.* In this section we will obtain an a-priori inequality for the coupled fluid-structure problem just presented. We will consider only the case of homogeneous boundary conditions, that is

$$\mathbf{g} = \mathbf{0}, \quad \alpha = \beta = 0,$$

for the coupled problem (5.12)–(5.16).

Lemma 5.1. *The coupled problem (5.12)–(5.16) with* $\mathbf{g} = \mathbf{0}$ *and* $\alpha = \beta = 0$ *satisfies the following energy equality for all* $t \in I$

$$\begin{aligned}\frac{d}{dt}\left[\frac{\omega}{2}\|\mathbf{u}(t)\|_{\mathbf{L}^2(\Omega_t)} + e_s(t)\right] + 2\omega\int_{\Omega_t}\nu\mathbf{D}(\mathbf{u}):\mathbf{D}(\mathbf{u}) + c\|\frac{\partial^2\eta}{\partial z\partial t}\|^2_{L^2(\Gamma_0^w)} \\ + \frac{\omega}{2}\int_{\Gamma_t^{out}}|\mathbf{u}|^2\mathbf{u}\cdot\mathbf{n} = \omega\int_{\Omega_t}\mathbf{f}\cdot\mathbf{u},\end{aligned} \tag{5.18}$$

where e_s *was defined in (4.29) and*

$$\omega = \frac{\rho}{\rho_w h_0}. \tag{5.19}$$

Moreover, if we assume that the net kinetic energy flux is non-negative on the outlet section, i.e.

$$\int_{\Gamma_t^{out}}|\mathbf{u}|^2\mathbf{u}\cdot\mathbf{n} \geq 0 \quad \forall t \in I \tag{5.20}$$

we obtain the a-priori *energy estimate*

(5.21)

$$\begin{aligned}\frac{\omega}{2}\|\mathbf{u}(t)\|_{\mathbf{L}^2(\Omega_t)} + e_s(t) + C_K\omega\nu_0\int_{t_0}^t\|\boldsymbol{\nabla}\mathbf{u}(\tau)\|^2_{\mathbf{L}^2(\Omega_\tau)}d\tau + c\int_{t_0}^t\|\frac{\partial^2\eta}{\partial z\partial t}(\tau)\|^2_{L^2(\Gamma_w^0)}d\tau \\ \leq \frac{\omega}{2}\|\mathbf{u}_0\|_{\mathbf{L}^2(\Omega_t)} + e_s(t_0) + \frac{\omega C_P^2}{4\nu C_K}\int_{t_0}^t\|\mathbf{f}(\tau)\|^2_{\mathbf{L}^2(\Omega_\tau)}d\tau, \quad t \in I.\end{aligned}$$

Proof. We recall expression (4.32) and we recast the right hand side on the current configuration Γ_t^w. By exploiting (4.4) and (4.5) we have

$$\begin{aligned}\int_{\Gamma_0^w} H\frac{\partial\eta}{\partial t}d\sigma_0 &= \frac{\rho}{\rho_w h_0}\int_{\Gamma_0^w}\left[\frac{R}{R_0}(\widetilde{p} - p_{ext}) - 2g\nu(\widetilde{\mathbf{D}(\mathbf{u})\cdot\mathbf{n}})\cdot\mathbf{e}_r\right]\frac{\partial\eta}{\partial t}d\sigma_0 \\ &= \omega\int_{\Gamma_0^w}\left[(\widetilde{p} - p_{ext})\mathbf{n}\cdot\mathbf{e}_r - 2\nu(\widetilde{\mathbf{D}(\mathbf{u})\cdot\mathbf{n}})\cdot\mathbf{e}_r\right]\frac{\partial\eta}{\partial t}gd\sigma_0 = \\ \omega\int_{\Gamma_0^w}\left[(\widetilde{p} - p_{ext})\mathbf{n} - 2\nu(\widetilde{\mathbf{D}(\mathbf{u})\cdot\mathbf{n}})\right]\cdot\widetilde{\mathbf{u}}gd\sigma_0 &= \omega\int_{\Gamma_t^w}[(p - p_{ext})\mathbf{n} - 2\nu(\mathbf{D}(\mathbf{u})\cdot\mathbf{n})]\cdot\mathbf{u}d\sigma,\end{aligned}$$

where we have used the interface conditions (5.16). Then,

$$\frac{1}{2}\frac{de_s}{dt} + c\|\frac{\partial^2\eta}{\partial z\partial t}\|^2_{L^2(\Gamma_0^w)} = \omega\int_{\Gamma_t^w}[(p - p_{ext})\mathbf{n} - 2\nu(\mathbf{D}(\mathbf{u})\cdot\mathbf{n})]\cdot\mathbf{u}d\sigma. \tag{5.22}$$

As for the fluid equations, we follow the same route of Lemma 3.4. In particular, we begin by multiplying (5.12) by $\mathbf{u}$ and integrating over Ω_t, obtaining

$$\int_{\Omega_t}\mathbf{u}\cdot\frac{D^{\mathcal{A}}}{Dt}\mathbf{u} + \int_{\Omega_t}\mathbf{u}\cdot[(\mathbf{u} - \mathbf{w})\cdot\boldsymbol{\nabla}]\,\mathbf{u} + \int_{\Omega_t}\mathbf{u}\cdot(\boldsymbol{\nabla}p - 2\nu\,\mathbf{div}\,\mathbf{D}(\mathbf{u})) = (\mathbf{f},\mathbf{u}). \tag{5.23}$$

We now analyse each term in turn. By exploiting the ALE transport theorem (5.10) we may derive that

$$\int_{\Omega_t} \mathbf{u}\cdot\frac{D^{\mathcal{A}}}{Dt}\mathbf{u} = \int_{\Omega_0} J_t\widetilde{\mathbf{u}}\cdot\frac{\partial\widetilde{\mathbf{u}}}{\partial t} = \frac{1}{2}\int_{\Omega_0} J_t\frac{\partial|\widetilde{\mathbf{u}}|^2}{\partial t} = \frac{1}{2}\int_{\Omega_t}\frac{D^{\mathcal{A}}}{Dt}|\mathbf{u}|^2 = \frac{1}{2}\frac{d}{dt}\int_{\Omega_t}|\mathbf{u}|^2 - \frac{1}{2}\int_{\Omega_t}|\mathbf{u}|^2\operatorname{div}\mathbf{w}. \tag{5.24}$$

The convective term gives

$$\int_{\Omega_t}\mathbf{u}\cdot[(\mathbf{u}-\mathbf{w})\cdot\boldsymbol{\nabla}]\,\mathbf{u} = -\frac{1}{2}\int_{\Omega_t}|\mathbf{u}|^2\operatorname{div}\mathbf{u} + \frac{1}{2}\int_{\Omega_t}|\mathbf{u}|^2\operatorname{div}\mathbf{w} + \frac{1}{2}\int_{\partial\Omega_t}|\mathbf{u}|^2(\mathbf{u}-\mathbf{w})\cdot\mathbf{n} = \frac{1}{2}\int_{\Omega_t}|\mathbf{u}|^2\operatorname{div}\mathbf{w} + \frac{1}{2}\int_{\Gamma_t^{out}}|\mathbf{u}|^2\mathbf{u}\cdot\mathbf{n}, \tag{5.25}$$

since $\operatorname{div}\mathbf{u} = 0$ in Ω_t while $\mathbf{w} = \mathbf{u}$ on Γ_t^w and $\mathbf{w} = \mathbf{0}$ on $\partial\Omega_t \setminus \Gamma_t^w$.

The other terms provide

$$\int_{\Omega_t}\mathbf{u}\cdot\boldsymbol{\nabla}p = (\text{since } p_{ext} = \text{const.})\ \int_{\Omega_t}\mathbf{u}\cdot\boldsymbol{\nabla}(p-p_{ext}) = -\int_{\Omega_t}(p-p_{ext})\operatorname{div}\mathbf{u} + \int_{\partial\Omega_t}(p-p_{ext})\mathbf{u}\cdot\mathbf{n} = \int_{\Gamma_t^{out}}(p-p_{ext})\mathbf{u}\cdot\mathbf{n} + \int_{\Gamma_t^w}(p-p_{ext})\mathbf{u}\cdot\mathbf{n}, \tag{5.26}$$

and

$$\int_{\Omega_t}\nu\mathbf{u}\cdot\mathbf{div}\,\mathbf{D}(\mathbf{u}) = -\int_{\Omega_t}\nu\boldsymbol{\nabla}\mathbf{u}:\mathbf{D}(\mathbf{u}) + \int_{\partial\Omega_t}\nu\mathbf{u}\cdot\mathbf{D}(\mathbf{u})\cdot\mathbf{n} = -\int_{\Omega_t}\nu\mathbf{D}(\mathbf{u}):\mathbf{D}(\mathbf{u}) + \int_{\partial\Omega_t}\nu\mathbf{u}\cdot\mathbf{D}(\mathbf{u})\cdot\mathbf{n} = -\int_{\Omega_t}\nu\mathbf{D}(\mathbf{u}):\mathbf{D}(\mathbf{u}) + \int_{\Gamma_t^{out}}\nu(\mathbf{D}(\mathbf{u})\cdot\mathbf{n})\cdot\mathbf{u} + \int_{\Gamma_t^w}\nu(\mathbf{D}(\mathbf{u})\cdot\mathbf{n})\cdot\mathbf{u}, \tag{5.27}$$

where we have exploited again the symmetry of $\mathbf{D}(\mathbf{u})$.

Using the results obtained in (5.24), (5.25), (5.26) and (5.27) into (5.23), rearranging the terms and recalling the boundary condition (5.15a) we can write

$$\frac{1}{2}\frac{d}{dt}\|\mathbf{u}\|^2_{\mathbf{L}^2(\Omega_t)} + 2\int_{\Omega_t}\nu\mathbf{D}(\mathbf{u}):\mathbf{D}(\mathbf{u}) + \frac{1}{2}\int_{\Gamma_t^{out}}|\mathbf{u}|^2\mathbf{u}\cdot\mathbf{n} + \int_{\Gamma_t^w}[(p-p_{ext})\mathbf{n} - 2\nu\mathbf{D}(\mathbf{u})\cdot\mathbf{n}]\cdot\mathbf{u} = \int_{\Omega_t}\mathbf{f}\cdot\mathbf{u}$$

We now recall expression (5.22) and recognise the equivalence of the integrals over Γ_t^w, which express the exchange of power (rate of energy) between fluid and structure. We multiply then the last equality by ω and add it to (5.22), obtaining (5.18).

Using (5.20), (3.2) and the fact that $\nu \geq \nu_0 > 0$,

$$\frac{d}{dt}\left[\frac{\omega}{2}\|\mathbf{u}(t)\|_{\mathbf{L}^2(\Omega_t)} + e_s(t)\right] + 2C_K\omega\nu_0\|\boldsymbol{\nabla}\mathbf{u}\|^2_{\mathbf{L}^2(\Omega_t)} + c\|\frac{\partial^2\eta}{\partial z\partial t}\|^2_{L^2(\Gamma_0^w)} \leq$$

$$\frac{d}{dt}\left[\frac{\omega}{2}\|\mathbf{u}(t)\|_{\mathbf{L}^2(\Omega_t)} + e_s(t)\right] + 2\omega\int_{\Omega_t}\nu\mathbf{D}(\mathbf{u}):\mathbf{D}(\mathbf{u}) + c\|\frac{\partial^2\eta}{\partial z\partial t}\|^2_{L^2(\Gamma_0^w)} \leq$$

$$\omega\int_{\Omega_t}\mathbf{f}\cdot\mathbf{u} \leq \frac{\omega}{4\epsilon}\|\mathbf{f}\|^2_{\mathbf{L}^2(\Omega_t)} + \omega\epsilon\|\mathbf{u}\|^2_{\mathbf{L}^2(\Omega_t)} \leq \frac{\omega}{4\epsilon}\|\mathbf{f}\|^2_{\mathbf{L}^2(\Omega_t)} + C_P^2\omega\epsilon\|\boldsymbol{\nabla}\mathbf{u}\|^2_{\mathbf{L}^2(\Omega_t)},$$

for any positive ϵ. To derive the last inequality we have applied the Poincaré inequality (3.1).

The desired result is then obtained by taking $\epsilon = \frac{\nu_0 C_K}{C_P^2}$ and integrating in time between t_0 and t. □

This last result shows that the energy associated to the coupled problem is bounded, at any time, by quantities which depend only on the initial condition and the applied volume forces. Moreover, since in blood flow simulation we neglect the volume force term $\mathbf{f}$ in the Navier-Stokes equations, estimate (5.21) simplifies into

$$\frac{\omega}{2}\|\mathbf{u}(t)\|_{\mathbf{L}^2(\Omega_t)} + e_s(t) + 2C_K\omega\nu_0\int_{t_0}^t\|\boldsymbol{\nabla}\mathbf{u}(\tau)\|^2_{\mathbf{L}^2(\Omega_\tau)}d\tau + c\int_{t_0}^t\|\frac{\partial^2\eta}{\partial z\partial t}(\tau)\|^2_{L^2(\Gamma_w^0)}d\tau$$
$$\leq \frac{\omega}{2}\|\mathbf{u}_0\|_{\mathbf{L}^2(\Omega_t)} + e_s(t_0), \quad \forall t \in I.$$

Remark 5.1. We may note that the non-linear convective term in the Navier-Stokes equations is crucial to obtain the stability result, because it generates a boundary term which compensates that coming from the treatment of the velocity time derivative. These two contributions are indeed only present in the case of a moving boundary.

♢

Remark 5.2. Should we replace the boundary condition (5.15a) by

$$2\nu\mathbf{D}(\mathbf{u})\cdot\mathbf{n} - (p - p_{ext} + \frac{1}{2}|\mathbf{u}|^2)\mathbf{n} = \mathbf{0} \qquad \text{on } \Gamma_t^{out},\ t \in I, \tag{5.28}$$

we would obtain the stability results without the restrictions on the outlet velocity (5.20).

Let us note that the above boundary condition amounts to imposing a zero value for the *total stress* at the outflow surface.

♢

Remark 5.3. Under slightly different assumptions, that is periodic boundary conditions in space and the presence of a further dissipative term proportional to $\frac{\partial^4\eta}{\partial z^4}$ in the generalised string model, H. Beirão da Veiga has recently proven [3] an existence result of strong solutions to the coupled fluid-structure problem.

♢

The hypothesis (5.20) is obviously satisfied if Γ_t^{out} is indeed an *outflow section*, i.e. $\mathbf{u}\cdot\mathbf{n} \geq 0$ for all $\mathbf{x} \in \Gamma_t^{out}$. As already pointed out, this is seldom true for vascular flow, particularly in large arteries.

We may observe that the "viscoelastic term" $-c\frac{\partial^3\eta}{\partial t\partial^2 z}$ in (4.23) allows to obtain the appropriate regularity of the velocity field $\mathbf{u}$ on the boundary (see [36]).

In the derivation of the energy inequality (5.21), we have considered homogeneous boundary conditions both for the fluid and the structure. However, the conditions

$\eta = 0$ at $z = 0$ and $z = L$, which correspond to hold the wall fixed at the two ends, are not realistic in the context of blood flow. Since the model (4.23) for the structure is of propagative type, the first order absorbing boundary conditions

$$\frac{\partial \eta}{\partial t} - \sqrt{a}\frac{\partial \eta}{\partial z} = 0 \qquad \text{at } z = 0, \tag{5.29}$$

$$\frac{\partial \eta}{\partial t} + \sqrt{a}\frac{\partial \eta}{\partial z} = 0 \qquad \text{at } z = L \tag{5.30}$$

look more suited to the problem at hand. An inequality of the type (5.21) could still be proven. Indeed the boundary term which appears in (4.31) would now read

$$-\left[a\frac{\partial \eta}{\partial z}\frac{\partial \eta}{\partial t} + c\frac{\partial^2 \eta}{\partial z \partial t}\frac{\partial \eta}{\partial t}\right]_{z=0}^{z=L} =$$
$$\sqrt{a}\left[\left(\frac{\partial \eta}{\partial t}\Big|_{z=0}\right)^2 + \left(\frac{\partial \eta}{\partial t}\Big|_{z=L}\right)^2\right] + \frac{c}{2}\sqrt{a}\frac{d}{dt}\left[\left(\frac{\partial \eta}{\partial t}\Big|_{z=0}\right)^2 + \left(\frac{\partial \eta}{\partial t}\Big|_{z=L}\right)^2\right].$$

This term, integrated in time, would eventually appear on the left hand side of inequality (5.21). We may note, however, that we obtain both for $z = 0$ and $z = L$ the following expression

$$\sqrt{a}\int_{t_0}^{t}\left(\frac{\partial \eta}{\partial t}(\tau)\right)^2 d\tau + \frac{c}{2}\sqrt{\frac{1}{a}}\left(\frac{\partial \eta}{\partial t}(t)\right)^2 = \frac{c}{2}\sqrt{\frac{1}{a}}\left(\frac{\partial \eta}{\partial t}(t_0)\right)^2. \tag{5.31}$$

This additional term is positive and depends only on initial conditions.

Yet, conditions (5.29) and (5.30) are not compatible with the homogeneous Dirichlet boundary conditions for the fluid; indeed, if $\eta|_{z=0} \neq 0$ and $\mathbf{u} = 0$ on Γ_t^{in}, the trace of $\mathbf{u}$ on the boundary is discontinuous and thus not compatible with the regularity required on the solution of (5.12) (see. e.g. [43]).

A possible remedy consists of changing the condition $\mathbf{u} = 0$ on Γ_t^{in} into

$$\mathbf{u} \cdot \mathbf{e}_z = g \circ \mathcal{A}_t^{-1}$$
$$\mathbf{T} \cdot \mathbf{n} - (\mathbf{T} \cdot \mathbf{n}) \cdot \mathbf{e}_z = \mathbf{0}$$

on Γ_t^{in}, where g is a given function defined on Γ_0^{in}, with $g = 0$ on $\partial\Gamma_0^{in}$. Here $\mathbf{T}$ is the stress tensor defined in (2.24). An energy inequality for the coupled problem can be derived also in this case with standard calculations, taking a suitable harmonic extension $\tilde{g}$ of the non homogeneous data g. The calculations are here omitted for the sake of brevity.

5.3. **An iterative algorithm to solve the coupled fluid-structure problem.** In this section we outline an algorithm that at each time-level allows the decoupling of the sub-problem related to the fluid from that related to the vessel wall. As usual, t^k, $k = 0, 1, \ldots$ denotes the k-th discrete time level; $\Delta t > 0$ is the time-step, while v^k is the approximation of the function (scalar or vector) v at time t^k.

The numerical solution of the fluid-structure interaction problem (5.12)-(5.13) will be carried out by constructing a suitable finite element approximation of each sub-problem. In particular, for the fluid we need to devise a finite element formulation suitable for moving domains (or, more precisely, moving grids). In this respect, the ALE formulation will provide an appropriate framework.

To better illustrate the situation we refer to Fig. 22 where we have drawn a 2D fluid structure interaction problem. The fluid domain is Ω_t and the movement of its upper boundary Γ_t^w is governed by a generalised string model. This geometry could be derived from an axisymmetric model of the flow inside a cylindrical vessel. However, in this case we should employ the Navier-Stokes equations in axisymmetric coordinates. Since this example is only for the purpose of illustrating a possible set-up a coupled fluid structure algorithm, for the sake of simplicity we consider here a

two-dimensional fluid structure problem governed by equations (5.12)-(5.13), with interface conditions (5.16), initial and boundary conditions (5.14) and the additional condition

$$\mathbf{u}|_{\Gamma^0} = \mathbf{0}, \quad t \in I.$$

The algorithm here presented may be readily extended to three dimensional problems.

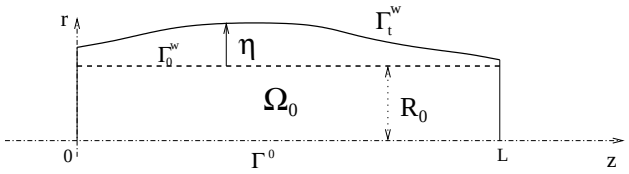

FIGURE 22. A simple fluid-structure interaction problem.

The structure on Γ_0^w will be discretised by means of a finite element triangulation $\mathcal{T}_h^s$, like the one we illustrate in Fig. 23. We have considered the space S_h of piecewise linear continuous (P1) finite elements functions to represent the approximate vessel wall displacement η_h. In the same figure we show the position at time t of the discretised vessel wall boundary $\Gamma_{t,h}^w$, corresponding to a given value of the discrete displacement field $\eta_h \in S_h$. Consequently, the fluid domain will be represented at every time by a polygon, which we indicate by $\Omega_{t,h}$. Its triangulation $\mathcal{T}_{t,h}^f$ will be constructed as the image by an appropriate ALE mapping $\mathcal{A}_t$ of a triangulation $\mathcal{T}_{0,h}^f$ of Ω_0, as shown in Fig. 24. Correspondingly, $\Omega_{t,h} = \mathcal{A}_t\Omega_{0,h}$, where $\Omega_{0,h}$ is the approximation of Ω_0 induced by the triangulation $\mathcal{T}_{t,h}^f$ (clearly, if Ω_0 has a polygonal boundary we have $\Omega_{0,h} = \Omega_0$.) The trace of $\mathcal{T}_{0,h}^f$ on Γ_0^w will coincide with the "triangulation" $\mathcal{T}_h^s$ of the vessel wall, thus we consider *geometrically conforming* finite elements between the fluid and the structure. The possibility of using a geometrically non-conforming finite element representation has been investigated in [26].

We then have to face the following problem. Suppose that we know at $t = t^{k+1}$ a discrete displacement field η_h^{k+1} and thus the corresponding position of the domain boundary $\partial\Omega_{t^{k+1},h}$. How to build a map $\mathcal{A}_{t^{k+1}}$ such that $\mathcal{A}_{t^{k+1}}(\mathcal{T}_{0,h}^f)$ is an acceptable finite element mesh for the fluid domain? This task is in general not simple. However, if we can assume that $\Omega_{t,h}$ is convex for all t and that the displacements are relatively small, the technique known as *harmonic extension* may well serve the purpose. Let $\mathbf{X}_h$ be the P1 finite element vector space associated to $\mathcal{T}_{0,h}^f$, while

$$\mathbf{X}_h^0 = \{\mathbf{w}_h \in \mathbf{X}_h : \quad \mathbf{w}_h|_{\partial\Omega_{0,h}} = \mathbf{0}\}$$

and let $\mathbf{g}_h : \partial\Omega_{0,h} \to \partial\Omega_{t^{k+1},h}$ be the function describing the fluid domain boundary. We build the map by seeking $\mathbf{y}_h \in \mathbf{X}_h$ such that

$$\begin{aligned} &\int_{\Omega_0} \nabla\mathbf{y}_h : \nabla\mathbf{z}_h = 0 \quad \forall \mathbf{z}_h \in \mathbf{X}_h^0, \\ &\mathbf{y}_h = \mathbf{g}_h, \quad \text{on } \partial\Omega_{0,h}, \end{aligned} \tag{5.32}$$

and then setting $\mathcal{A}_{t^{k+1}}(\mathbf{Y}) = \mathbf{y}_h(\mathbf{Y}), \quad \forall \mathbf{Y} \in \Omega_{0,h}$. This technique has indeed been adopted for the mesh in Fig. 24. From a practical point of view, the value of $\mathbf{y}_h$ in correspondence to the nodes of $\mathcal{T}_{0,h}^f$ gives the position of the corresponding node in $\mathcal{T}_{t,h}^f$ at time t^{k+1}. A more general discussion on the construction of the ALE mapping may be found in [17, 36] as well as in [23].

Remark 5.4. Adopting P1 elements for the construction of the ALE map ensures that the triangles of $\mathcal{T}_{h,0}^f$ are mapped into triangles, thus $\mathcal{T}_{h,t}^f$ is a valid triangulation, under the requirement of invertibility of the map (which is assured if the domain is convex and the wall displacements are small).

$\diamondsuit$

As for the time evolution, we may adopt a linear time variation within each time slab $[t^k, t^{k+1}]$ by setting

$$\mathcal{A}_t = \frac{t-t^k}{\Delta t}\mathcal{A}_{t^{k+1}} - \frac{t-t^{k+1}}{\Delta t}\mathcal{A}_{t^k}, \quad t \in [t^k, t^{k+1}].$$

Then, the corresponding domain velocity $\mathbf{w}_h$ will be constant on each time slab.

We are now in the position of describing a possible finite element scheme for both the structure and the fluid problem, to be adopted in the sub-structuring algorithm. We first give more details on the adopted finite element discretisation.

5.3.1. *Discretisation of the structure.* For the structure we consider a *mid-point* scheme. We introduce the additional variable $\dot\eta^k$ which is the approximation of the displacement velocity at time t^k.

The time advancing scheme reads:

$\forall k \geq 0$ *find* η^{k+1} *and* $\dot\eta^{k+1}$ *that satisfy the following system*

$$\frac{\eta^{k+1}-\eta^k}{\Delta t} = \frac{\dot\eta^k + \dot\eta^{k+1}}{2}, \tag{5.33a}$$

$$\frac{\dot\eta^{k+1}-\dot\eta^k}{\Delta t} - a\frac{\partial^2}{\partial z^2}\frac{\eta^k+\eta^{k+1}}{2} + b\frac{\eta^{k+1}+\eta^k}{2} - c\frac{\partial^2}{\partial z^2}\frac{\dot\eta^{k+1}+\dot\eta^k}{2} = H^{k+\frac12}, \tag{5.33b}$$

with

$$\eta^{k+1}|_{z=0} = \alpha(t^{k+1}), \quad \eta^{k+1}|_{z=L} = \beta(t^{k+1}), \tag{5.34a}$$

and

$$\dot\eta^{k+1}|_{z=0} = \frac{\partial}{\partial t}\alpha(t^{k+1}), \quad \dot\eta^{k+1}|_{z=L} = \frac{\partial}{\partial t}\beta(t^{k+1}), \tag{5.34b}$$

while the value of η^0 *and* $\dot\eta^0$ *are given by the initial conditions.*

Here, $H^{k+\frac12}$ is a suitable approximation of H at time $t^k + \frac12\Delta t$ which in the context of a sub-structuring iteration for the coupled problem is a known quantity and whose calculation from the Navier-Stokes data will be made precise later.

System (5.33) is then discretised in space by taking $\eta_h^k \in S_h$ and $\dot\eta_h^k \in S_h$. We set $S_h^0 = \{s_h \in S_h : \quad s_h(0) = 0,\, s_h(L) = 0\}$ and the finite element problem reads

For all $k \geq 0$ *find* $\eta_h^{k+1} \in S_h$ *and* $\dot\eta_h^{k+1} \in S_h$ *that satisfy the following system*

$$(2\eta_h^{k+1} - \Delta t\dot\eta_h^{k+1}, s_h) = (2\eta_h^k + \Delta t\dot\eta_h^k, s_h), \tag{5.35a}$$

$$\begin{aligned}&(\frac{1}{\Delta t}\dot\eta_h^{k+1} + \frac{b}{2}\eta_h^{k+1}, s_h) + \frac12(a\frac{\partial\eta_h^{k+1}}{\partial z} + c\frac{\partial\dot\eta_h^{k+1}}{\partial z}, \frac{\partial s_h}{\partial z}) = \\ &(H^{k+\frac12}, s_h) + (\frac{1}{\Delta t}\dot\eta_h^k + \frac{b}{2}\eta_h^k, s_h) - \frac12(a\frac{\partial\eta_h^k}{\partial z} + c\frac{\partial\dot\eta_h^k}{\partial z}, \frac{\partial s_h}{\partial z}),\end{aligned} \tag{5.35b}$$

$\forall s_h \in S_h^0$, *together with the boundary conditions*

$$\eta_h^{k+1}|_{z=0} = \alpha(t^{k+1}), \quad \eta_h^{k+1}|_{z=L} = \beta(t^{k+1}), \tag{5.36a}$$

$$\dot\eta_h^{k+1}|_{z=0} = \frac{\partial}{\partial t}\alpha(t^{k+1}), \quad \dot\eta_h^{k+1}|_{z=L} = \frac{\partial}{\partial t}\beta(t^{k+1}), \tag{5.36b}$$

and the initial conditions

$$\eta_h^0 = \pi_{S_h}\eta^0, \quad \eta_h^0 = \pi_{S_h}\eta^0,$$

being π^{S_h} the standard interpolation operator upon S_h.

5.3.2. *Discretisation of the fluid problem.* In the frame of our splitting scheme the velocity field at Γ_t^w as well as the current domain configuration are provided by the calculation of η_h; they can thus be considered as given data. We consider the following finite element spaces. $\widetilde{Q}_h$ is the space of continuous piece-wise linear finite elements, while $\widetilde{\mathbf{V}}_h$ is that of vector functions whose components are in the space $\widetilde{V}_h$ of continuous piece-wise quadratic (or P1-isoP2) finite elements. Both refer to the triangulation $\mathcal{T}_{0,h}^f$ of Ω_0. For a precise definition of these finite element spaces the reader may refer to [43] or [5].

We will also need to define

$$\widetilde{\mathbf{V}}_h^0 = \{\widetilde{\mathbf{v}}_h \in \widetilde{\mathbf{V}}_h : \quad \widetilde{\mathbf{v}}_h|_{\partial\Omega_0 \setminus \Gamma_0^{in}} = \mathbf{0}, \}$$

and the space $\widetilde{V}_h^{\Gamma_0^w}$ formed by function in Γ_0^w which are the trace of a function in $\widetilde{V}_h$.

The corresponding spaces on the current configuration will be given by

$$Q_{h,t} = \{q_h : \quad q_h \circ \mathcal{A}_t \in \widetilde{Q}_h\},$$

$$\mathbf{V}_{h,t} = \{\mathbf{v}_h : \quad \mathbf{v}_h \circ \mathcal{A}_t \in \widetilde{\mathbf{V}}_h\},$$

and analogously for $\mathbf{V}_{h,t}^0$.

Remark 5.5. The functions belonging to $Q_{h,t}$ and $\mathbf{V}_{h,t}$ depend also on time through the ALE mapping. A thorough presentation of finite element spaces in an ALE framework is contained in [17] and [36].

$\Diamond$

We will employ an implicit Euler time advancing scheme with a semi-explicit treatment of the convective term. Let us assume that the solution $(\mathbf{u}_h^k, p_h^k)$ at time step t^k is known, as well as the domain configuration $\Omega_{t^{k+1},h}$ at time t^{k+1} (and thus the corresponding ALE map).

The numerical solution at t^{k+1} can be computed as follows:

Find $\mathbf{u}_h^{k+1} \in \mathbf{V}_{h,t^{k+1}}$ and $p_h^{k+1} \in Q_{h,t^{k+1}}$ such that

$$\begin{aligned} &\frac{1}{\Delta t}(\mathbf{u}^{k+1}, \widetilde{\mathbf{v}}_h)_{k+1} - c_{k+\frac{1}{2}}(\mathbf{w}^{k+\frac{1}{2}}, \mathbf{u}^{k+1}, \widetilde{\mathbf{v}}_h) + c_{k+1}(\mathbf{u}^k, \mathbf{u}^{k+1}, \widetilde{\mathbf{v}}_h) + \\ &d_{k+\frac{1}{2}}(\mathbf{w}^{k+\frac{1}{2}}, \mathbf{u}^{k+1}, \widetilde{\mathbf{v}}_h) + b_{k+1}(\widetilde{\mathbf{v}}_h, p^{k+1}) + a_{k+1}(\mathbf{u}^{k+1}, \widetilde{\mathbf{v}}_h) = \\ &(\mathbf{f}^{k+1}, \widetilde{\mathbf{v}}_h)_{k+1} + \frac{1}{\Delta t}(\mathbf{u}^k, \widetilde{\mathbf{v}}_h)_k, \quad \forall \widetilde{\mathbf{v}}_h \in \widetilde{\mathbf{V}}_h^0 \end{aligned} \tag{5.37a}$$

$$b_{k+1}(\mathbf{u}^{k+1}, \widetilde{q}_h) = 0, \quad \forall \widetilde{q}_h \in \widetilde{Q}_h, \tag{5.37b}$$

and

$$\mathbf{u}_h^{k+1} = \mathbf{g}_h^{k+1}, \quad \text{on } \Gamma_{t^{k+1}}^{in}, \tag{5.38a}$$

$$\mathbf{u}_h^{k+1} = \left(\Pi_h^{\Gamma_0^w} \dot{\eta}_h^{k+1}\right) \circ \mathcal{A}_{t^{k+1}}^{-1} \mathbf{e}_r, \quad \text{on } \Gamma_{t^{k+1}}^{w}. \tag{5.38b}$$

We have defined

$$(\mathbf{w},\widetilde{\mathbf{v}})_k = \int_{\Omega_{t^k}} \mathbf{w}\cdot(\widetilde{\mathbf{v}}\circ\mathcal{A}_{t^k}^{-1}),$$

$$c_k(\mathbf{w},\mathbf{z},\widetilde{\mathbf{v}}) = \int_{\Omega_{t^k}} ((\mathbf{w}\cdot\boldsymbol{\nabla})\mathbf{z})\cdot(\widetilde{\mathbf{v}}\circ\mathcal{A}_{t^k}^{-1}),$$

$$d_k(\mathbf{w},\mathbf{z},\widetilde{\mathbf{v}}) = \int_{\Omega_{t^k}} (\operatorname{div}\mathbf{w})\mathbf{z}\cdot(\widetilde{\mathbf{v}}\circ\mathcal{A}_{t^k}^{-1}),$$

$$b_k(\mathbf{w},\widetilde{q}) = \int_{\Omega_{t^k}} \operatorname{div}\mathbf{w}\,(\widetilde{q}\circ\mathcal{A}_{t^k}^{-1}), \quad b_k(\widetilde{\mathbf{w}},q) = \int_{\Omega_{t^k}} \operatorname{div}(\widetilde{\mathbf{w}}\circ\mathcal{A}_{t^k}^{-1})\,q,$$

$$a_k(\mathbf{w},\widetilde{\mathbf{v}}) = \int_{\Omega_{t^k}} 2\nu\mathbf{D}(\mathbf{w}) : \mathbf{D}(\widetilde{\mathbf{v}}\circ\mathcal{A}_{t^k}^{-1}).$$

The function $\mathbf{g}_h^{k+1}$ is the finite element interpolant of the boundary data $\mathbf{g}(t^{k+1})$ on the space of restrictions of $\mathbf{V}_{h,t^{k+1}}$ on $\Gamma_{t^{k+1}}^{in}$. Moreover, $\Pi_h^{\Gamma_0^w} : S_h \to \widetilde{V}_h^{\Gamma_0^w}$ is the interpolation operator required to project the discrete vessel velocity computed by the structure solver on the trace space of discrete fluid velocity on the vessel wall. Since we are using geometrically conforming finite elements, this operator is quite simple to build up.

It is understood that when the approximation of $\mathbf{u}$ and $\mathbf{w}$ in (5.37) are not evaluated at the same time as the integral, they need to be mapped on the correct domain by means of the ALE transformation.

Remark 5.6. The term involving the domain velocity $\mathbf{w}$ has been computed on the intermediate geometry $\Omega_{t^{k+\frac{1}{2}}}$ in order to satisfy the so-called Geometric Conservation Law (GCL) [27]. A discussion on the significance of the GCL for the problem at hand may be found in [36].

$\diamondsuit$

5.3.3. *Recovering the forcing term for the vessel wall.* We need now to compute the forcing term $H^{k+\frac{1}{2}}$ in (5.35) as the residual of the discrete momentum equation (5.37b) for time step t^{k+1}. Let us define

$$R_h^{k+1}(\widetilde{\mathbf{v}}_h) = (\mathbf{f}^{k+1},\widetilde{\mathbf{v}}_h)_{k+1} + \frac{1}{\Delta t}(\mathbf{u}^k,\widetilde{\mathbf{v}}_h)_k - \frac{1}{\Delta t}(\mathbf{u}^{k+1},\widetilde{\mathbf{v}}_h)_{k+1} +$$
$$c_{k+\frac{1}{2}}(\mathbf{w}^{k+\frac{1}{2}},\mathbf{u}^{k+1},\widetilde{\mathbf{v}}_h) - c_{k+1}(\mathbf{u}^k,\mathbf{u}^{k+1},\widetilde{\mathbf{v}}_h) -$$
$$d_{k+\frac{1}{2}}(\mathbf{w}^{k+\frac{1}{2}},\mathbf{u}^{k+1},\widetilde{\mathbf{v}}_h) - b_{k+1}(\widetilde{\mathbf{v}}_h,p^{k+1}) - a_{k+1}(\mathbf{u}^{k+1},\widetilde{\mathbf{v}}_h), \quad \forall\widetilde{\mathbf{v}}_h\in\widetilde{\mathbf{V}}_h.$$

Note that $R_h^{k+1}(\widetilde{\mathbf{v}}_h) = 0$, for all $\widetilde{\mathbf{v}}_h\in\widetilde{\mathbf{V}}_h^0$. We define the following operator

$$boldsymbol{\mathcal{S}}_h : S_h \to \widetilde{\mathbf{V}}_h, \qquad \boldsymbol{\mathcal{S}}_h s_h = [\mathcal{R}_h(\Pi_h^{\Gamma_0^w} s_h)]\mathbf{e}_r,$$

where $\mathcal{R}_h : \widetilde{V}_h^{\Gamma_0^w} \to \widetilde{V}_h$ is a finite element extension operator such that

$$(\mathcal{R}_h v_h)|_{\Gamma_0^w} = v_h, \quad \forall v_h\in\widetilde{V}_h^{\Gamma_0^w},$$

for instance the one obtained by extending by zero at all internal nodes (see [44]). We then take

$$(H^{k+\frac{1}{2}},s_h) = \frac{\omega}{2}\left[R_h^{k+1}(\boldsymbol{\mathcal{S}}_h s_h) + R_h^k(\boldsymbol{\mathcal{S}}_h s_h)\right]. \tag{5.39}$$

5.3.4. *The algorithm.* We are now in the position of describing an iteration algorithm for the solution of the coupled problem. As usual, we assume to have all quantities available at $t = t^k$, $k \geq 0$, provided either by previous calculations or by the initial data and we wish to advance to the new time step t^{k+1}. For ease of notation we here omit the subscript h, with the understanding that we are referring exclusively to finite element quantities.

The algorithm requires to choose a *tolerance* $\tau > 0$, which is used to test the convergence of the procedure, and a *relaxation parameter* $0 < \theta \leq 1$. In the following, the subscript $j \geq 0$ denotes the sub-iteration counter.

The algorithm reads:

A1 Extrapolate the vessel wall structure displacements and velocity:

$$\eta_{(0)}^{k+1} = \eta^k + \Delta t \dot{\eta}^k, \qquad \dot{\eta}_{(0)}^{k+1} = \dot{\eta}^k.$$

A2 Set $j = 0$.

A2.1 By using $\eta_{(j)}^{k+1}$ compute the new grid for the fluid domain Ω_t and the ALE map by solving (5.32).

A2.2 Solve the Navier-Stokes problem (5.37) to compute $\mathbf{u}_{(j+1)}^{k+1}$ and $p_{(j+1)}^{k+1}$, using as velocity on the wall boundary the one calculated from $\dot{\eta}_{(j)}^{k+1}$.

A2.3 Solve (5.35) to compute η_*^{k+1} and $\dot{\eta}_*^{k+1}$ using as forcing term the one recovered from $\mathbf{u}_{(j+1)}^{k+1}$ and $p_{(j+1)}^{k+1}$ using (5.39).

A2.4 Unless $\|\eta_*^{k+1} - \eta_{(j)}^{k+1}\|_{L^2(\Gamma_0^w)} + \|\dot{\eta}_*^{k+1} - \dot{\eta}_{(j)}^{k+1}\|_{L^2(\Gamma_0^w)} \leq \tau$, set

$$\eta_{(j+1)}^{k+1} = \theta\eta_{(j)}^{k+1} + (1-\theta)\eta_*^{k+1}, \ \dot{\eta}_{(j+1)}^{k+1} = \theta\dot{\eta}_{(j)}^{k+1} + (1-\theta)\dot{\eta}_*^{k+1},$$

and $j \leftarrow j + 1$. Then return to step 2a.

A3 Set

$$\eta^{k+1} = \eta_*^{k+1}, \qquad \dot{\eta}^{k+1} = \dot{\eta}_*^{k+1}.$$
$$\mathbf{u}^{k+1} = \mathbf{u}_{(j+1)}^{k+1}, \qquad p^{k+1} = p_{(j+1)}^{k+1}.$$

If the algorithm converges, $\lim_{j\to\infty} \mathbf{u}_{(j)}^{k+1} = \mathbf{u}^{k+1}$ and $\lim_{j\to\infty} \eta_{(j)}^{k+1} = \eta^{k+1}$, where $\mathbf{u}^{k+1}$ and η^{k+1} are the solution at time step t^{k+1} of the coupled problem.

The algorithm entails, at each sub-iteration, the computation of the generalised string equation (5.35)–(5.36), the Navier-Stokes equations and the solution of two Laplace equations (5.32), one for every displacement component.

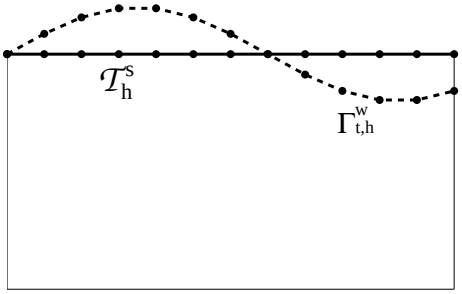

FIGURE 23. Position of the discretised vessel wall corresponding to a possible value of η_h.

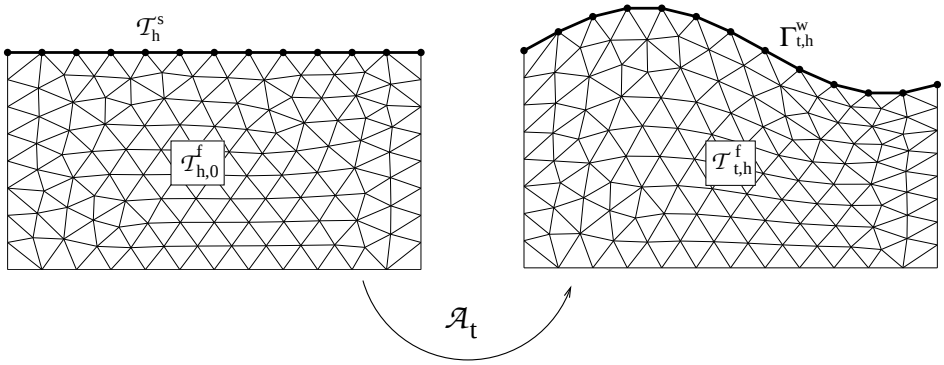

FIGURE 24. The triangulation used for the fluid problem at each time t is the the image through a map $\mathcal{A}_t$ of a mesh constructed on Ω_0.

6. ONE DIMENSIONAL MODELS OF BLOOD FLOW IN ARTERIES

In this Section we introduce a simple 1D model to describe the flow motion in arteries and its interaction with the wall displacement. In the absence of branching, a short section of an artery may be considered as a cylindrical compliant tube. As before we denote by $I = (t_0, t_1)$ the time interval of interest and by Ω_t the spatial domain which is supposed to be a circular cylinder filled with blood.

As already done in Sect. 4, we will employ cylindrical coordinates and indicate with $\mathbf{e}_r$, $\mathbf{e}_\theta$ and $\mathbf{e}_z$ the radial, circumferential and axial unit vectors, respectively, and with (r, θ, z) the corresponding coordinates system. The vessel extends from $z = 0$ to $z = L$ and the vessel length L is constant with time.

The basic model is deduced by making the following assumptions, some of which are analogous to the ones made in Sect. 4.

- A1 *Axial symmetry.* All quantities are independent from the angular coordinate θ. As a consequence, every axial section z =const remains circular during the wall motion. The tube radius R is a function of z and t.
- A2 *Radial displacements.* The wall displaces along the radial direction solely, thus at each point on the tube surface we may write $\boldsymbol{\eta} = \eta \mathbf{e}_r$, where $\eta = R - R_0$ is the displacement with respect to the reference radius R_0.
- A3 *Constant pressure.* We assume that the pressure P is constant on each section, so that it depends only on z and t.
- A4 *No body forces.* We neglect body forces (the inclusion of the gravity force, if needed, is straightforward); thus we put $\mathbf{f} = \mathbf{0}$ in the momentum equation (3.5a).
- A5 *Dominance of axial velocity.* The velocity components orthogonal to the z axis are negligible compared to the component along z. The latter is indicated by u_z and its expression in cylindrical coordinates reads

$$u_z(t, r, z) = \overline{u}(t, z) s\left(\frac{r}{R(z)}\right) \tag{6.1}$$

where $\overline{u}$ is the *mean velocity* on each axial section and $s : \mathbb{R} \to \mathbb{R}$ is a *velocity profile*[6].

A generic axial section will be indicated by $\mathcal{S} = \mathcal{S}(t, z)$. Its measure A is given by

$$A(t, z) = \text{meas}(\mathcal{S}(t, z)) = 2\pi R^2(t, z) = 2\pi(R_0(z) + \eta(t, z))^2. \tag{6.2}$$

The mean velocity $\overline{u}$ is then given by

$$\overline{u} = A^{-1} \int_{\mathcal{S}} u_z d\sigma,$$

and from (6.1) it follows that

$$\int_{\mathcal{S}} s d\sigma = A.$$

We will indicate with α the *momentum-flux correction coefficient*, (sometimes called Coriolis coefficient) defined as

$$\alpha = \frac{\int_{\mathcal{S}} {u_z}^2 d\sigma}{A\overline{u}^2} = \frac{\int_{\mathcal{S}} s^2 d\sigma}{A}, \tag{6.3}$$

where the dependence of the various quantities on the spatial and time coordinates is understood. It is immediate to verify that $\alpha \geq 1$. In general this coefficient will vary in time and space, yet in our model is taken constant as a consequence of (6.1).

[6]The fact that the velocity profile does not vary is in contrast with experimental observations and numerical results carried out with full scale models. However, it is a necessary assumption for the derivation of the reduced model. One may then think s as being a profile representative of an average flow configuration.

One possible choice for the profile law is the parabolic profile $s(y) = 2(1-y^2)$, which corresponds to the Poiseuille solution characteristic of steady flow in circular tubes. In this case we have $\alpha = \frac{4}{3}$. However, for blood flow in arteries it has been found that the velocity profile is, on average, rather flat. Indeed, a profile law often used for blood flow in arteries (see for instance [53]) is a power law of the type $s(y) = \gamma^{-1}(\gamma+2)(1-y^\gamma)$, with typically $\gamma = 9$ (the value $\gamma = 2$ gives again the parabolic profile). Correspondingly, we have $\alpha = 1.1$. Furthermore, we will see that the choice $\alpha = 1$, which indicates a completely flat velocity profile, would lead to a certain simplification in our analysis.

The mean flux Q, defined as

$$Q = \int_{\mathcal{S}} u_z d\sigma = A\overline{u},$$

is one of the main variables of our problem, together with A and the pressure P.

6.1. **The derivation of the model.** There are (at least) three ways of deriving our model. The first one moves from the incompressible Navier-Stokes equations with constant viscosity and performs an asymptotic analysis by assuming that the ratio $\frac{R_0}{L}$ is small, thus discarding the higher order terms with respect to $\frac{R_0}{L}$ (see [2]). The second approach derives the model directly from the basic conservation laws written in integral form. The third approach consists of integrating the Navier-Stokes equations on a generic section $\mathcal{S}$.

We will indicate with Γ_t^w the wall boundary of Ω_t, which now reads

$$\Gamma_t^w = \{(r,\theta,z) : r = R(z,t), \theta \in [0,2\pi)\, z \in (0,L)\}$$

while $\mathbf{n}$ is the outwardly oriented normal to $\partial\Omega_t$. Under the previous assumption, the momentum and continuity equations along z are

$$\frac{\partial u_z}{\partial t} + \operatorname{div}(u_z \mathbf{u}) + \frac{1}{\rho}\frac{\partial P}{\partial z} - \nu \Delta u_z = 0, \quad z \in (0,L),\, t \in I \tag{6.4a}$$

$$\operatorname{div} \mathbf{u} = 0, \quad z \in (0,L),\, t \in I, \tag{6.4b}$$

and on the tube wall we have

$$\mathbf{u} = \dot{\boldsymbol{\eta}}, \text{ on } \Gamma_t^w,\, t \in I.$$

We have written the convective term in divergence form, like in (2.23), because it simplifies the further derivation.

To ease notation, in this section we will omit to explicitly indicate the time dependence, with the understanding that all variables are considered at time t. Let us consider the portion $\mathcal{P}$ of Ω_t, sketched in Fig. 25, comprised between $z = z^* - \frac{dz}{2}$ and $z = z^* + \frac{dz}{2}$, with $z^* \in (0,L)$ and $dz > 0$ small enough so that $z^* + \frac{dz}{2} < L$ and $z^* - \frac{dz}{2} > 0$. The part of $\partial\mathcal{P}$ laying on the tube wall is indicated by $\Gamma_{\mathcal{P}}^w$. The reduced model is derived by integrating (6.4b) and (6.4a) on $\mathcal{P}$ and passing to the limit as $dz \to 0$, assuming that all quantities are smooth enough

We will first illustrate a result derived from the application of the ALE transport theorem (Theorem 5.1) to $\mathcal{P}$.

Lemma 6.1. *Let $f : \Omega_t \times I \to \mathbb{R}$ be an axisymmetric function, i.e. $\dfrac{\partial f}{\partial \theta} = 0$. Let us indicate by f_w the value of f on the wall boundary and by $\overline{f}$ its mean value on each axial section, defined by*

$$\overline{f} = A^{-1}\int_{\mathcal{S}} f d\sigma.$$

We have the following relation

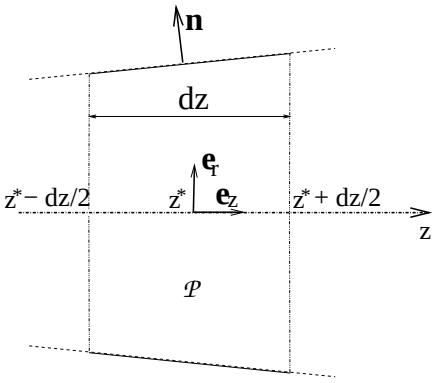

FIGURE 25. A longitudinal section (θ =const.) of the tube and the portion between $z = z^* - \frac{dz}{2}$ and $z = z^* + \frac{dz}{2}$ used for the derivation of the 1D reduced model.

$$\frac{\partial}{\partial t}(A\overline{f}) = A\overline{\frac{\partial f}{\partial t}} + 2\pi R\dot{\eta} f_w. \tag{6.5}$$

In particular taking $f = 1$ yields

$$\frac{\partial A}{\partial t} = 2\pi R\dot{\eta}. \tag{6.6}$$

Proof. The application of (5.10) to $\mathcal{P}$ gives

$$\frac{d}{dt}\int_{\mathcal{P}} f = \int_{\mathcal{P}} \frac{\partial f}{\partial t} + \int_{\partial\mathcal{P}} f\mathbf{g}\cdot\mathbf{n}, \tag{6.7}$$

where $\mathbf{g}$ denotes the velocity of the boundary of $\mathcal{P}$, i.e.

$$\mathbf{g} = \begin{cases} \dot{\boldsymbol{\eta}} & \text{on } \Gamma_{\mathcal{P}}^w, \\ \mathbf{0} & \text{on } \partial\mathcal{P}\setminus\Gamma_{\mathcal{P}}^w. \end{cases} \tag{6.8}$$

Then, by applying the mean-value theorem to both sides of (6.7) we have

$$\frac{d}{dt}[A(z^*)\overline{f}(z^*)dz + o(dz)] = A\overline{\frac{\partial f}{\partial t}} + o(dz) + \int_{\Gamma_{\mathcal{P}}^w} f\dot{\eta}\mathbf{e}_r\cdot\mathbf{n}.$$

We recall relation (4.6), already used in the derivation of the models for the wall structure dynamics, to write

$$\int_{\Gamma_{\mathcal{P}}^w} f\dot{\eta}\mathbf{e}_r\cdot\mathbf{n} = \int_0^{2\pi}\int_{z^*-\frac{dz}{2}}^{z^*+\frac{dz}{2}} f\dot{\eta}R\,dz\,d\theta = [2\pi\dot{\eta}(z^*)R(z^*)f_w(z^*)dz + o(dz)]. \tag{6.9}$$

By substituting into (6.7), dividing by dz and passing to the limit as $dz \to 0$ we obtain the desired result. □

We are now ready to derive our reduced model. We start first from the continuity equation. Using the divergence theorem, we obtain

$$0 = \int_{\mathcal{P}} \operatorname{div} \mathbf{u} = -\int_{\mathcal{S}^-} u_z + \int_{\mathcal{S}^+} u_z + \int_{\Gamma_{\mathcal{P}}^w} \mathbf{u}\cdot\mathbf{n} = -\int_{\mathcal{S}^-} u_z + \int_{\mathcal{S}^+} u_z + \int_{\Gamma_{\mathcal{P}}^w} \dot{\boldsymbol{\eta}}\cdot\mathbf{n}. \tag{6.10}$$

We have exploited (6.8) and the fact that $\mathbf{n} = -\mathbf{e}_z$ on $\mathcal{S}^-$ while $\mathbf{n} = \mathbf{e}_z$ on $\mathcal{S}^+$. Now, since $\dot{\boldsymbol{\eta}} = \dot{\eta}\mathbf{e}_r$, we deduce

$$\int_{\Gamma_{\mathcal{P}}^w} \dot{\boldsymbol{\eta}}\cdot\mathbf{n} = [2\dot{\eta}\pi R(z^*)dz + o(dz)] = \text{ (by (6.6)) } = \frac{\partial}{\partial t}A(z^*)dz + o(dz).$$

By substituting into (6.10), using the definition of Q, and passing to the limit as $dz \to 0$, we finally obtain

$$\frac{\partial A}{\partial t} + \frac{\partial Q}{\partial z} = 0,$$

which is the reduced form of the continuity equation.

We will now consider all terms in the momentum equation in turn. Again, we will integrate them over $\mathcal{P}$ and consider the limit as dz tends to zero.

$$\int_{\mathcal{P}} \frac{\partial u_z}{\partial t} = \frac{d}{dt}\int_{\mathcal{P}} u_z - \int_{\partial\mathcal{P}} u_z \mathbf{g}\cdot\mathbf{n} = \frac{d}{dt}\int_{\mathcal{P}} u_z.$$

In order to eliminate the boundary integral we have exploited the fact that $u_z = 0$ on $\Gamma_{\mathcal{P}}^w$ and $\mathbf{g} = \mathbf{0}$ on $\mathcal{S}^-$ and $\mathcal{S}^+$. We may then write

$$\int_{\mathcal{P}} \frac{\partial u_z}{\partial t} = \frac{\partial}{\partial t}[A(z^*)\overline{u}(z^*)dz + o(dz)] = \frac{\partial Q}{\partial t}(z^*)dz + o(dz).$$

Moreover, we have

$$\int_{\mathcal{P}} \operatorname{div}(u_z\mathbf{u}) = \int_{\partial\mathcal{P}} u_z\mathbf{u}\cdot\mathbf{n} = -\int_{\mathcal{S}^-} {u_z}^2 + \int_{\mathcal{S}^+} {u_z}^2 + \int_{\Gamma_{\mathcal{P}}^w} u_z\mathbf{g}\cdot\mathbf{n} =$$

$$\alpha[A(z^* + \frac{dz}{2})\overline{u}^2(z^* + \frac{dz}{2}) - A(z^* - \frac{dz}{2})\overline{u}^2(z^* - \frac{dz}{2})] = \frac{\partial \alpha A\overline{u}^2}{\partial z}(z^*)dz + o(dz).$$

Again, we have exploited the condition $u_z = 0$ on $\Gamma_{\mathcal{P}}^w$.

Since the pressure is assumed to be constant on each section, we obtain

$$\int_{\mathcal{P}} \frac{\partial P}{\partial z} = -\int_{\mathcal{S}^-} P + \int_{\mathcal{S}^+} P + \int_{\Gamma_{\mathcal{P}}^w} Pn_z = A(z^* + \frac{dz}{2})P(z^* + \frac{dz}{2}) - A(z^* - \frac{dz}{2})P(z^* - \frac{dz}{2}) + \int_{\Gamma_{\mathcal{P}}^w} Pn_z \tag{6.11}$$

Since

$$\int_{\partial\mathcal{P}} n_z = 0,$$

we may write that

$$\int_{\Gamma_{\mathcal{P}}^w} Pn_z = P(z^*)\int_{\Gamma_{\mathcal{P}}^w} n_z + o(dz) = -P(z^*)\int_{\partial\mathcal{P}\setminus\Gamma_{\mathcal{P}}^w} n_z + o(dz) = -P(z^*)(A(z^* + \frac{dz}{2}) - A(z^* - \frac{dz}{2})) + o(dz)$$

By substituting the last result into (6.11) we have

$$\int_{\mathcal{P}} \frac{\partial P}{\partial z} = A(z^* + \frac{dz}{2})P(z^* + \frac{dz}{2}) - A(z^* - \frac{dz}{2})P(z^* - \frac{dz}{2}) - P(z^*)[A(z^* + \frac{dz}{2}) - A(z^* - \frac{dz}{2})] + o(dz)$$
$$= \frac{\partial (AP)}{\partial z}(z^*)dz - P(z^*)\frac{\partial A}{\partial z}(z^*)dz + o(dz) = A\frac{\partial P}{\partial z}(z^*)dz + o(dz).$$

We finally consider the viscous term,

$$\int_{\mathcal{P}} \Delta u_z = \int_{\partial \mathcal{P}} \boldsymbol{\nabla} u_z \cdot \mathbf{n} = -\int_{\mathcal{S}^-} \frac{\partial u_z}{\partial z} + \int_{\mathcal{S}^+} \frac{\partial u_z}{\partial z} + \int_{\Gamma_{\mathcal{P}}^w} \boldsymbol{\nabla} u_z \cdot \mathbf{n}.$$

We neglect $\frac{\partial u_z}{\partial z}$ by assuming that its variation along z is small compared to the other terms. Moreover, we split $\mathbf{n}$ into two vector components, the radial component $\mathbf{n}_r = n_r \mathbf{e}_r$ and $\mathbf{n}_z = \mathbf{n} - \mathbf{n}_r$. Owing to the cylindrical geometry, $\mathbf{n}$ has no component along the circumpherential coordinate and, consequently, $\mathbf{n}_z$ is indeed oriented along z. We may thus write

$$\int_{\mathcal{P}} \Delta u_z = \int_{\Gamma_{\mathcal{P}}^w} (\boldsymbol{\nabla} u_z \cdot \mathbf{n}_z + \boldsymbol{\nabla} u_z \cdot \mathbf{e}_r n_r)\, d\sigma.$$

Again, we neglect the term $\boldsymbol{\nabla} u_z \cdot \mathbf{n}_z$, which is proportional to $\frac{\partial u_z}{\partial z}$. We recall relation (6.1) to write

$$\int_{\mathcal{P}} \Delta u_z = \int_{\Gamma_{\mathcal{P}}^w} n_r \boldsymbol{\nabla} u_z \cdot \mathbf{e}_r d\sigma = \int_{\Gamma_{\mathcal{P}}^w} \overline{u} R^{-1} s'(1) \mathbf{n} \cdot \mathbf{e}_r d\sigma = 2\pi \int_{z^* - \frac{dz}{2}}^{z^* + \frac{dz}{2}} \overline{u} s'(1) dz,$$

where we have used the relation $n_r d\sigma = 2\pi R dz$ and indicated by s' the first derivative of s.

Then,

$$\int_{\mathcal{P}} \Delta u_z \approx 2\pi \overline{u}(z^*) s'(1) dz.$$

By substituting all results into (6.4a), dividing all terms by dz and passing to the limit as $dz \to 0$, we may finally write the momentum equation of our one dimensional model as follows

$$\frac{\partial Q}{\partial t} + \frac{(\partial \alpha A \overline{u}^2)}{\partial z} + \frac{A}{\rho}\frac{\partial P}{\partial z} + K_r \overline{u} = 0,$$

where

$$K_r = -2\pi\nu s'(1)$$

is a *friction parameter*, which depends on the type of profile chosen, i.e. on the choice of the function s in (6.1). For a profile law given by $s(y) = \gamma^{-1}(\gamma + 2)(1 - y^\gamma)$ we have $K_r = 2\pi\nu(\gamma + 2)$. In particular, for a parabolic profile $K_r = 8\pi\nu$, while for $\gamma = 9$ we obtain $K_r = 22\pi\nu$.

To conclude, the final system of equations reads

$$\frac{\partial A}{\partial t} + \frac{\partial Q}{\partial z} = 0, \quad z \in (0, L),\, t \in I, \tag{6.12a}$$

$$\frac{\partial Q}{\partial t} + \alpha \frac{\partial}{\partial z}\left(\frac{Q^2}{A}\right) + \frac{A}{\rho}\frac{\partial P}{\partial z} + K_r\left(\frac{Q}{A}\right) = 0, \quad z \in (0, L),\, t \in I, \tag{6.12b}$$

where the unknowns are A, Q and P and α is here taken constant.

6.2. **Accounting for the vessel wall displacement.** In order to close system (6.12) we provide a relation for the pressure. A possibility is to resort to an algebraic relation linking pressure to the wall deformation and consequently to the vessel section A.

More generally, we may assume that the pressure satisfies a relation like

$$P(t,z) - P_{ext} = \psi(A(t,z); A_0(z), \boldsymbol{\beta}(z)), \tag{6.13}$$

where we have outlined that the pressure will in general depend also on $A_0 = \pi R_0^2$ and on a set of coefficients $\boldsymbol{\beta} = (\beta_0, \beta_1, \cdots, \beta_p)$, related to physical and mechanical properties, that are, in general, *given* functions of z. Here P_{ext} indicates, as in Sect. 4, the external pressure. We require that ψ be (at least) a C^1 function of all its arguments and be defined for all $A > 0$ and $A_0 > 0$, while the range of variation of $\boldsymbol{\beta}$ will depend by the particular mechanical model chosen for the vessel wall.

Furthermore, we require that for all allowable values of A, A_0 and $\boldsymbol{\beta}$

$$\frac{\partial \psi}{\partial A} > 0, \quad \text{and} \quad \psi(A_0; A_0, \boldsymbol{\beta}) = 0. \tag{6.14}$$

By exploiting the linear elastic law provided in (4.17), with the additional simplifying assumption (4.16), and using the fact that

$$\eta = (\sqrt{A} - \sqrt{A_0})/\sqrt{\pi} \tag{6.15}$$

we can obtain the following expression for ψ

$$\psi(A; A_0, \beta_0) = \beta_0 \frac{\sqrt{A} - \sqrt{A_0}}{A_0}. \tag{6.16}$$

We have identified $\boldsymbol{\beta}$ with the single parameter $\beta_0 = \frac{\sqrt{\pi} h_0 E}{1-\xi^2}$. The latter depends on z only in those cases where the Young modulus E or the vessels thickness h_0 are not constant.

For ease of notation, the dependence of A, A_0 and $\boldsymbol{\beta}$ from their arguments will be understood. It is immediate to verify that all the requirements in (6.14) are indeed satisfied.

Another commonly used expression for the pressure-area relationship is given by [28, 53]

$$\psi(A; A_0, \boldsymbol{\beta}) = \beta_0 \left[\left(\frac{A}{A_0} \right)^{\beta_1} - 1 \right].$$

In this case, $\boldsymbol{\beta} = (\beta_0, \beta_1)$, where $\beta_0 > 0$ is an elastic coefficient while $\beta_1 > 0$ is normally obtained by fitting the stress-strain response curves obtained by experiments.

Another alternative formulation [32] is

$$\psi(A; A_0, \boldsymbol{\beta}) = \beta_0 \tan \left[\pi \left(\frac{A - A_0}{2A_0} \right) \right],$$

where again the coefficients vector $\boldsymbol{\beta}$ reduces to the single coefficient β_0.

In the following, whenever not strictly necessary we will omit to indicate the dependence of the various quantities on A_0 and $\boldsymbol{\beta}$, which is however always understood.

6.3. **The final model.** By exploiting relation (6.13) we may eliminate the pressure P from the momentum equation. To that purpose we will indicate by $c_1 = c_1(A; A_0, \boldsymbol{\beta})$ the following quantity

$$c_1 = \sqrt{\frac{A}{\rho} \frac{\partial \psi}{\partial A}}, \tag{6.17}$$

which has the dimension of a velocity and, as we will see later on, is related to the speed of propagation of simple waves along the tube.

By simple manipulations (6.12) may be written in *quasi-linear* form as follows

$$\frac{\partial}{\partial t}U + \mathbf{H}(U)\frac{\partial U}{\partial z} + B(U) = \mathbf{0}, \quad z \in (0, L),\, t \in I \tag{6.18}$$

where,

$$U = \begin{bmatrix} A \\ Q \end{bmatrix},$$

$$\mathbf{H}(U) = \begin{bmatrix} 0 & 1 \\ \dfrac{A}{\rho}\dfrac{\partial \psi}{\partial A} - \alpha \overline{u}^2 & 2\alpha\overline{u} \end{bmatrix} = \begin{bmatrix} 0 & 1 \\ c_1^2 - \alpha\left(\dfrac{Q}{A}\right)^2 & 2\alpha\dfrac{Q}{A} \end{bmatrix}, \tag{6.19}$$

and

$$B(U) = \begin{bmatrix} 0 \\ K_R\left(\dfrac{Q}{A}\right) + \frac{A}{\rho}\dfrac{\partial \psi}{\partial A_0}\dfrac{dA_0}{dz} + \dfrac{A}{\rho}\dfrac{\partial \psi}{\partial \boldsymbol{\beta}}\dfrac{d\boldsymbol{\beta}}{dz} \end{bmatrix}.$$

Clearly, if A_0 and $\boldsymbol{\beta}$ are constant the expression for B becomes simpler. A *conservation form* for (6.18) may be found as well and reads

$$\frac{\partial U}{\partial t} + \frac{\partial F}{\partial z}(U) + S(U) = 0, \tag{6.20}$$

where

$$F(U) = \begin{bmatrix} Q \\ \alpha\frac{Q^2}{A} + C_1 \end{bmatrix}$$

is the vector of fluxes,

$$S(U) = B(U) - \begin{bmatrix} 0 \\ \dfrac{\partial C_1}{\partial A_0}\dfrac{dA_0}{dz} + \dfrac{\partial C_1}{\partial \boldsymbol{\beta}}\dfrac{d\boldsymbol{\beta}}{dz}, \end{bmatrix}$$

and C_1 is a primitive of c_1^2 with respect to A, given by

$$C_1(A; A_0, \boldsymbol{\beta}) = \int_{A_0}^{A} c_1^2(\tau; A_0, \boldsymbol{\beta})\, d\tau.$$

Again, if A_0 and $\boldsymbol{\beta}$ are constant, the source term S simplifies and becomes $S = B$. System (6.20) allows to identify the vector U as the the *conservation variables* of our problem.

Remark 6.1. In the case we use relation (6.16) we have

$$c_1 = \sqrt{\frac{\beta_0}{2\rho A_0}}A^{\frac{1}{4}}, \quad C_1 = \frac{\beta_0}{3\rho A_0}A^{\frac{3}{2}}. \tag{6.21}$$

$\diamondsuit$

Lemma 6.2. *If $A \geq 0$, the matrix $\mathbf{H}$ possesses two real eigenvalues. Furthermore, if $A > 0$ the two eigenvalues are distinct and (6.18) is a strictly hyperbolic system of partial differential equations.*

Proof. By straightforward computations we have the following expression for the eigenvalues of $\mathbf{H}$

$$\lambda_{1,2} = \alpha\overline{u} \pm c_\alpha, \tag{6.22}$$

where

$$c_\alpha = \sqrt{c_1^2 + \overline{u}^2\alpha\,(\alpha - 1)}.$$

Since $\alpha \geq 1$, c_α is a real number. If $c_\alpha > 0$ the two eigenvalues are distinct. A sufficient condition to have $c_\alpha > 0$ is $c_1 > 0$ and, thanks to the definition of c_1 and (6.14), this is always true if $A > 0$. If $\alpha = 1$, this condition is also necessary.

The existence of a complete set of (right and left) eigenvectors is an immediate consequence of $\mathbf{H}$ having distinct eigenvalues. □

Remark 6.2. System (6.12) shares many analogies with the 1D compressible Euler equations, after identifying the section area A with the density. The equivalence is not complete since the term $\frac{\partial P}{\partial z}$ in the Euler equations is here replaced by $A\frac{\partial P}{\partial z}$.

♢

6.3.1. *Characteristics analysis.* Let $(\mathbf{l}_1, \mathbf{l}_2)$ and $(\mathbf{r}_1, \mathbf{r}_2)$ be two couples of left and right eigenvectors of the matrix $\mathbf{H}$ in (6.19), respectively. The matrices $\mathbf{L}$, $\mathbf{R}$ and $\mathbf{\Lambda}$ are defined as

$$\mathbf{L} = \begin{bmatrix} \mathbf{l}_1^T \\ \mathbf{l}_2^T \end{bmatrix}, \qquad \mathbf{R} = \begin{bmatrix} \mathbf{r}_1 & \mathbf{r}_2 \end{bmatrix}, \qquad \mathbf{\Lambda} = \operatorname{diag}(\lambda_1, \lambda_2) = \begin{bmatrix} \lambda_1 & 0 \\ 0 & \lambda_2 \end{bmatrix}. \tag{6.23}$$

Since right and left eigenvectors are mutually orthogonal, without loss of generality we choose them so that $\mathbf{LR} = \mathbf{I}$. Matrix $\mathbf{H}$ may then be decomposed as

$$\mathbf{H} = \mathbf{R}\mathbf{\Lambda}\mathbf{L}, \tag{6.24}$$

and system (6.18) written in the equivalent form

$$\mathbf{L}\frac{\partial U}{\partial t} + \mathbf{\Lambda}\mathbf{L}\frac{\partial U}{\partial z} + \mathbf{L}B(U) = \mathbf{0}, \quad z \in (0, L),\, t \in I. \tag{6.25}$$

If there exist two quantities W_1 and W_2 which satisfy

$$\frac{\partial W_1}{\partial U} = \mathbf{l}_1, \quad \frac{\partial W_2}{\partial U} = \mathbf{l}_2 \tag{6.26}$$

we will call them *characteristic variables* of our hyperbolic system. We point out that in the case where the coefficients A_0 and β are not constant, W_1 and W_2 are not autonomous functions of U.

By setting $W = [W_1, W_2]^T$ system (6.25) may be elaborated into

$$\frac{\partial W}{\partial t} + \mathbf{\Lambda}\frac{\partial W}{\partial z} + G = \mathbf{0}, \quad z \in (0, L),\, t \in I, \tag{6.27}$$

where

$$G = \mathbf{L}B - \frac{\partial W}{\partial A_0}\frac{dA_0}{dz} - \frac{\partial W}{\partial \beta}\frac{d\beta}{dz}. \tag{6.28}$$

In the case where $B = 0$ and the coefficients A_0 and β are constant, (6.27) takes the simpler form

$$\frac{\partial W}{\partial t} + \mathbf{\Lambda}\frac{\partial W}{\partial z} = \mathbf{0}, \quad z \in (0, L),\, t \in I, \tag{6.29}$$

which component-wise reads

$$\frac{\partial W_i}{\partial t} + \lambda_i\frac{\partial W_i}{\partial z} = 0, \quad z \in (0, L),\, t \in I,\, i = 1, 2 \tag{6.30}$$

Remark 6.3. From definition (6.26) and the fact that the left and right eigenvectors $\mathbf{l}_i$, and $\mathbf{r}_i$ are mutually orthogonal it follows that

$$\frac{\partial W_1}{\partial U}(U) \cdot \mathbf{r}_2(U) = 0,$$

thus W_1 is a 2-*Riemann invariant* of our hyperbolic system [25]. Analogously, one may show that W_2 is a 1-Riemann invariant.

$\diamondsuit$

From (6.30) we have that W_1 and W_2 are constant along the two *characteristic curves* in the (z,t) plane described by the differential equations

$$\frac{dz}{dt} = \lambda_1 \quad \text{and} \quad \frac{dz}{dt} = \lambda_2,$$

respectively. In the more general case (6.27) we may easily show that W_1 and W_2 satisfy a coupled system of ordinary differential equations.

The expression for the left eigenvectors $\mathbf{l}_1$ and $\mathbf{l}_2$ is given by

$$\mathbf{l}_1 = \zeta \begin{bmatrix} c_\alpha - \alpha\overline{u} \\ 1 \end{bmatrix}, \qquad \mathbf{l}_2 = \zeta \begin{bmatrix} -c_\alpha - \alpha\overline{u} \\ 1 \end{bmatrix},$$

where $\zeta = \zeta(A, \overline{u})$ is any arbitrary smooth function of its arguments with $\zeta > 0$. Here we have expressed $\mathbf{l}_1$ and $\mathbf{l}_2$ as functions of $(A, \overline{u})$ instead of (A, Q) as is more convenient for the next developments. Thus, relations (6.26) become

$$\frac{\partial W_1}{\partial A} = \zeta\left[c_\alpha - \overline{u}\,(\alpha - 1)\right], \quad \frac{\partial W_1}{\partial \overline{u}} = \zeta A \tag{6.31a}$$

$$\frac{\partial W_2}{\partial A} = \zeta\left[-c_\alpha - \overline{u}\,(\alpha - 1)\right], \quad \frac{\partial W_2}{\partial \overline{u}} = \zeta A. \tag{6.31b}$$

For a hyperbolic system of two equations is always possible to find the characteristic variables (or, equivalently, the Riemann invariants) locally, that is in a sufficiently small neighbourhood of any point U [25, 33], yet the existence of global characteristic variables is not in general guaranteed. However, in the special case $\alpha = 1$, (6.31) takes the much simpler form

$$\frac{\partial W_1}{\partial A} = \zeta c_1, \quad \frac{\partial W_1}{\partial \overline{u}} = \zeta A$$
$$\frac{\partial W_2}{\partial A} = -\zeta c_1, \quad \frac{\partial W_2}{\partial \overline{u}} = \zeta A.$$

Let us show that a set of global characteristic variables for our problem does exist in this case. We remind that the characteristic variable W_1 exists if and only if

$$\frac{\partial^2 W_1}{\partial A \partial \overline{u}} = \frac{\partial^2 W_1}{\partial \overline{u} \partial A},$$

for all allowable values of A and $\overline{u}$. Since now c_1 does not depend on $\overline{u}$, the above condition yields

$$c_1 \frac{\partial \zeta}{\partial \overline{u}} = \zeta + A \frac{\partial \zeta}{\partial A}.$$

In order to satisfy this relation, it is sufficient to take $\zeta = \zeta(A)$ such that $\zeta = -A\frac{\partial \zeta}{\partial A}$. A possible instance is $\zeta = A^{-1}$. The resulting differential form is

$$\partial W_1 = \frac{c_1}{A}\partial A + \partial \overline{u},$$

and by proceeding in the same way for W_2 we have

$$\partial W_2 = -\frac{c_1}{A}\partial A + \partial \overline{u},$$

To integrate it in the $(A, \overline{u})$ plane we need to fix the value at a reference state, for instance $W_1 = W_2 = 0$ for $(A, \overline{u}) = (A_0, 0)$. We finally obtain

$$W_1 = \overline{u} + \int_{A_0}^{A} \frac{c_1(\tau)}{\tau} d\tau, \qquad W_2 = \overline{u} - \int_{A_0}^{A} \frac{c_1(\tau)}{\tau} d\tau. \tag{6.32}$$

Remark 6.4. If we adopt relation (6.16) and use the expression for c_1 given in (6.21), after simple computations we have

$$W_1 = \overline{u} + 4(c_1 - c_{1,0}), \qquad W_2 = \overline{u} - 4(c_1 - c_{1,0}), \tag{6.33}$$

where $c_{1,0}$ is the value of c_1 corresponding to the reference vessel area A_0.

$\diamondsuit$

Under physiological conditions, typical values of the flow velocity and mechanical characteristics of the vessel wall are such that $c_\alpha >> \alpha\overline{u}$. Consequently $\lambda_1 > 0$ and $\lambda_2 < 0$, i.e. the flow is sub-critical everywhere. Furthermore, the flow is smooth. Discontinuities, which would normally appear when treating a non-linear hyperbolic system, do not have indeed the time to form in our context because of the pulsatility of the boundary conditions. It may be shown [7] that, for the typical values of the mechanical and geometric parameters in physiological conditions and the typical vessel lengths in the arterial tree, the solution of our hyperbolic system remains smooth, in accordance to what happens in the actual physical problem (which is however dissipative, a feature which has been neglected in our one-dimensional model).

In the light of the previous considerations, from now on we will always assume sub-critical regime and smooth solutions.

6.3.2. *Boundary conditions.* System (6.12) must be supplemented by proper boundary conditions. The number of conditions to apply at each end equals the number of characteristics entering the domain though that boundary. Since we are only considering sub-critical flows we need to impose exactly one boundary condition at both $z = 0$ and $z = L$.

An important class of boundary conditions, called non-reflecting or 'absorbing', are those that allow the simple wave associated to the outgoing characteristic to exit the computational domain with no reflections. Following [56, 29] non-reflecting boundary conditions for one dimensional systems of non-linear hyperbolic equation like (6.20) may be written as

$$\mathbf{l}_1 \left(\frac{\partial U}{\partial t} + S(U) \right) = 0 \text{ at } z = 0, \quad \mathbf{l}_2 \left(\frac{\partial U}{\partial t} + S(U) \right) = 0 \text{ at } z = L,$$

for all $t \in I$. When $S = 0$ these conditions are equivalent to impose a constant value (typically set to zero) to the incoming characteristic variable. When $S \neq 0$ they take into account the "natural variation" of the characteristic variables due to the presence of the source term. A boundary condition of this type is quite convenient at the outlet section.

At the inlet instead one usually desires to impose values of pressure or mass flux derived from measurements or other means. Let us suppose that $z = 0$ is an inlet section (the following discussion may be readily extended to the boundary $z = L$). Whenever an explicit formulation of the characteristic variables is available, the boundary condition may be expressed directly in terms of the entering characteristic variable W_1, i.e., for all $t \in I$

$$W_1(t) = g_1(t) \text{ at } z = 0, \tag{6.34}$$

g_1 being a given function. However, seldomly one has directly g_1 at disposal, as the available boundary data is normally given in terms of physical variables. Let us suppose that we know the time variation of both pressure and mass flux at that boundary (for instance taken from measurements). We may derive the corresponding value of g_1 using directly the definition of the characteristic variable W_1. If $P_m = P_m(t)$ and $Q_m = Q_m(t)$ are the measured average pressure and mass

flux at $z = 0$ for $t \in I$ and $W_1(A, Q)$ indicates the characteristic variable W_1 as function of A and Q, we may pose

$$g_1(t) = W_1\left(\psi^{-1}(P_m(t) - P_{ext}), Q_m(t)\right), \quad t \in I,$$

in (6.34). This means that P_m and Q_m are not imposed exactly at $z = 0$ (this would not be possible since our system accounts for only one boundary condition at each end of the computational domain), yet we require that at all times t the value of A and Q at $z = 0$ lies on the curve in the (A, Q) plane defined by

$$W_1(A, Q) - W_1\left(\psi^{-1}(P_m(t) - P_{ext}), Q_m(t)\right) = 0.$$

If instead one has at disposal the time history $q(t)$ of a just one physical variable $\phi = \phi(A, Q)$ the boundary condition

$$\phi(A(t), Q(t)) = q(t), \quad \forall t \in I, \quad \text{at } z = 0,$$

is admissible under certain restrictions [43], which in our case reduce to exclude the case where ϕ may be expressed as function of only W_2. In particular, it may be found that for the problem at hand the imposition of either average pressure or mass flux are both admissible.

Remark 6.5. If the integration of (6.26) is not feasible (as, for instance, in the case $\alpha \neq 1$), one may resort to the *pseudo-characteristic* variables [43], $Z = [Z_1, Z_2]^T$, defined by linearising (6.26) around an appropriately chosen reference state. One obtains

$$Z = \overline{Z} + \mathbf{L}(\overline{U})\left(U - \overline{U}\right) \tag{6.35}$$

where $\overline{U}$ is the chosen reference state and $\overline{Z}$ the corresponding value for $\mathbf{Z}$. One may then use the pseudo-characteristic variables instead of W, by imposing

$$Z_1(t) = g_1(t) \text{ at } z = 0, \quad Z_2(t) = 0 \text{ at } z = L.$$

In the context of a time advancing scheme for the numerical solution of (6.20) the pseudo-characteristics are normally computed linearising around the solution computed at the previous time step.

♢

Remark 6.6. When considering the numerical discretisation, we need in general to provide an additional equation at each end point in order to close the resulting algebraic system. Typically, this extra relation is provided by the so-called *compatibility conditions* [43], which read as follows

$$\mathbf{l}_2^T\left(\frac{\partial}{\partial t}U + \mathbf{H}\frac{\partial U}{\partial z} + B\right) = 0, \quad z = 0,\ t \in I, \tag{6.36a}$$

$$\mathbf{l}_1^T\left(\frac{\partial}{\partial t}U + \mathbf{H}\frac{\partial U}{\partial z} + B\right) = 0, \quad z = L,\ t \in I. \tag{6.36b}$$

♢

6.3.3. *Energy conservation for the 1D model.* Most of the results presented in this section are taken from [15] and [7].

Lemma 6.3. *Let us consider the hyperbolic problem (6.18) and assume that the initial and boundary conditions are such that* $\forall z \in (0, L)$

$$A(0, z) > 0, \quad \textit{and } A(t, 0) > 0, A(t, L) > 0, \forall t \in I,$$

and that the solution U is smooth for all $(t, z) \in I \times (0, L)$. Then $A(t, z) > 0$ for all $(t, z) \in I \times (0, L)$.

Proof. Let us suppose that we have $A(t^*, z^*) = 0$ at a generic point $(t^*, z^*) \in I \times (0, L)$. From the definition of λ_1 and λ_2 the line $l = \{(t, z) |\ z = z_u(t)\}$ satisfying

$$\frac{dz_u}{dt}(t) = \overline{u}(t, z_u(t))$$

and ending at the point (t^*, z^*), lies between the two characteristic curves passing through the same point. Therefore, it completely lies inside the domain of dependence of (t^*, z^*) and either intersects the segment $z \in (0, L)$ at $t = 0$ or one of the two semi-lines $z = 0$ or $z = L$ at $t \geq 0$. We indicate this intersection point by $(\overline{t}, \overline{z})$. The corresponding value of A, call it $\overline{A}$, is positive by hypothesis. From the continuity equation, A satisfies along the line l the following ordinary differential equation

$$\frac{dA}{dt} = -A\frac{\partial \overline{u}}{\partial z},$$

where here the $\frac{dA}{dt}$ indicates the directional derivative along l. Therefore,

$$A(t^*, z^*) = \overline{A} \int_{\overline{t}}^{t^*} \frac{\partial \overline{u}}{\partial z}(\tau, z_u(\tau)) d\tau > 0,$$

in contradiction with the hypothesis. Therefore we must have $A > 0$. □

Here we derive now an *a priori* estimate for the solution of system (6.18) under the hypotheses of $\alpha = 1$, sub-critical smooth flow, and $A > 0$. We will consider the following initial and boundary conditions

(6.37) initial conditions $\quad A(0, z) = A^0(z), \quad Q(0, z) = Q^0(z) \qquad z \in (0, L)$

(6.38) boundary conditions $\quad \begin{array}{l} W_1(t, 0) = g_1(t), \quad t \in I \\ W_2(t, L) = g_2(t), \quad t \in I \end{array}$

Let the quantity e be defined as

$$e = \frac{\rho}{2} A\overline{u}^2 + \Psi \tag{6.39}$$

where $\Psi = \Psi(A)$ is given by

$$\Psi(A) = \int_{A_0}^{A} \psi(\zeta) d\zeta. \tag{6.40}$$

Here and in what follows we omit to indicate the dependence of ψ on A_0 and β, since it is not relevant to obtain the desired result, which can be however extended also to the general case where the coefficients A_0 and β depend on z.

An energy of the 1D model is given by

$$\mathcal{E}(t) = \int_0^L e(t, z) dz, \quad t \in I. \tag{6.41}$$

Indeed, owing to the assumptions we have made on ψ in (6.14), we may observe that ψ attains a minimum at $A = A_0$, since

$$\Psi(A_0) = \Psi'(A_0) = 0 \qquad \text{and } \Psi''(A) > 0 \quad \forall A > 0.$$

it follows that $\Psi(A) \geq 0, \quad \forall A > 0$. Consequently, $\mathcal{E}(t)$ is a positive function for all Q and $A > 0$ and, moreover,

$$\mathcal{E}(t) = 0 \quad \text{iff } (A(t, z), Q(t, z)) = (A_0, 0), \quad \forall z \in (0, L).$$

The following Lemma holds

Lemma 6.4. *In the special case $\alpha = 1$, system (6.12), supplied with an algebraic pressure-area relationship of the form (6.13) and under conditions (6.14), satisfies the following conservation property, $\forall t \in I$*

$$\mathcal{E}(t) + \rho K_R \int_{t_0}^{t}\int_0^L \overline{u}^2 dz d\tau + \int_{t_0}^{t} Q\left(P_{tot} - P_{ext}\right)\Big|_0^L dt = \mathcal{E}(0), \tag{6.42}$$

where $\mathcal{E}(0)$ depends only on the initial data A^0 and Q^0, while $P_{tot} = P + \frac{1}{2}\rho\overline{u}^2$ is the fluid total pressure.

Proof. Let us multiply the second equation of (6.12) by $\overline{u}$ and integrate over $(0, L)$. We will analyse separately the four terms that are obtained.

- First term

$$I_1 = \int_0^L \frac{\partial(A\overline{u})}{\partial t}\overline{u}dz = \frac{1}{2}\int_0^L A\frac{\partial\overline{u}^2}{\partial t}dz + \int_0^L \frac{\partial A}{\partial t}\overline{u}^2 dz = \frac{1}{2}\frac{d}{dt}\int_0^L A\overline{u}^2 dz + \frac{1}{2}\int_0^L \overline{u}^2\frac{\partial A}{\partial t}dz \tag{6.43}$$

- Second term

$$I_2 = \alpha\int_0^L \frac{\partial(A\overline{u}^2)}{\partial z}\overline{u}dz = \alpha\left[\int_0^L \frac{\partial(A\overline{u})}{\partial z}\overline{u}^2 dz + \int_0^L A\overline{u}^2\frac{\partial\overline{u}}{\partial z}dz\right] = \alpha\left[\frac{1}{2}\int_0^L \frac{\partial(A\overline{u})}{\partial z}\overline{u}^2 dz + \frac{1}{2}\int_0^L \frac{\partial A}{\partial z}\overline{u}^3 dz + \frac{3}{2}\int_0^L A\overline{u}^2\frac{\partial\overline{u}}{\partial z}dz\right] = \alpha\left[\frac{1}{2}\int_0^L \frac{\partial Q}{\partial z}\overline{u}^2 dz + \frac{1}{2}\int_0^L \frac{\partial(A\overline{u}^3)}{\partial z}dz\right] \tag{6.44}$$

Now, using the continuity equation we obtain

$$I_2 = \frac{\alpha}{2}\left[-\int_0^L \frac{\partial A}{\partial t}\overline{u}^2 dz + (A\overline{u}^3)\Big|_0^L\right] \tag{6.45}$$

- Third term

$$I_3 = \int_0^L \frac{A}{\rho}\frac{\partial P}{\partial z}\overline{u}dz = \frac{1}{\rho}\int_0^L A\frac{\partial}{\partial z}\left(P - P_{ext}\right)\overline{u}dz = \frac{1}{\rho}\left[-\int_0^L \frac{\partial Q}{\partial z}\psi(A)dz + (P - P_{ext})Q\Big|_0^L\right] \tag{6.46}$$

Again, using the first of (6.12) we have

$$I_3 = \frac{1}{\rho}\left[\int_0^L \frac{\partial A}{\partial t}\psi(A)dz + (P - P_{ext})Q\Big|_0^L\right] = \frac{1}{\rho}\left[\frac{d}{dt}\int_0^L \Psi(A)dz + (P - P_{ext})Q\Big|_0^L\right]$$

- Fourth term

$$I_4 = \int_0^L K_r\frac{Q}{A}\overline{u}dz = K_r\int_0^L \overline{u}^2 dz \tag{6.47}$$

By summing the four terms and multiplying by ρ, we obtain the following equality when $\alpha = 1$,

$$\frac{1}{2}\rho\frac{d}{dt}\int_0^L A\overline{u}^2 dz + \frac{d}{dt}\int_0^L \Psi(A)dz + \rho K_r\int_0^L \overline{u}^2 dz + Q\left(P_{tot} - P_{ext}\right)\Big|_0^L = 0 \tag{6.48}$$

Integrating equation (6.48) in time between t_0 and t leads to the desired result. □

In order to draw an energy inequality from (6.42), we need to investigate the sign of the last term on the left hand side. With this aim, let us first analyse the homogeneous case $g_1 = g_2 = 0$.

We will rewrite the boundary term in (6.42) as a function of A, $\psi(A)$ and c_1 (which, in its turn, depends on A, see (6.17)).

If $g_1 = g_2 = 0$ in (6.38), then

$$\text{at z = 0} \qquad W_1 = \overline{u} + \int_{A_0}^{A} \frac{c_1(\zeta)}{\zeta} d\zeta = 0 \qquad \Longrightarrow \qquad \overline{u}(t,0) = -\int_{A_0}^{A} \frac{c_1(\zeta)}{\zeta} d\zeta$$

$$\text{at z = L} \qquad W_2 = \overline{u} - \int_{A_0}^{A} \frac{c_1(\zeta)}{\zeta} d\zeta = 0 \qquad \Longrightarrow \qquad \overline{u}(t,L) = \int_{A_0}^{A} \frac{c_1(\zeta)}{\zeta} d\zeta$$

and thus

$$Q\,(P_{tot} - P_{ext})\,\Big|_0^L = F(A(t,0)) + F(A(t,L)), \tag{6.49}$$

where

$$F(A) = A \int_0^A \frac{c_1(\zeta)}{\zeta} d\zeta \left[\psi(A) + \frac{1}{2}\rho \left(\int_{A_0}^{A} \frac{c_1(\zeta)}{\zeta} d\zeta \right)^2 \right]. \tag{6.50}$$

From our assumption of sub-critical flow we have $|\overline{u}| < c_1$ which implies that at $z = 0$ and $z = L$ we have

$$\left| \int_{A_0}^{A} \frac{c_1(\zeta)}{\zeta} d\zeta \right| < c_1(A) \tag{6.51}$$

We are now in the position to conclude with the following result.

Lemma 6.5. *If the function pressure-area relationship $P = \psi(A)$ is such that $F(A) > 0$ whenever (6.51) is satisfied, then inequality*

$$\mathcal{E}(t) + \rho K_r \int_{t_0}^{t}\int_0^L \overline{u}^2 dz d\tau \le \mathcal{E}(0) \tag{6.52}$$

holds for system (6.12), provided homogeneous conditions on the characteristic variables, $W_1 = 0$ and $W_2 = 0$, are imposed at $z = 0$ and $z = L$, respectively.

Proof. It is an immediate consequence of (6.42), (6.49) and (6.50). □

By straightforward computations one may verify that the pressure-area relationship given in (6.16) satisfies the hypotheses of Lemma 6.5 (see [15]). Therefore, in that case the 1D model satisfies the energy inequality (6.52).

Under relation (6.16), we can prove a more general energy estimate, valid also in the case of non homogeneous boundary conditions. We state the following result.

Lemma 6.6. *If the pressure-area relationship is given by (6.16), and the boundary data satisfy*

$$g_1(t) > -4c_{1,0}(0) \quad \text{and} \quad g_2(t) < 4c_{1,0}(L) \qquad \forall t \in I, \tag{6.53}$$

where $c_{1,0}(z) = \sqrt{\frac{\beta_0(z)}{\rho}} A_0(z)^{-\frac{1}{4}}$ is the value of c_1 at the reference vessel area, then there exists a positive quantity $G(t)$ which continuously depends on the boundary data $g_1(t)$ and $g_2(t)$, as well as on the values of the coefficients A_0 and β, at $z = 0$ and $z = L$, such that, for all $t \in I$

$$\mathcal{E}(t) + \rho K_r \int_{t_0}^{t}\int_0^L \overline{u}^2 dz d\tau \le \mathcal{E}(0) + \int_0^t G(t) dt. \tag{6.54}$$

Proof. We will consider only the case where $g_1 \neq 0$ and $g_2 = 0$, since the most general case may be derived in a similar fashion. We recall that relationship (6.16) together with the assumption of sub-critical flow, complies with the conditions stated for $F(A)$ in Lemma 6.5. Then from (6.48) we obtain the following inequality

$$\frac{d}{dt}\mathcal{E}+\rho K_r \int_0^L \overline{u}^2 dz \leq Q\left(P_{tot} - P_{ext}\right)\Big|_{z=0} \leq \left(A|\overline{u}||\psi(A)| + \frac{1}{2}\rho A|\overline{u}|^3\right)\Big|_{z=0} \tag{6.55}$$

At $z = 0$, we have from (6.33) that

$$\overline{u} + 4(c_1 - c_{1,0}) = g_1.$$

On the other hand, the condition $\lambda_1 = \overline{u} + c_1 > 0$ gives

$$c_1 < \frac{1}{3}(g_1 + 4c_{1,0}). \tag{6.56}$$

Since c_1 is a non-negative quantity, we must necessarily have $g_1 > -4c_{1,0}$. We now note that from (6.16) and the definition of $c_{1,0}$ we may write

$$\psi(A) = 2\rho(c_1^2(A) - c_{1,0}^2)$$

which together with (6.56) and the fact that $c_{1,0}$ is a positive function, allows us to state that, at $z = 0$,

$$\psi(A) \leq \frac{2\rho}{9}(g_1^2 + 15c_{1,0}^2 + 8g_1c_{1,0}) \equiv f_1(g_1), \tag{6.57}$$

where f_1 is a positive continuous function depending parametrically on the values of A_0 and β_0 at $z = 0$. Furthermore, condition $|\overline{u}| < c_1$ together with inequality (6.56) imply that

$$|\overline{u}| \leq f_2(g_1),$$

being f_2 another positive and continuous function. Finally, from the definition of ψ and $c_{1,0}$ we have

$$A = \frac{A_0^2}{\beta_0^2}(\psi(A) + \sqrt{A_0})^2 \leq \frac{2A_0^2}{\beta_0^2}(\psi^2(A) + A_0) \leq \frac{2A_0^2}{\beta_0^2}\left(f_1^2(g1) + A_0\right) \equiv f_3(g_1),$$

where we have exploited (6.57). By combining all previous inequalities we deduce that the right hand side in (6.55) may be bounded by a positive and continuous function of the boundary data g_1 that depend parametrically on the value of A_0 and β_0 at $z = 0$. By repeating a similar argument for the boundary conditions at $z = L$ we then obtain the desired stability inequality. □

6.3.4. *Weak form.* We consider the hyperbolic system (6.20) with initial condition $U = U_0$, at $t = t_0$, and appropriate boundary conditions at $z = 0$ and $z = L$. We indicate by $C_0^1((0, L) \times [t_0, t_1))$ the set of functions which are the restriction to $(0, L) \times [t_0, t_1)$ of C^1 functions with compact support in $(0, L) \times (-\infty, t_1)$. We will assume that U_0 is a bounded measurable function in $(0, L)$.

A function $U \in [L^\infty((0, L) \times [t_0, t_1))]^2$ is a weak solution of the equation in conservation form (6.20) if for all $\boldsymbol{\phi} \in [C_0^1((0, L) \times [t_0, t_1))]^2$ we have

$$\int_{t_0}^{t^1}\int_0^L \left(U \cdot \frac{\partial \boldsymbol{\phi}}{\partial t} + F(U) \cdot \frac{\partial \boldsymbol{\phi}}{\partial z} - S(U) \cdot \boldsymbol{\phi}\right) dzdt + \int_0^L U_0 \cdot \boldsymbol{\phi}|_{t=0} \; = \; 0. \tag{6.58}$$

Moreover, we will require that U complies given boundary conditions.

A solution of (6.58) is called a weak solution of our hyperbolic system. Clearly "classical" smooth solutions of (6.20) are also weak solutions. Conversely, it may be shown that a smooth weak solution, i.e. belonging to $[C^1((0, L) \times [t_0, t_1))]^2$, is

also solution of (6.20) in a classical sense. However, the weak form accommodates also for less regular U. In particular, weak solutions of our hyperbolic problem may be discontinuous. The weak form is furthermore the basis of a class of numerical schemes, in particular the finite element method, as already seen for the Navier-Stokes equations.

Remark 6.7. The conservation formulation (6.20) accounts also for mechanical properties which vary smoothly along z. However, there are some fundamental difficulties in extending it to the case of discontinuous mechanical characteristics (e.g. discontinuous β). On the other hand, this situation has a certain practical relevance, for instance in stented arteries or in the presence of a vascular prosthesis. A stent is a metal meshed wire structure inserted into a stenotic artery (typically a coronary) by angioplasty, in order to restore the original lumen dimension. Vascular prostheses are used to treat degenerative pathologies, such as aneurysms, or when angioplasty is not possible.

A possibility [19] is to model the sharp variation of the Young modulus at the interface between the artery and the prosthesis by a regular function. Fig 26 illustrates a possible description of the change in the Young modulus due to the presence of a prosthesis. One may argue what would happen when the parameter δ in figure tends to zero. Numerical experiments have shown that the solution remains bounded although it becomes discontinuous at the location of the discontinuity in the Young modulus. This fact has been recently investigated in [6] where an expression for the jump of mass flow and area across the discontinuity is derived by computing a particular limit of weak solutions of a regularised problem. More details are found in the cited reference.

$\Diamond$

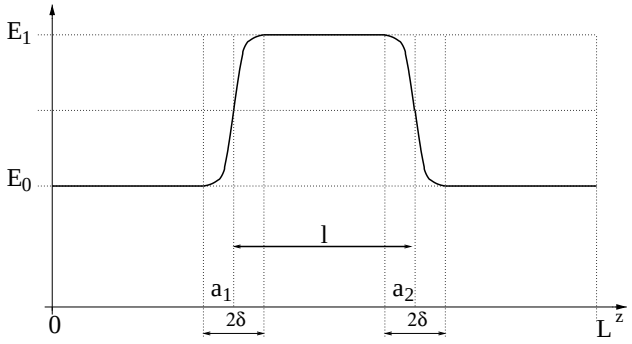

FIGURE 26. The sharp variation of the Young Modulus E from the value E_0 to the value E_1, due to the presence of a prosthesis, is modeled by a smooth function. One may argue what would happen when the parameter δ in figure tends to zero.

6.3.5. *An entropy function for the 1D model.* Let us consider the hyperbolic system written in quasi-linear form (6.18). A pair of functions $e : \mathbb{R}^2 \to \mathbb{R}$ and $F_e : \mathbb{R}^2 \to \mathbb{R}$ is called *entropy pair* for the system if e is a convex function of U (called *entropy*) and the following condition is satisfied

$$(\frac{de}{dU})^T \mathbf{H}(U) = \frac{\partial F_e}{\partial U} \tag{6.59}$$

for all admissible values of U.

F_e is the *entropy flux* associated to the entropy e. If the hyperbolic system admits an entropy pair then the entropy function satisfies a conservation law of the form

$$\frac{\partial e}{\partial t} + \frac{\partial F_e}{\partial z} + B_e(U) = 0,$$

where

$$B_e(U) = \frac{de}{dU} \cdot B(U) - \frac{\partial F_e}{\partial A_0}\frac{dA_0}{dz} - \frac{\partial F_e}{\partial \beta}\frac{d\beta}{dz}$$

is a source term. The last two terms in the previous expression account for the possible dependence of the coefficients A_0 and β on z.

The existence of an entropy pair is of a certain importance when studying the weak solution of the hyperbolic problem and in particular discontinuous solutions (more details in [33] and [25]). Although we have here considered only smooth solutions, the identification of an entropy for our problem is important to set the basis for the extension of the model to more general situations.

In the case $\alpha = 1$,

$$e = \frac{1}{2}\rho A\overline{u}^2 + \Psi(A) = \frac{1}{2}\rho\frac{Q^2}{A} + \Psi(A)$$

is indeed an entropy for the problem at hand, with associated flux

$$F_e = Q\left(\psi(A) + \frac{1}{2}\rho\overline{u}^2\right) = Q(P_{tot} - P_{ext}).$$

Indeed, we have

$$\frac{\partial e}{\partial U} = \begin{bmatrix} -\dfrac{\rho\overline{u}^2}{2} + \psi(A) \\ \rho\overline{u} \end{bmatrix}, \quad \frac{\partial F_e}{\partial U} = \begin{bmatrix} Q\dfrac{\partial \psi}{\partial A}(A) - \rho\overline{u}^3 \\ \psi(A) + \dfrac{3}{2}\rho\overline{u}^2 \end{bmatrix}.$$

and we may directly verify condition (6.59) by recalling (6.19). Furthermore $B_e = \rho K_r \overline{u}^2$ and the entropy balance equation thus read

$$\frac{\partial}{\partial t}\left(\frac{1}{2}\rho A\overline{u}^2 + \Psi(A)\right) + \frac{\partial}{\partial z}\left[Q\left(\psi(A) + \frac{1}{2}\rho\overline{u}^2\right)\right] + \rho K_r\overline{u}^2 = 0. \tag{6.60}$$

It is valid for any smooth solution of our hyperbolic model. Furthermore, the following Lemma ensures the convexity of e.

Lemma 6.7. *The entropy*

$$e(A, Q) = \frac{\rho}{2}\frac{Q^2}{A} + \Psi(A)$$

is convex for all $A > 0$.

Proof. By a straightforward calculation one finds that the Hessian of e is given by

$$H_e = \begin{bmatrix} \dfrac{\partial^2 e}{\partial A^2} & \dfrac{\partial^2 e}{\partial A \partial Q} \\ \dfrac{\partial^2 e}{\partial A \partial Q} & \dfrac{\partial^2 e}{\partial Q^2} \end{bmatrix} = \frac{\rho}{A}\begin{bmatrix} \overline{u}^2 + c_1^2 & -\overline{u} \\ -\overline{u} & 1 \end{bmatrix}.$$

Its eigenvalues are

$$\lambda_{1,2}(H_e) = \rho\frac{c_1^2 + \overline{u}^2 + 1 \pm \sqrt{(c_1^2 + \overline{u}^2 + 1)^2 - 4c_1^2}}{2A}$$

The condition for the discriminant to be positive is

$$4c_1^2 \leq (c_1^2 + \overline{u}^2 + 1)^2$$

Since $c_1 > 0$ whenever $A > 0$, this inequality is equivalent to impose that

$$c_1^2 + \overline{u}^2 + 1 - 2c_1 = (c_1 - 1)^2 + \overline{u}^2 \geq 0,$$

which it is always true. Therefore, the two eigenvalues are strictly positive for all $A > 0$. This completes our proof. □

6.4. **More complex wall laws that account for inertia and viscoelasticity.** The algebraic relation (6.13) assumes that the wall is instantaneously in equilibrium with the pressure forces acting on it. Indeed, this approach correspond to the independent ring model introduced in Sect. 4.

At the price of some approximations it is possible to maintain the simple structure of a two-equations system while introducing effects, such as the inertia, which depend on the time derivative of the wall displacement.

We will consider as starting point relation (4.18) where we account for the inertia term and we model the viscoelastic property of the wall by adding a term proportional to the displacement rate, while we will still use the approximation (4.16) for the forcing term. We may thus write

$$P - P_{ext} = \gamma_0 \frac{\partial^2 \eta}{\partial t^2} + \gamma_1 \frac{\partial \eta}{\partial t} + \psi(A; A_0, \boldsymbol{\beta}), \tag{6.61}$$

where $\gamma_0 = \rho_w h_0$, $\gamma_1 = \frac{\gamma}{R_0^2}$ and the last term is the elastic response, modelled is the same way as done before. Here γ is the same viscoelasticity coefficient of (4.18) and η is the wall displacement, linked to A by (6.2).

In the following, we indicate by $\dot{A}$ and $\ddot{A}$ the first and second time derivative of A. We will substitute the following identities

$$\frac{\partial \eta}{\partial t} = \frac{1}{2\sqrt{\pi A}} \dot{A}, \qquad \frac{\partial^2 \eta}{\partial t^2} = \pi^{-\frac{1}{2}} \left(\frac{1}{2\sqrt{A}} \ddot{A} - \frac{1}{4\sqrt{A^3}} \dot{A}^2 \right),$$

that are derived from (6.2), into (6.61) to obtain a relation that links the pressure also to the time derivatives of A, which we write in all generality as

$$P - P_{ext} = \tilde{\psi}(A, \dot{A}, \ddot{A}; A_0) + \psi(A; A_0, \boldsymbol{\beta}),$$

where $\tilde{\psi}$ is a non-linear function which derives from the treatment of the terms containing the time derivative of η. Since it may be assumed that the contribution to the pressure is in fact dominated by the term ψ, we will simplify this relationship by linearising $\tilde{\psi}$ around the state $A = A_0$, $\dot{A} = \ddot{A} = 0$. By doing that, after some simple algebraic manipulations, one finds

$$P - P_{ext} = \frac{\gamma_0}{2\sqrt{\pi A_0}} \ddot{A} + \frac{\gamma_1}{2\sqrt{\pi A_0}} \dot{A} + \psi(A; A_0, \boldsymbol{\beta}), \tag{6.62}$$

Replacing this expression for the pressure in the momentum equation requires to compute the term

$$\frac{A}{\rho} \frac{\partial P}{\partial z} = \frac{\gamma_0 A}{2\rho\sqrt{\pi A_0}} \frac{\partial^3 A}{\partial z \partial t^2} + \frac{\gamma_1 A}{2\rho\sqrt{\pi A_0}} \frac{\partial^2 A}{\partial z \partial t} + \frac{A}{\rho} \frac{\partial \psi}{\partial z}.$$

The last term in this equality may be treated as previously, while the first two terms may be further elaborated by exploiting the continuity equation. Indeed, we have

$$\frac{\partial^2 A}{\partial z \partial t} = -\frac{\partial^2 Q}{\partial z^2}, \quad \frac{\partial^3 A}{\partial z \partial t^2} = -\frac{\partial^3 Q}{\partial t \partial z^2}$$

Therefore, the momentum equation with the additional terms deriving from inertia and viscoelastic forces becomes

$$\frac{\partial Q}{\partial t} + \frac{\partial F_2}{\partial z} - \frac{\gamma_0 A}{2\rho\sqrt{\pi A_0}} \frac{\partial^3 Q}{\partial t \partial z^2} - \frac{\gamma_1 A}{2\rho\sqrt{\pi A_0}} \frac{\partial^2 Q}{\partial z^2} + S_2 = 0, \tag{6.63}$$

where with F_2 and S_2 we have indicated the second component of F and S, respectively.

Remark 6.8. This analysis puts into evidence that the wall inertia introduces a *dispersive* term into the momentum equation, while the viscoelasticity has a *diffusion* effect.

$\Diamond$

6.5. **Some further extensions.** More general one dimensional models may be derived by accounting for vessel curvature. This may be accomplished by enriching the description of the velocity field on each vessel section to allow asymmetries of the velocity profile to develop.

Another enhancement of the model is to account for vessel branching. By employing domain decomposition techniques, each branch is simulated by a separate one dimensional model and interface conditions are used to account for the appropriate "transfer" of mass and momentum across the branching point. All these aspects are not covered in these notes. They are subject of current research and preliminary results may be found in [16].

Beside providing valuable information about average pressure and mass flux along an arterial segment, a one-dimensional model of blood flow may be used in the context of a multiscale/multimodel description of the cardiovascular system. In the multiscale framework, models of different level of complexity of the various cardiovascular elements are coupled together with the objective of simulating the whole cardiovascular system. Only the elements of major interest for the problem under study will be simulated at the highest level of detail (e.g. by employing a three dimensional fluid-structure interaction model), while reduced models are adopted in the remaining parts. This technique allows us to account (at least partially) for the complex feedback mechanisms of the complete cardiovascular system, while keeping the overall computational costs at a resonable level. More details on this technique may be found in [20, 15, 39] while in [38] a first example on the use of this multiscale approach for a realistic clinical application is presented.

7. SOME NUMERICAL RESULTS

We provide some numerical results to illustrate applications of the techniques discussed in the previous sections. The aim here is to show the potential of the numerical modelling to reproduce realistic flow fields relevant for medical investigations. Many of the results here presented are substantially taken from previous works of the authors, in particular from [42], [15] and [19]. More details and other examples may be found in the cited references.

7.1. **Compliant pipe.** Here we consider two examples of a fluid structure-interaction problem like the one presented in subsection 5.3, namely a 2D and a 3D computation of a pressure wave in a compliant tube.

In the 2D case, we have considered a rectangular domain of height $1cm$ and length $L = 6cm$. The fluid is initially at rest and an over pressure of 15mmHg ($2 \cdot 10^4\, dynes/cm^2$) has been imposed at the inlet for 0.005 seconds. The viscosity of the fluid is equal to $0.035\, poise$, its density is $1\, g/cm^3$, the Young modulus of the structure is equal to $0.75 \cdot 10^6\, dynes/cm^2$, its Poisson coefficient is 0.5, its density is $1.1\, g/cm^3$ and its thickness is $0.1\, cm$.

In the 3D case, our computation has been made on a cylindrical domain of radius $R_0 = 0.5cm$ and length $L = 5cm$, with the following physical parameters: fluid viscosity: $0.03\, poise$, fluid density: $1\, g/cm^3$, Young modulus of the structure: $3 \cdot 10^6\, dynes/cm^2$, Poisson coefficient: 0.3 and structure density: $1.2\, g/cm^3$. Again, an over-pressure of 10mmHg ($1.3332 \cdot 10^4\, dynes/cm^2$) is imposed at the inlet for 0.005 seconds.

The fluid equations are solved using the ALE approach, with a piecewise linear finite element space discretisation. More precisely, for the 2D case the pressure is piecewise linear on triangular elements and the velocity is linear over each of the four sub-triangles obtained by joining the midpoints of the edges of each pressure triangle (this is the so called P1isoP2–P1 discretisation). We have employed the Yosida technique illustrated in subsection 3.7.2. For the 3D case we have used a stabilised scheme [31] and piecewise linear elements for both velocity and pressure.

For the 2D case, the equation for the structure displacement (5.13) has been solved using a P^1 finite element space discretisation, with nodes coincident with the ones of the pressure discretisation. In the 3D case, we have used a shell-type formulation [51, 52] to describe the dynamics of the wall structure. In both cases, the coupling scheme adopts a sub-iterations strategy of the type illustrated in subsection 5.3.

In order to reduce spurious wave reflections at the outlet, we have coupled the fluid-structure interaction problem with a one dimensional system of the type described in Sect. 6. For more details on this technique see [15], as well as [18].

Figures 27 and 28 show the fluid pressure and the domain deformation in the 2D and the 3D case respectively. For the sake of clarity, the displacements shown in Fig. 28 are magnified by a factor 10.

7.2. **Anastomosis models.** Anastomosis is the a surgical operation by which the functionality of a blocked artery (typically a coronary) is restored thanks to by-pass. The flow condition when the blood in the by-pass re-joins the main artery may be critical. If we have a large recirculation area, the higher latency time of blood particles there may favor plaque growing and cause a new blockage further downstream.

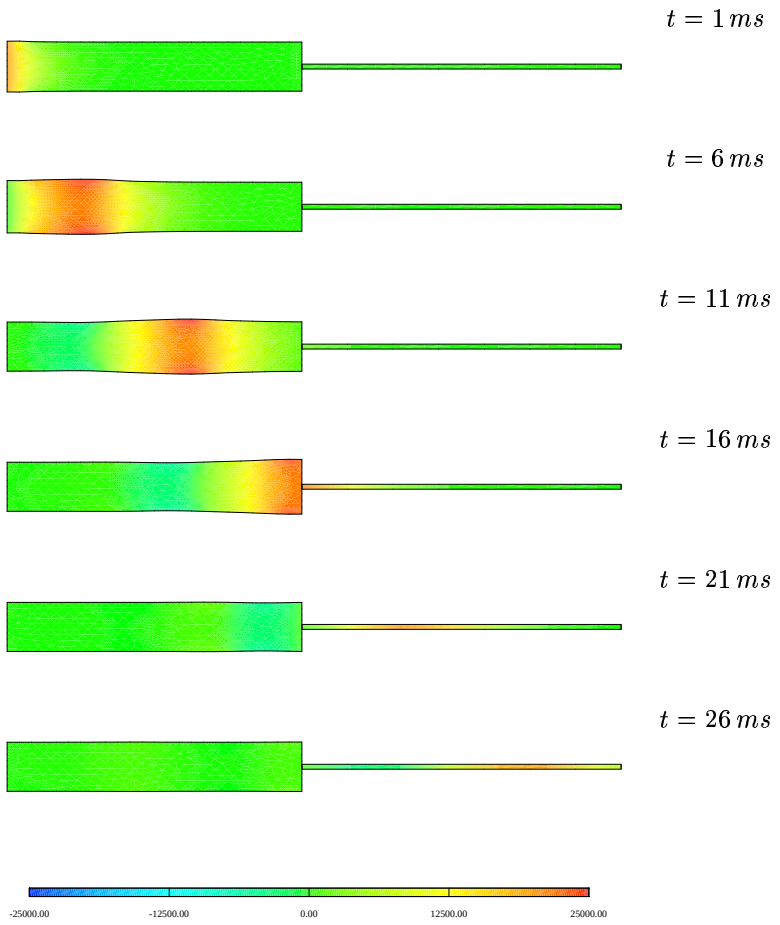

FIGURE 27. Pressure pulse entering at the *inflow*. A non-reflecting boundary condition at the outlet has been obtained by the coupling with a 1D hyperbolic model. Solutions every $5\,ms$.

The simulations here presented aim at highlight the problem. We illustrate the flow in the median plane of a 3D model of an anastomosis. [7]. The junction angle is 15 degrees. The diameter of the occluded branch (below) is 1 cm, and the one of the by-pass (above) is 0.96 cm. The simulations have been carried out setting the dynamic viscosity $\mu = 0.04$ g cm^{-1} s^{-1} and the density $\rho = 1$ g cm^{-3}. In this simulation the vessel wall has been assumed fixed and the boundary conditions prescribe null velocity on the walls and on the upstream section of the stenotic branch (100% stenosis), while a parabolic velocity profile has been prescribed at the inlet section with a peak velocity of 56 cm s^{-1}, corresponding to a flow rate of 1320 ml min^{-1}. On the downstream section a Neumann–type condition has been assigned.

Fig. 29 clearly illustrates the appearance and the evolution of the flow recirculation zones during the different phases of the heart beat.

7.3. **Pressure wave modification caused by a prosthesis.** Here we present a numerical simulation obtained using the one dimensional model (6.12) to investigate

[7] The model geometry has been provided by the Vascular Surgery Skejby Sygheus of the Aahrus University Hospital in Denmark.

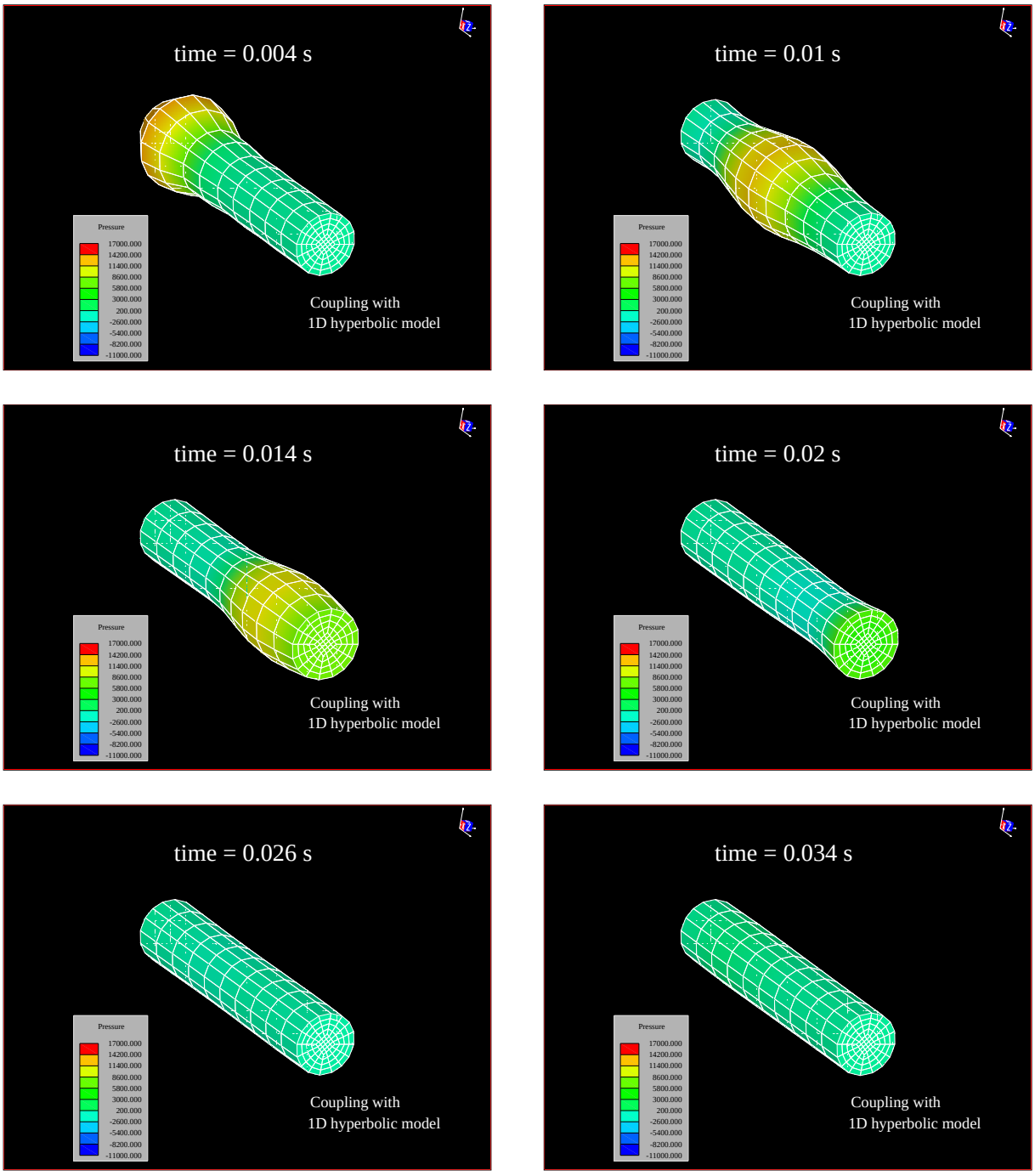

FIGURE 28. A pressure pulse traveling in a 3D compliant vessel. The displacement of the structure has been magnified by a factor 10. A non-reflecting boundary condition at the outlet has been obtained by the coupling with a 1D hyperbolic model (not shown in the picture).

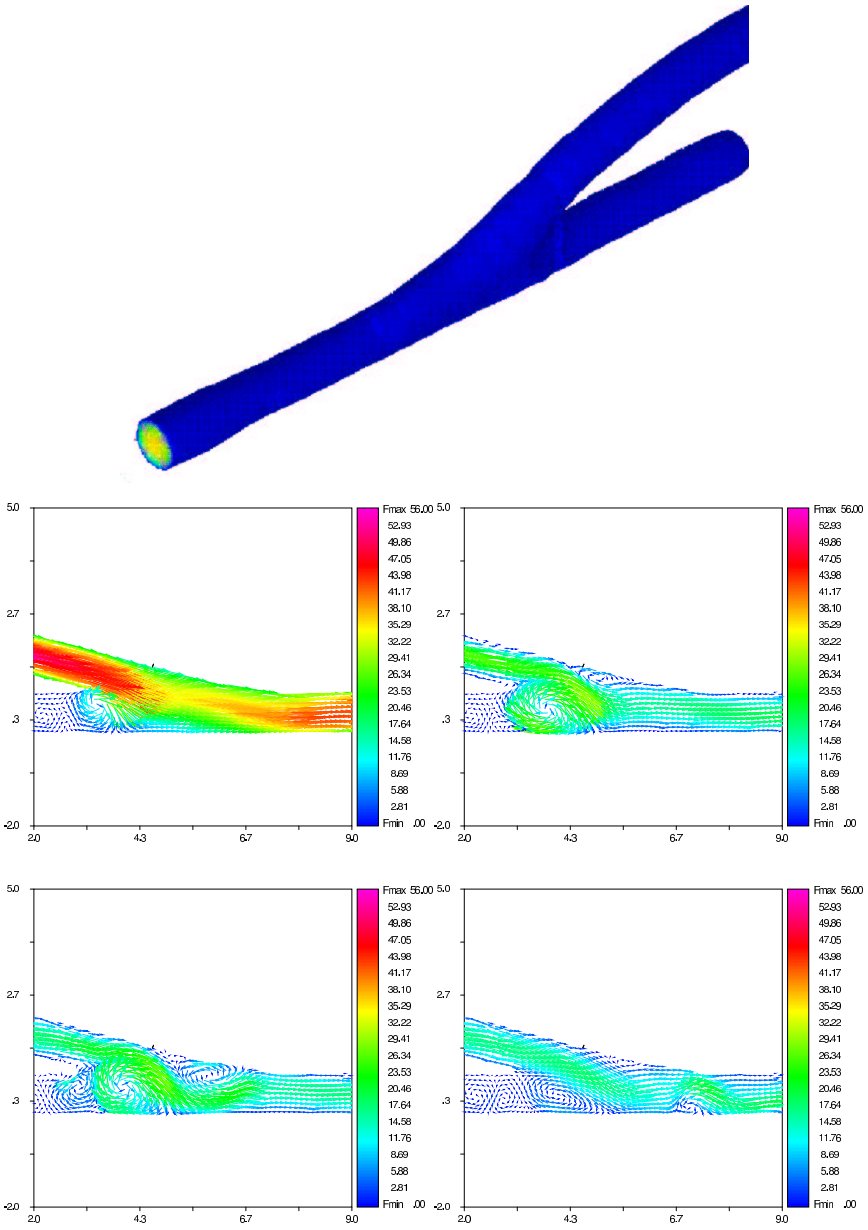

FIGURE 29. A model of a coronary by-pass anastomosis (top) and the velocity vector field on the median plane at four different instants of the heart beat. Flow at systole (top, left), initial deceleration phase (top, right), beginning of diastole (bottom, left) and end of diastole (bottom, right). The recirculation regions upstream and downstream of the junction are evident.

the effect of a prosthesis in an artery, in particular with respect to the alteration of the pressure wave pattern. To that purpose we have considered the portion of an artery of length L and a prosthesis of length l (see Fig. 30) and a Young modulus varying as already illustrated in Fig. 26.

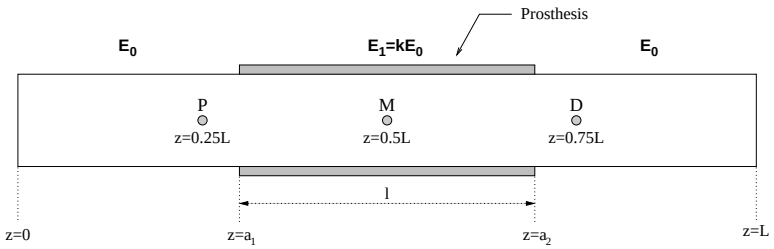

FIGURE 30. The layout of our numerical experiment. The points P, M and D are used as 'monitoring stations' to assess the modifications on the pressure wave caused by the prosthesis.

In order to assess the effect of the changes in vessel wall elastic characteristic on the pressure pattern, we have devised several numerical experiments. Two types of pressure input have been imposed at $z = 0$, namely an impulse input, that is a single sine wave with a small time period and a single sine wave with a more realistic time period (see Fig. 31). The impulse has been used to better highlight the reflections induced by the vascular prosthesis.

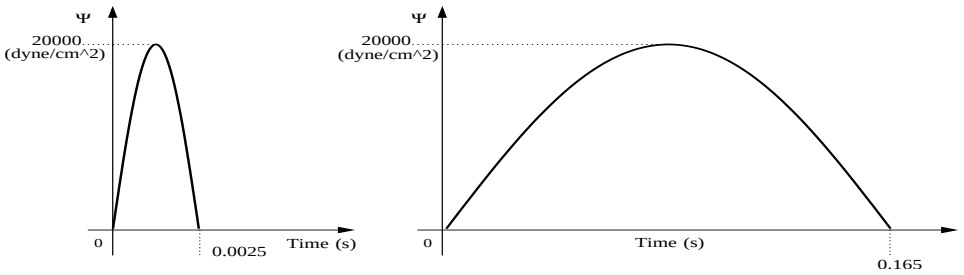

FIGURE 31. The two types of pressure input profiles used in the numerical experiments: an impulse (left) and a more realistic sine wave (right).

The part that simulates the presence of the prosthesis or stent of length L is comprised between coordinates a_1 and a_2. The corresponding Young's modulus has been taken as a multiple of the basis Young's modulus E_0 associated to the physiological tissue.

Three locations along the vessel have been identified and indicated by the letters D (distal), M (medium) and P (proximal). They will be taken as monitoring point for the pressure variation. Different prosthesis length L have been considered; in all cases points P and D are located outside the region occupied by the prosthesis. Table 1 indicates the basic data which have been used in all numerical experiments. In this numerical experiment we have considered the the conservation form (6.20) setting the friction term K_r to zero. The numerical scheme adopted is a second order Taylor-Galerkin [13]. A time step $\Delta t = 2 \times 10^{-6}$s and the initial values $A = A_0$ and $Q = 0$ have been used throughout.

At the outlet boundary $z = L$ we have kept W_2 constant and equal to its initial value (non-reflecting boundary condition). At the inlet boundary we have imposed the chosen pressure input in an approximate fashion, following a technique of the type illustrated in subsection 6.3.2.

7.3.1. *Case of an impulsive pressure wave.* In Fig. 32 we show the results obtained for the case of a pressure impulse. We compare the results obtained with uniform

TABLE 1. Data used in the numerical experiments.

	Parameters	**Value**
	Input Pressure Amplitude	$20\text{x}10^3\text{dyne/cm}^2$
FLUID	Viscosity, ν	0.035poise
	Density, ρ	1g/cm^3
	Young's Modulus, E_0	$3\text{x}10^6\text{dyne/cm}^2$
STRUCTURE	Wall Thickness, h	0.05cm
	Reference Radius, R_0	0.5cm

Young's modulus E_0 and the corresponding solution when $E_1 = 100E_0$, $l = 5$cm and the transition zone between healthy artery and prosthesis is $\delta = 0.5$cm. We have taken $L = 15$cm and a non uniform mesh of 105 finite elements, refined around the points a_1 and a_2. When the Young modulus is uniform, the impulse travels along the tube undisturbed. The numerical solution shows a little dissipation and dispersion due to the numerical scheme. In the case of variable E the situation changes dramatically. Indeed, as soon as the wave enters the region at higher Young's modulus it gets partially reflected (the reflection is registered by the positive pressure value at point P and $t \approx 0.015$s) and it accelerates. Another reflection occurs at the exit of the 'prosthesis', when E returns to its reference value E_0. The point M indeed registers an oscillatory pressure which corresponds to the waves that are reflected back and forth between the two ends of the prosthesis. The wave at point D is much weaker, because part of the energy has been reflected back and part of it has been 'captured' inside the prosthesis itself.

7.3.2. *Case of a sine wave.* Now, we present the case of the pressure input given by the sine wave with a larger period shown in Fig. 31, which describes a situation closer to reality than the impulse. We present again the results for both cases of a constant and a variable E. All other problem data have been left unchanged from the previous simulation. Now, the interaction among the reflected waves is more complex and eventually results in a less oscillatory solution (see Fig. 33). The major effect of the presence of the stent is a pressure increase at the proximal point P, where the maximum pressure is approximately 2500dynes/cm^2 higher than in the constant case. At a closer inspection one may note that the interaction between the incoming and reflected waves shows up in discontinuities in the slope, particularly for the pressure history at point P. In addition, the wave is clearly accelerated inside the region where E is larger.

In Table 2 we show the effect of a change in the length of the prosthesis by comparing the maximum pressure value recorded for a prosthesis of 4, 14 and 24 cm, respectively. The values shown are the maximal values in the whole vessel, over one period. Here, we have taken $L = 60$cm, $\delta = 1$cm, a mesh of 240 elements and we have positioned in the three cases the prosthesis in the middle of the model. The maximum value is always reached at a point upstream the prosthesis. In the table we give the normalised distance between the upstream prosthesis section and of the point where the pressure attains its maximum.

Finally, we have investigated the variation of the pressure pattern due to an increase of $k = E/E_0$. Fig. 34 shows the result corresponding to $L = 20$cm and $\delta = 1$cm and various values for k. The numerical result confirms the fact that a stiffer prosthesis causes a higher excess pressure in the proximal region, a fact that may have negative effects on the heart.

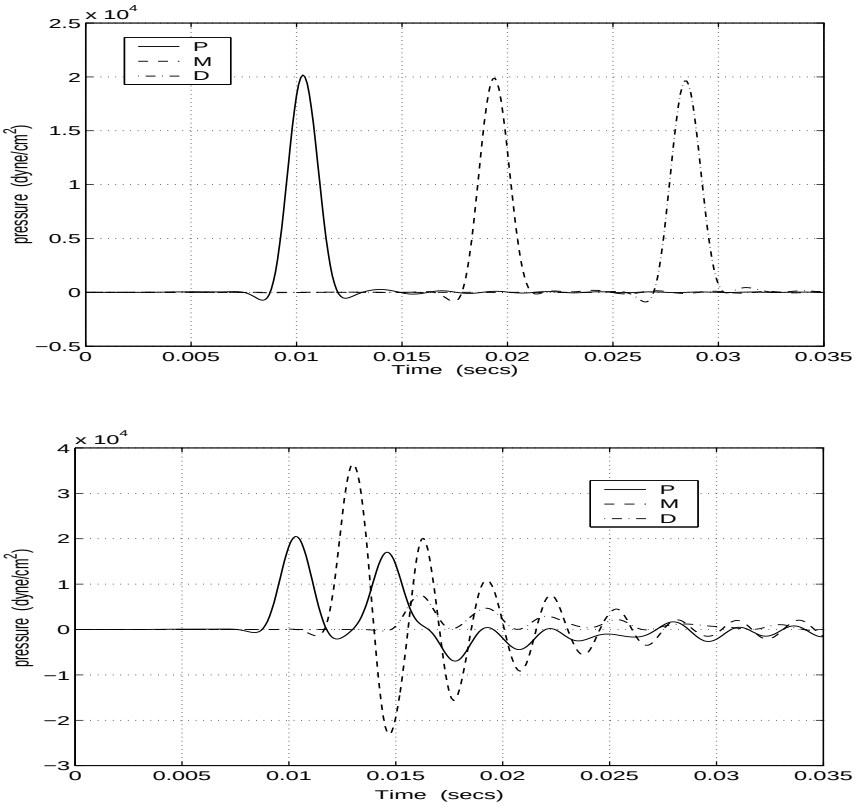

FIGURE 32. Pressure history at points P, M and D of figure 30, for an impulsive input pressure, in the case of constant (upper) and variable (lower) E.

TABLE 2. Maximum pressure value for prosthesis of different length.

Prosthesis length (cm)	*Maximal pressure* (dyne/cm^2)	*Maximum location* $z_{\max}/l$
4	23.5×10^3	0.16
14	27.8×10^3	0.11
24	30.0×10^3	0.09

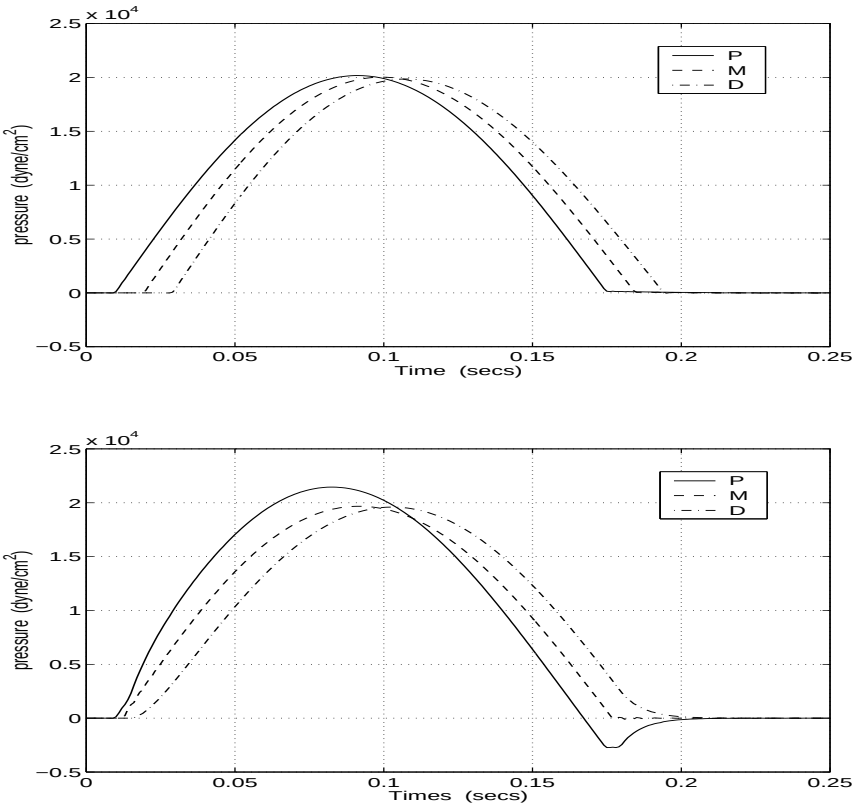

FIGURE 33. Pressure history at points P, M and D of Fig. 30, for a sine wave input pressure, in the case of constant (upper) and variable (lower) E.

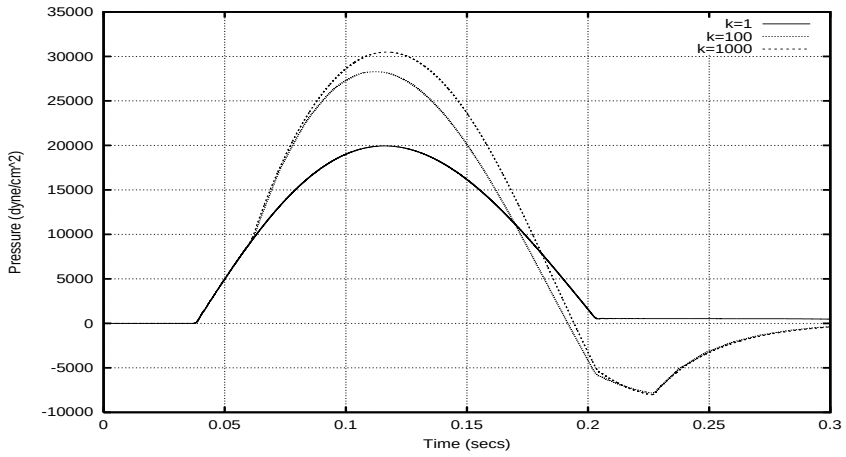

FIGURE 34. Pressure history at point P of Fig. 30, for a sine wave input pressure and different Young's moduli $E = kE_0$.

References

[1] R. Aris. *Vectors, Tensors and the Basic Equations of Fluid Mechanics*. Prentice Hall, 1962.

[2] A.C.L. Barnard, W.A. Hunt, W.P. Timlake, and E. Varley. A theory of fluid flow in compliant tubes. *Biophys. J.*, 6:717–724, 1966.

[3] H. Beirão da Veiga. On the existence of strong solutions to a coupled fluid-structure evolution problem. *Arch. Rat. Mech. and Analysis*, 2001. submitted.

[4] H. Brezis. *Analyse Fonctionnelle*. Masson, Paris, 1983.

[5] F. Brezzi and M. Fortin. *Mixed and Hybrid Finite Elements*. SSCM n. 5, Springer–Verlag, 1991.

[6] S. Canic. Blood flow through compliant vessels after endovascular repair: wall deformations induced by the discontinuous wall properties. *Computing and Visualisation in Science*, 2002. to appear.

[7] S. Canic and E.H. Kim. Mathematical analysis of the quasilinear effects in a hyperbolic model of blood flow through compliant axi-symmetric vessels. Preprint of the Department of Mathematics, University of Huston, 2001.

[8] A.J. Chorin and J.E. Marsden. *A Mathematical Introduction to Fluid Mechanics*, volume 4 of *Texts in Applied Mathematics*. Springer-Verlag, New York, 3 edition, 1990.

[9] P.G. Ciarlet. *Mathematical Elasticity. Volume 1: Three Dimensional Elasticity*, volume 20 of *Studies in Mathematics and its Applications*. North Holland, 1988.

[10] P.G. Ciarlet. *Introduction to Linear Shell Theory*. Gauthiers-Villars, 1998.

[11] P.G. Ciarlet. *Mathematical Elasticity. Vol. III. Theory of shells*. North-Holland, Amsterdam, 2000.

[12] G.R. Cokelet. The rheology and tube flow of blood. In R.Skalak and S. Chen, editors, *Handbook of Bioengineering*. McGraw-Hill, 1987.

[13] J. Donea, S. Giuliani, H. Laval, and L. Quartapelle. Time-accurate solutions of advection-diffusion problems by finite elements. *Comp. Meth. Appl. Mech. Engng.*, 45:123–145, 1984.

[14] G. Duvaut and J-L. Lions. *Inequalities in Mechanics and Physics*. Springer-Verlag, Berlin, 1976.

[15] L. Formaggia, J.-F. Gerbeau, F. Nobile, and A. Quarteroni. On the coupling of 3D and 1D Navier-Stokes equations for flow problems in compliant vessels. *Comp. Methods in Appl. Mech. Engng.*, 191:561–582, 2001.

[16] L. Formaggia, D. Lamponi, and A. Quarteroni. One dimensional models for blood flow circulation. in preparation, 2002.

[17] L. Formaggia and F. Nobile. A stability analysis for the Arbitrary Lagrangian Eulerian formulation with finite elements. *East-West J. Numer. Math.*, 7:105–131, 1999.

[18] L. Formaggia, F. Nobile, J.-F. Gerbeau, and A. Quarteroni. Numerical treatment of defective boundary conditions for the Navier-Stokes equations. *SIAM J. Num. An.*, 2002. (to appear).

[19] L. Formaggia, F. Nobile, and A. Quarteroni. A one dimensional model for blood flow: application to vascular prosthesis. In I. Babuska, T. Miyoshi, and P.G. Ciarlet, editors, *Mathematical Modeling and Numerical Simulation in Continuum Mechanics*, volume 19 of *Lecture Notes in Computational Science and Engineering*, pages 137–153, Berlin, 2002. Springer-Verlag.

[20] L. Formaggia, F. Nobile, A. Quarteroni, and A. Veneziani. Multiscale modelling of the circulatory system: a preliminary analysis. *Computing and Visualisation in Science*, 2:75–83, 1999.

[21] Y.C. Fung. *Biodynamics: Circulation*. Springer-Verlag, New York, 1984.

[22] Y.C. Fung. *Biomechanics: Mechanical Properties of Living Tissues*. Springer-Verlag, New York, 1993.

[23] L. Gastaldi. A priori error estimates for the arbitrary Lagrangian Eulerian formulation with finite elements. *East-West J. Numer. Math.*, 9(2):123–156, 2001.

[24] V. Girault and P.-A. Raviart. *Finite Element Methods for Navier-Stokes Equations, Theory and Algorithms*. Number 5 in Springer Series in Computational Mathematics. Springer-Verlag, Berlin, 1986.

[25] E. Godlewski and P.-A. Raviart. *Numerical Approximation of Hyperbolic Systems of Conservation Laws*, volume 118 of *Applied Mathematical Sciences*. Springer, New York, 1996.

[26] C. Grandmont and Y. Maday. Nonconforming grids for the simulation of fluid-structure interaction. In *Domain Decomposition Methods, 10 (Boulder, CO, 1997)*, pages 262–270. Amer. Math. Soc., Providence, RI, 1998.

[27] H. Guillard and C. Farhat. On the significance of the geometric conservation law for flow computations on moving meshes. *Comput. Methods Appl. Mech. Engng.*, 190(11-12):1467–1482, 2000.

[28] K. Hayashi, K. Handa, S. Nagasawa, and A. Okumura. Stiffness and elastic behaviour of human intracranial and extracranial arteries. *J. Biomech.*, 13:175–184, 1980.

[29] G.W. Hedstrom. Nonreflecting boundary conditions for nonlinear hyperbolic systems. *J. Comp. Physics*, 30:222–237, 1979.

[30] G.A. Holzapfel, T.C. Gasser, and R.W. Ogden. A new constitutive framework for arterial wall mechanics and a comparative study of material models. *Journal of Elasticity*, 61:1–48, 2000.

[31] T.J. Hughes, L. P. Franca, and M. Balestra. A new finite element formulation for computational fluid dynamics: V. Circumventing the Babuska Brezzi condition: a stable Petrov-Galerkin formulation of the Stokes problem accomodating equal-order interpolation. *Comp. Meth. Appl. Mech. Engng.*, 59:85–99, 1986.

[32] G.L. Langewouters, K.H. Wesseling, and W.J.A. Goedhard. The elastic properties of 45 human thoracic and 20 abdominal aortas *in vitro* and the parameters of a new model. *J. Biomech.*, 17:425–435, 1984.

[33] P.D. Lax. *Hyperbolic Systems of Conservation Laws and the Mathematical Theory of Shock Waves*. SIAM, Philadelphia, Pa., 1973. Conference Series in Applied Mathematics, No. 11.

[34] J. L. Lions and E. Magenes. *Problèmes aux Limites non Homogènes et Applications, 1*. Dunod, Paris, 1968.

[35] C.D. Meyer. *Matrix Analysis and Applied Linear Algebra*. SIAM, Philadelphia, USA, 2000.

[36] F. Nobile. *Numerical approximation of fluid-structure interaction problems with application to hemodynamics*. PhD thesis, École Polytechnique Fédérale de Lausanne (EPFL), 2001. Thesis N. 2458.

[37] B. Perot. An analysis of the fractional step method. *J. Comp. Phys.*, 108:51–58, 1993.

[38] R. Pietrabissa, A. Quarteroni, G. Dubini, A. Veneziani, F. Migliavacca, and S. Ragni. From the global cardiovascular hemodynamics down to the local blood motion: preliminary applications of a multiscale approach. In E. Onate et al., editor, *ECCOMAS 2000*, Barcelona, 2000.

[39] A. Quarteroni, S. Ragni, and A. Veneziani. Coupling between lumped and distributed models for blood problems. *Computing and Visualisation in Science*, 4:111–124, 2001.

[40] A. Quarteroni, F. Saleri, and A. Veneziani. Analysis of the Yosida method for the incompressible Navier-Stokes equations. *J. Math. Pure et Appl.*, 78:473–503, 1999.

[41] A. Quarteroni, F. Saleri, and A. Veneziani. Factorization methods for the numerical approximation of the incompressible Navier-Stokes equations. *Comp. Meth. Appl. Mech. Engng.*, 188:505–526, 2000.

[42] A. Quarteroni, M. Tuveri, and A. Veneziani. Computational vascular fluid dynamics: Problems, models and methods. *Computing and Visualisation in Science*, 2:163–197, 2000.

[43] A. Quarteroni and A. Valli. *Numerical Approximation of Partial Differential Equations*. Springer-Verlag, Berlin, 1994.

[44] A. Quarteroni and A. Valli. *Domain Decomposition Methods for Partial Differential Equations*. The Clarendon Press Oxford University Press, New York, 1999. Oxford Science Publications.

[45] A. Quarteroni, A. Veneziani, and P. Zunino. Mathematical and numerical modelling of solute dynamics in blood flow and arterial walls. *SIAM J. Numer. Analysis*, 2001. (to appear).

[46] K.R. Rajagopal. Mechanics of non-newtonian fluids. In G. Galdi and J. Necas, editors, *Recent Developments in Theoretical Fluid Mechanics*. Pitman Research Notes in Mathematics (291) - Longman, 1993.

[47] G. Rappitsch and K. Perktold. Pulsatile albumin transport in large arteries: a numerical simulation study. *ASME J. of Biomech. Eng.*, 118:511–519, 1996.

[48] B.D. Reddy. *Introductory Functional Analysis. With applications to boundary value problems and finite elements*. Springer-Verlag, New York, 1998.

[49] L.A. Segel. *Mathematics Applied to Continuum Mechanics*. Dover Publications, New York, 1987.

[50] J. Serrin. Mathematical principles of classical fluid mechanics. In S. Flugge and C. Truesdell, editors, *Handbuch der Physik*, volume VIII. Springer-Verlag, Berlin, 1959.

[51] J.C. Simo and D.D. Fox. On a stress resultant geometrically exact shell model, Part I: formulation and optimal parametrization. *Comput. Meths. Appl. Mech. Engng.*, 72:267–304, 1989.

[52] J.C. Simo, D.D. Fox, and M.S. Rifai. On a stress resultant geometrically exact shell model, Part II: the linear theory; computational aspects. *Comput. Meths. Appl. Mech. Engng.*, 73:53–92, 1989.

[53] N.P. Smith, A.J. Pullan, and P.J. Hunter. An anatomically based model of coronary blood flow and myocardial mechanics. *SIAM J. Appl. Math.*, 2002. (to appear).

[54] C.A. Taylor, M.T. Draney, J.P. Ku, D. Parker, B.N. Steele, K. Wang, and C.K. Zarins. Predictive medicine: Computational techniques in therapeutic decision-making. *Computer Aided Surgery*, 4(5):231–247, 1999.

[55] R. Temam. *Navier-Stokes Equations, Theory and Numerical Analysis.* North-Holland, Amsterdam, 2nd edition, 1984.

[56] K.W. Thompson. Time dependent boundary conditions for hyperbolic systems. *J. Comp. Physics*, 68:1–24, 1987.

[57] J.R. Womersley. Method for the calculation of velocity, rate of flow and viscous drag in arteries when the pressure gradient is known. *J. of Physiol.*, 127:553–563, 1955.

(Alfio Quarteroni) MOX, Department of Mathematics, Politecnico di Milano, Italy and, Institute of Mathematics, EPFL, Lausanne, Switzerland
E-mail address: Alfio.Quarteroni@epfl.ch

(Luca Formaggia) Institute of Mathematics, EPFL, Lausanne, Switzerland
E-mail address: Luca.Formaggia@epfl.ch